Master's thesis

NTNU
Norwegian University of Science and Technology
Faculty of Engineering
Department of Energy and Process Engineering

Martin Andre Righetti Nilsen

Industrial Drying of Raw Materials and By-products in Aluminium Production

Master's thesis in Energy and Environmental Engineering
Supervisor: Trygve Magne Eikevik
June 2021

NTNU
Kunnskap for en bedre verden

Martin Andre Righetti Nilsen

Industrial Drying of Raw Materials and By-products in Aluminium Production

Master's thesis in Energy and Environmental Engineering
Supervisor: Trygve Magne Eikevik
June 2021

Norwegian University of Science and Technology
Faculty of Engineering
Department of Energy and Process Engineering

NTNU

Kunnskap for en bedre verden

Abstract

In this thesis, the case of utilizing excess heat from surplus heat from process off-gases in the aluminium production process for industrial drying of raw materials and by-products is investigated.

Initially, some fundamental principles, as well as some basic economic considerations, were introduced. Furthermore, a literature review of where the research is at currently with regards to the challenges faced when capturing heat from the exhaust gasses in the aluminium industry was conducted. In addition, drying research literature which is related to the range of available drying technologies and techniques was reviewed. A mapping and evaluation of potential heat sources available in the Alcoa Mosjøen plant was carried out. Furthermore, experiments on the moisture content and drying kinetics of aluminium oxide, anode mass and petroleum coke were conducted, so that drying calculations could be made with the aim being to give an estimate of how much energy is available as surplus heat, and to determine the specific heat expenditure of drying the by-products. The results showed that there was a significantly larger amount of available heat than the required amount.

A subsequent analysis of the costs related to the purchase, installation and operation of an industrial rotary dryer was used as a basis for an analysis of the profitability of investing in a dryer, where the payback period of the project was evaluated. The conclusion of the aforementioned analysis yielded a payback period of between four months, as a best-case scenario, and three years, as a worst-case scenario, depending on various factors.

Sammendrag

I denne masteroppgaven utforskes muligheten for å bruke spillvarme fra avgasser i aluminiumsproduksjonsprosessen med det formål å tørke biprodukter som oppstår og råmaterialer som inngår i denne prosessen.

Innledningsvis ble fundamentale prinsipper i tillegg til noen generelle økonomiske betraktninger introdusert. Deretter ble det utført en litteraturstudie der fronten i teknologiutviklingen beskrives, med fokus på hvilke utfordringer som møtes i forbindelse med utnyttelse av spillvarme i aluminiumsindustrien. I tillegg ble ulike teknologier og teknikker innenfor industriell tørking beskrevet. Deretter ble det foretatt en kartlegging og evaluering av hvilke varmekilder og varmestrømmer på fabrikken til Alcoa i Mosjøen som er mulig å utnytte. Videre ble det gjennomført eksperimenter for å fastslå fuktinnhold og tørkekinetikk i aluminiumsoksid, anodemasse og petroleumskoks, med det formål å kunne gjøre innledende beregninger på energi og effektbruk i tørkeprosessen. Resultatene viste at det var betydelig mer varme tilgjengelig enn varmebehovet for tørking.

Senere ble det gjennomført en kostnadsanalyse der kostnader knyttet til kjøp, installasjon og drift av en industriell rotasjonstørker. Denne analysen dannet grunnlaget for en analyse av profitabiliteten til investeringen i en tørker, der tilbakebetalingstiden på prosjektet ble evaluert. Konklusjonen av denne analysen viste en estimert tilbakebetalingstid på fire måneder, i beste tilfelle, og 3 år, i verste tilfelle, avhengig av ulike faktorer.

Preface

This thesis, which is a continuation of my project thesis, concludes my master's degree in Energy and Environmental engineering at the Norwegian University of Science and Technology (NTNU). The thesis was written in the spring of 2021 at the department of Energy and Process engineering in cooperation with Alcoa.

I would like to thank my supervisor, Trygve M. Eikevik, for his excellent guidance. In spite of his many endeavours, he found time to provide me with valuable mentoring which has been of an immense help to me. Furthermore, I would like to express my gratitude to Martin Grimstad, Ellen Myrvold and Roger Moen at Alcoa. Their forthcoming attitude made asking difficult questions much easier. In addition, I would also like to thank Trond Andresen at SINTEF for his guidance, data and input. I would also like to recognise Ignat Tolstorebrov for his help and guidance during my experiments in the dewatering laboratory.

Finally, I would like to extend my deepest gratitude to my parents. Their unbounded support has helped me through everything.

Contents

List of Symbols

Symbol	Explanation
X_{cr}	Critical moisture content
p	Pressure
P_0	Pressure of pure water
a_w	Water activity
c_p	Specific heat
m	Mass
h	Enthalpy
T	Temperature
y	Mole fraction
mf	Mass fraction
Q	Energy
q''	Heat transfer rate per unit area
k	Thermal conductivity
h_{conv}	Convection heat transfer coefficient
E_b	Emissive power
σ	Stefan-Boltzmann constant
ε	Emissivity
G	Irradiation
FC	Fixed costs
VC	Variable costs
TC	Total costs
Q	Output
VUC	Variable unit cost
MC	Marginal cost
TUC	Total unit costs
MB	Marginal benefits
Q	Market price
MPC	Marginal private cost
MSC	Marginal social cost
t	Tax

Symbol	Explanation
$\dot{V}$	Volumetric flow
ρ	Density
$\dot{Q}$	Heat
ΔH_{vap}	Latent heat of vaporization
m_{sample}	Weight of a sample
r	Radius
d	Thickness
M_d	Moisture content dry basis
M_w	Moisture content wet basis
W_w	Weight of water in solid
W_d	Weight of dry matter
MR	Moisture Ratio
m_{init}	Initial weight of a sample
$m_{dry,init}$	Initial weight of a sample which is used to measure the dry weight
m_{dry}	Weight of a sample when the dry weight of the material was reached
$\bar{\tau}$	Average residence time
H	Holdup
F	Feedrate
L	Length
D	Diameter
N	Rotations per minute
α	Slope of dryer
n	Dynamic angle of repose
V	Volume
n	Mole
R	Gas constant
M	Molar mass
p_{LNG}	Price of LNG

List of Terms

Term	Explanation
COP21	2015 United Nations Climate Change Conference
GHG	Greenhouse Gas
EMC	Equilibrium Moisture Content
ETS	Emissions Trading System
EU	European Union
FBD	Fluidized Bed Dryer
LHV	Lower Heating Value
LNG	Liquefied Natural Gas
NDC	Nationally Determined Contributions
NOK	Norwegian Krone

1 Introduction

In the industry of today, the focus is ever increasing on the environment. Cutting energy expenditure and reducing the amount of waste material is of importance when trying to lower the environmental footprint. Drying of industrial raw material and by-products that can be reintroduced into processes, preferably by utilization of process waste heat, may help reduce the energy expended and in addition a greater utilization of the materials may be achieved.

Aluminium makes up about 8.3% of the weight of the earths crust and is the third most plentiful element on earth (Tangstad, 2013, p. 26). According to Gautam et al. (2018), approximately 21% of global greenhouse gas emissions are contributed by the industrial sector, of which aluminum industries accounted for around 1.0%. In 2014 in Norway, around 1 400 000 tonnes of aluminium were produced, accounting for 2.4% of the total production worldwide (Pedersen, 2018). The Norwegian aluminium industry benefits of hydroelectricity, which makes the aluminium produced in Norway one of the cleanest in the world in terms of CO_2 emissions (Tangstad, 2013). In Table 1 from (Tangstad, 2013, p. 50) the CO_2 emissions in the different stages of aluminium production are tabulated. For production of aluminium based on hydroelectricity, production of alumina and electrolysis are the stages where most carbon dioxide is released. The aim is to dry alumina, which is reintroduced in the process by using waste heat from, among other processes, the electrolysis process. Thus, a reduced amount of new alumina is needed, and less energy is wasted from the electrolysis. These improvements will be in the two most polluting stages in the aluminium production process.

Table 1: "Emissions of CO_2 from various steps of aluminium production. Average numbers for emissions from various energy sources also given" (Tangstad, 2013, p. 50).

	General $\frac{kgCO_2}{kgAl}$	Hydro $\frac{kgCO_2}{kgAl}$	Gas $\frac{kWhCO_2}{kgAl}$	Coal $\frac{\%CO_2}{kgAl}$	Hydro $\frac{\%CO_2}{kgAl}$	Gas $\frac{\%CO_2}{kgAl}$	Coal $\frac{\%CO_2}{kgAl}$
Alumina prod.	1.70	1.70	1.70	1.70	43.2	17.5	9.7
Anode prod.	0.30	0.30	0.30	0.30	7.6	3.1	1.7
Electrolysis	1.50	1.50	1.50	1.50	38.1	15.4	8.6
Anode effect	0.30	0.30	0.30	0.30	7.6	3.1	1.7
Casthouse	0.06	0.06	0.06	0.06	1.5	0.6	0.3
Recycling	0.08	0.08	0.08	0.08	1.9	0.8	0.4
Hydro power	0.0	0.00			0.0		
Gas fired power plant	5.8		5.8			59.6	
Coal fired power plant	13.6			13.60			77.6
Total		3.94	9.74	17.54	100.00	100.00	100.00

The conventional method for producing aluminium, on an industrial scale, is by the Hall-Héroult process. The process was invented in 1886 by Paul Louis Héroult and Charles Martin Hall, independent of each other. In the Hall-Héroult process, aluminium oxide is reduced in an electrolytic bath consisting of molten cryolite and aluminium fluoride to create molten aluminium (Prasad, 2000). The molten aluminium is formed at the cathode and the oxygen gas produced at

the anode reacts with the carbon of the anode to form carbon dioxide (Pedersen, 2017). In Figure 1, a cross section of the electrolysis cell is shown with annotations of its most conspicuous features.

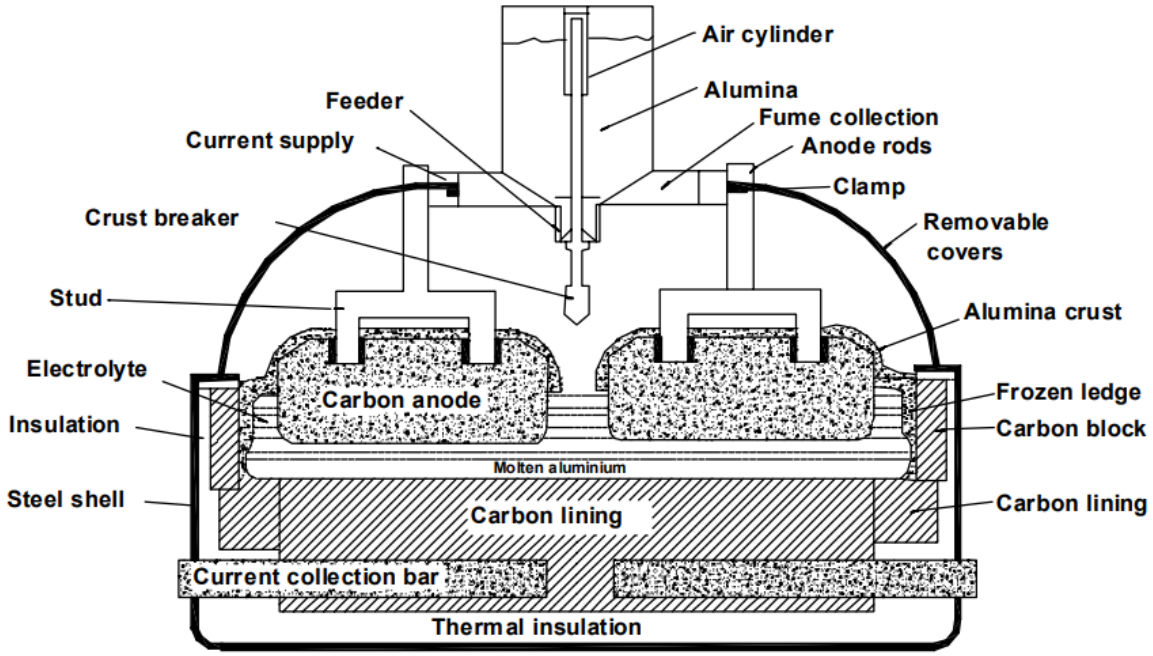

Figure 1: A cross sectional view of a Hall-Héroult electrolysis cell for aluminium production (Prasad, 2000).

After the aluminium electrolysis process, aluminium oxide particles are separated from electrolysis exhaust gas using a wet scrubber. The aluminium oxide particles come into contact with the water in the scrubber and is transported to a basin, where it is stored temporarily before being deposited in a treatment facility. In Figure 2 the artificial lake where the aluminium oxide is deposited is pictured. The yearly average accumulation of aluminium oxide is estimated to 500 tonnes per year. Even though the aluminium oxide is being deposited, it can still be reintroduced into the process. But before being reintroduced, the aluminium oxide must be completely dry, as it is being heated to around 960 °C. If the particles are not completely dry, the rapid heating of the moist aluminium oxide could cause an explosion. Hence, it is of high importance to assure that the product is completely dry. Preferably, the drying process should use excess heat from the aluminium process itself. The aim will be to utilize some of the exhaust gas to either use directly for drying or indirectly by a heat recovery heat exchanger.

Another possible drying case from the aluminium industry is the large amount of petroleum coke that is shipped to the factory. According to Alcoa, the amount of petroleum coke is 220 000 tonnes yearly, and it has a moisture content which is estimated to constitute 0.1 - 0.3 % of its total weight. The petroleum coke arrives by ship to the factory and is loaded to a conveyor belt, which brings the petroleum coke to a silo for temporary storage, before being mixed with pitch to make anodes. During the baking of the anodes the relatively small moisture content initially present in the petroleum coke, is removed. Thus, heat generated from burning of natural gas is

Figure 2: Aluminium oxide deposited in an artificial lake in Mosjøen.

used to remove moisture from the petroleum coke in the anode baking process. It could possibly be feasible to remove this moisture using surplus heat, instead of the moisture being removed while baking. This would contribute to lowering the CO_2 footprint of the process because the same drying process, which takes place in the anode baking furnace which uses natural gas would be conducted using surplus heat which otherwise would be discarded.

A different, albeit related, drying case is assocoated with the possibility of drying the excess carbon-rich anode sludge, or anode mass, which is created during the anode baking process. This anode mass consists of a mixture of petroleum coke and pitch. In prebaked anodes, which is the type of anode from which the anode mass originates, petroleum coke makes up around 65 % while the pitch makes up 15 %. The final 20 % is made up of anode butts, which are remains of previous anodes (Chevarin et al., 2016). The petroleum coke and the pitch are mixed in a mould and formed. During this process, the anode is cooled in a water basin. It is during this cooling period in the basin that some anodes lose an amount of anode mass. A yearly accumulation of 40 tonnes of anode mass is estimated. This mass is considered as hazardous waste if deposited, and therefore depositing it could be relatively expensive compared to drying and re-using it. More recently, the anode mass has been re-introduced into the anode baking process without drying it. Although this is a better alternative than depositing it, LNG is needed in order to increase the temperature and remove the moisture from the anode mass. Consequently, utilizing a dryer that uses recovered waste heat would be an alternative solution which could prove less costly whilst reducing the GHG-emissions.

2 Fundamentals

2.1 Drying

Drying is the process of removing moisture from a material to yield a solid product. The process of thermally drying a wet solid includes the transfer of energy from the surrounding environment to the solid in order to evaporate the surface moisture, and the transfer of internal moisture to the surface of the solid for it to be evaporated (Mujumdar, 2007, p. 4). The rate of which moisture is removed is called the drying rate. During the first stage of drying, the drying rate usually is constant. In Figure 3, the first drying stage is the the constant drying rate stage. During this stage, the free moisture at the surface of the solid is transported from the solid to the environment. Thus, in this phase, the rate of diffusion of the water vapour across the air-moisture interface of the solid is the main factor affecting the drying rate, according to Mujumdar (2007). After some drying has occurred, the internal moisture is moved by capillary forces from the inside of the solid towards the surface. When the surface film of the solid has been reduced so much that dry spots appear on the solid, the moisture content is at the critical moisture content, X_{cr}. The second and third stages of drying are often referred to as the "falling rate phase" and are phases where the surface is unsaturated. When the solid loses weight, shrinkage may occur. If the surface area of the solid decreases, this will lead to a reduction of total moisture removal rate. The drying rate of the third and last phase is limited by the movement of moisture from the internal part of the solid and to the surface. This rate is controlled by difference in gradients of concentration within the product. The heat transfer of this final phase is convective between the surface and the dry air, and conductive inside the solid.

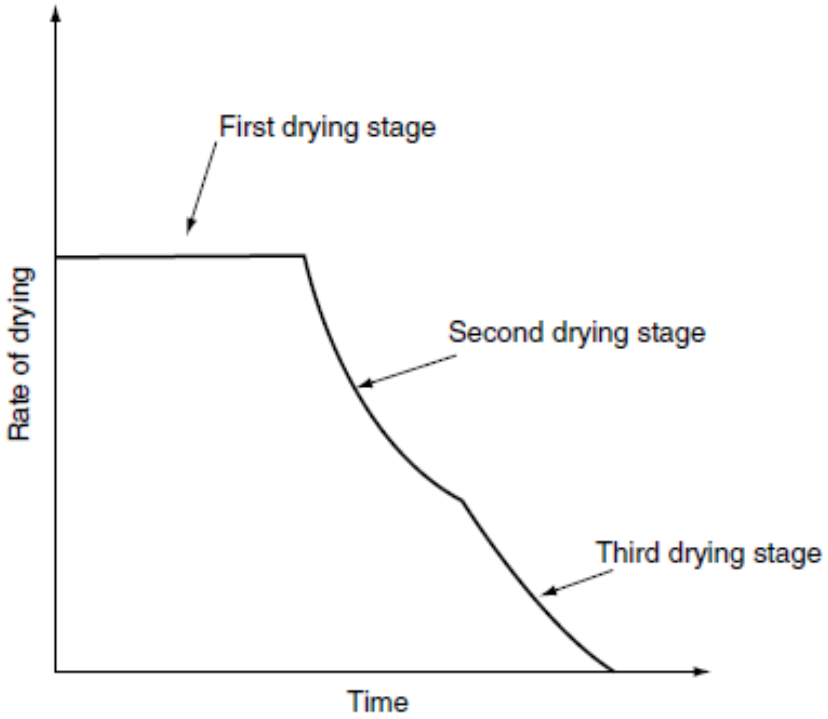

Figure 3: Characteristic drying rate curve as a function of time for a hygroscopic material (Mujumdar, 2007, p. 17).

2.2 Equilibrium moisture content and water activity

Considering a moist product which is to be dried by means of a heated gas stream, in this case, hot air. Depending on the gradient of vapour pressure of water present in the product and the partial pressure of vapour in the gas stream, the product will gain or lose moisture. Assuming that the partial pressure of vapour in the gas stream is constant and lower than in the product, the product will lose moisture until the equilibrium conditions are reached (Mujumdar, 2007, p. 14-15). The moisture content in the product at this equilibrium condition is called equilibrium moisture content (EMC), and it depends on the temperature and relative humidity of the surrounding air as well as the chemical composition and physical structure of the product (Mujumdar, 2007, p. 102-103). Plotting the EMC at different equilibrium relative humidities at constant temperatures, one can determine the sorption isotherms of the product. Depending on if the relative humidity in the gas stream is higher or lower than in the product itself, i.e. if the product is wetted or dried, the adsorption or desorption isotherm is obtained. In the drying process, the desorption isotherm is of interest because it shows the kinetics of the drying process.

Water activity, a_w, is the ratio of partial pressure of water in a substance, p, to the saturated vapour pressure of pure water at the same temperature, p_0:

$$a_w = \frac{p}{p_0} \tag{1}$$

According to (Mujumdar, 2007, p. 524), "Water activity relates to the chemical activity of moisture in the food during drying and storage", and is often used in the food industry as a means of determining the microbiological activity and consequently the shelf-life of a product.

The relationship between the equilibrium material moisture content and the corresponding water activity at a given temperature is known as the sorption isotherm (Mujumdar, 2007, p. 102). Moisture sorption isotherms are used to determine the minimum value of moisture a product can attain during a drying process at the given relative humidity. The relationship between EMC and water activity is complex and usually non-linear and the sorption isotherms are determined experimentally. In Figure 4, an example of desorption and adsorption isotherms are shown. The desorption isotherm is obtained when a solid is dried, and the adsorption isotherm is obtained when a product is gaining moisture. The adsorption and desorption isotherms deviate from one another, and the phenomenon of hysteresis is observed. This phenomenon is yet to be quantitatively described (Mujumdar, 2007, p. 102).

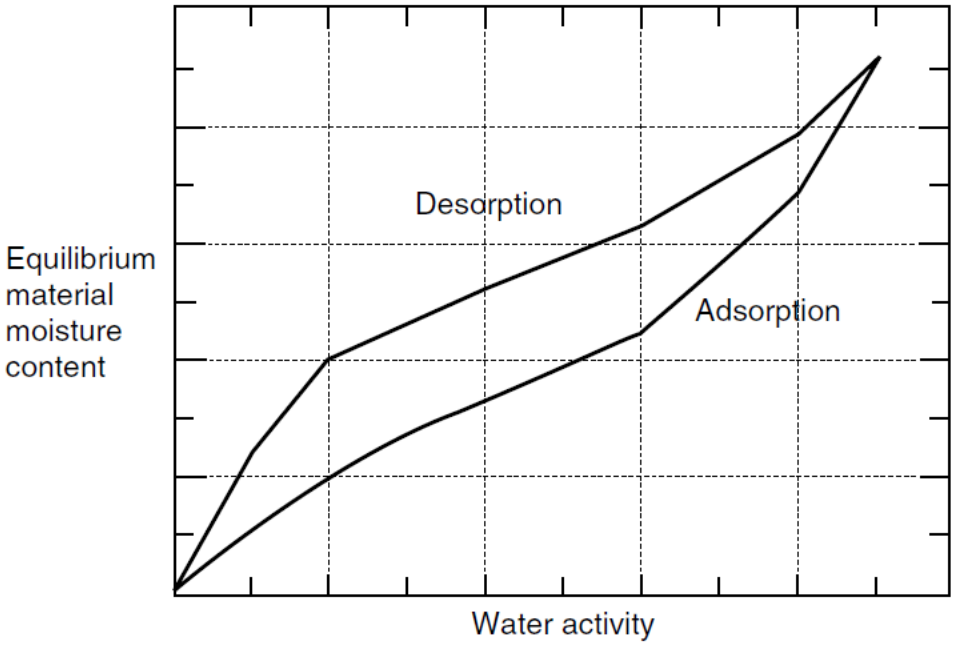

Figure 4: Hysteresis phenomenon in adsorption and desorption isotherms (Mujumdar, 2007, p. 102).

2.3 Specific heat

Specific heat, or heat capacity, is an intensive property related to the internal energy of matter (Moran and Shapiro, 2015, p. 104). For pure, simple compressible substances, isobaric specific heat, c_p, is defined as:

$$c_p = \left(\frac{\partial h}{\partial T}\right)_{p=constant} \tag{2}$$

Where h is enthalpy, T is temperature and p is pressure. The subscript $p = constant$ in Equation 2 denotes that the pressure is held fixed during differentiation.

Enthalpy can be either be expressed on a unit mass basis or on a unit mole basis, with SI units kJ/kg · K, or kJ/kmol · K (Moran and Shapiro, 2015).

For mixtures of solids, the specific heat of the mixture on a molar basis can be found as the sum of the products of mole fractions and specific heats of each component:

$$\overline{c}_p = \sum_{i=1}^{j} y_i \overline{c}_{p,i} \tag{3}$$

Where y_i is the mole fraction and $\overline{c}_{p,i}$ is the specific heat of the i-th component of the mixture (Moran and Shapiro, 2015, p. 632). Equation 3 works on a molar basis. Substituting the molar fraction y with mass fraction mf, the expression for specific heat on a mass basis becomes:

$$\overline{c}_p = \sum_{i=1}^{j} mf_i \overline{c}_{p,i} \tag{4}$$

Where mf_i is the mass fraction of the i-th and $\overline{c}_{p,i}$ is the specific heat of the i-th component of the mixture (Moran and Shapiro, 2015, p. 633).

2.4 Energy requirement in drying

Drying of materials implies removing the water inside the material. To do so, the minimum amount of heat that needs to be added is equal to the latent heat of vaporization of water, ΔH_{vap}. In addition, the materials will be heated during the drying process. The energy related to heating the materials is given as:

$$Q = m \cdot c_p \cdot \Delta T[kJ] \tag{5}$$

Where m [kg] is mass, c_p [kJ/kg $\cdot$ K] is the specific heat and ΔT [K] is the temperature difference between the upper and lower temperature in the heating process.

According to Mujumdar (2007), textiles, minerals and inorganic minerals are products where almost the entire moisture content is free. Thus, an approximation where constant drying rate is assumed in the energy requirement calculations will not be significantly inaccurate. Based on this assumption, the heat required to evaporate the water inside the solid is approximated to be equal to the heat required to evaporate a similar amount of free water.

2.5 Heat transfer

Incropera et al. (2017) states that "Heat transfer (or heat) is thermal energy in transit due to a spatial temperature difference". The transfer of heat can occur in different modes: mainly through conduction, convection and radiation. In industrial dryers, the most common modes of heat transfer are conduction and convection, where heat is transferred to the surface and inside of the wet solid. However, when radiation is applied, heat can be generated internally in the wet material. (Mujumdar, 2007, p. 4).

2.5.1 Conduction

Conductive heat transfer is the transfer of heat through a stationary medium, which may be either a solid or a fluid (Incropera et al., 2017, p. 2). Fourier's law is a rate equation which may be used to describe the energy transfer rate per unit time. Fourier's law in differential form is given as:

$$q'' = -k\nabla T \tag{6}$$

Where q'' [W/m^2] is the heat transfer rate per unit area perpendicular to the heat transfer direction, k [W/m $\cdot$ K] is the thermal conductivity, and ∇T [K/m] is the temperature gradient. In Figure 5, one-dimensional heat conduction through a wall with an arbitrary temperature difference is illustrated.

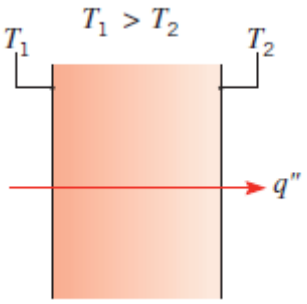

Figure 5: "Conduction through a solid or a stationary fluid" (Incropera et al., 2017, p. 2)

The thermal conductivity, k, is a transport property and is a characteristic of the material in which the heat is conducted. Pure metals and alloys have higher values of thermal conductivity than, e.g., liquids and gases. Hence, the metals and alloys will have a higher rate of heat transfer than the liquids and gases if all other parameters remain unchanged. There are several other factors affecting the thermal conductivity of a material, including temperature and the state of matter (Incropera et al., 2017, p. 62-71).

2.5.2 Convection

Convection heat transfer is comprised of two mechanisms: the diffusion of energy and the advection, or bulk motion, of the fluid (Incropera et al., 2017, p. 6). Mujumdar (2007) states that: "Convection is possibly the most common mode of drying particulate or sheet-form or pasty solids". In direct drying systems, the material which is to be dried is exposed directly to a drying medium. According to (Mujumdar, 2007, p. 21), "Heat for evaporation is supplied by convection to the exposed surface of the material and the evaporated moisture carried away by the drying medium".

Convection heat transfer is described by the rate equation known as Newton's law of cooling:

$$q'' = h_{conv}(T_s - T_\infty) \tag{7}$$

Where q'' [W/m^2] is the heat transfer rate per unit area, h_{conv} [W/m^2 $\cdot$ K] is the convection heat transfer coefficient, T$_s$ [K] is the temperature of the surface, and T$_\infty$ [K] is the fluid temperature. In Figure 6, convective heat transfer between a surface with a higher temperature than the passing fluid is illustrated. The direction of heat transfer is from the surface to the fluid.

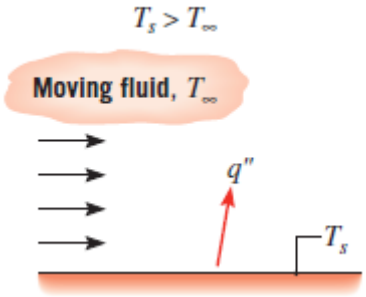

Figure 6: "Convection from a surface to a moving fluid" (Incropera et al., 2017, p. 2)

The nature of the stream of fluid determines whether the convection can be classified as forced or natural. Forced convection occurs when the flow is caused by external means (Incropera et al., 2017, p. 6). As an example, flow caused by a fan or flow such as atmospheric wind are classified as forced convection cases. Natural convection occurs when the flow is caused by buoyancy forces occurring as a consequence of density and temperature differences in the fluid (Incropera et al., 2017, p. 6). As an example, the heat generated from hot components in a computer will transfer to the surrounding air. When the air is heated, its density will decrease, and the buoyancy will induce an upward stream of air. However, if the amount of heat which is generated by the components in the computer is larger than the heat rejected by natural convection, the computer risks overheating. By inducing a flow of air with a speed such that enough heat is rejected, a computer fan could prevent overheating.

2.5.3 Radiation

Incropera et al. defines thermal radiation as "energy emitted by matter that is at a nonzero temperature" (Incropera et al., 2017, p. 8). Solids, liquids and gases emit thermal radiation in the form of electromagnetic waves at temperatures above zero Kelvin. In contrast to conduction and convection, heat transfer by radiation is not dependent on a material medium to occur, but is most effective in a vacuum (Incropera et al., 2017, p. 8-9). Figure 7 illustrates a basic case of radiation heat exchange between two arbitrary surfaces. The upper limit for how much emissive power can be radiated from a surface is given by the Stefan-Boltzmann law:

$$E_b = \sigma T_s^4 \tag{8}$$

Where E_b [W/m^2] is the emissive power of the surface, T_s is the absolute temperature of the surface and $\sigma = 5.67 \times 10^{-8}$ [W/m$^2 \cdot$ K^4] is the Stefan-Boltzmann constant.

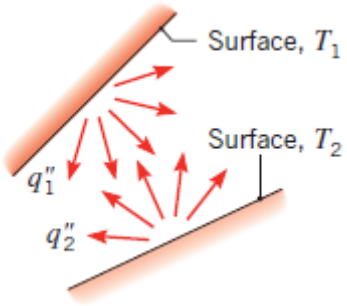

Figure 7: "Net radiation heat exchange between two surfaces" (Incropera et al., 2017, p. 2)

Equation 8 prescribes the emissive power of an ideal radiator, which is called a blackbody. The thermal radiation of a real surface will be lower than that of an ideal surface. For a real surface, the relation between emissive power and temperature is given by:

$$E = \varepsilon \sigma T_s^4 \tag{9}$$

Where ε is the emissivity, a radiative property of the surface. The emissivity has values in the range of $0 \leq \varepsilon \leq 1$, so the surface emissive power of a real body will always be lower than that of a blackbody.

Incropera et al. (2017) states that: "Radiation may also be incident on a surface from its surroundings. The radiation may originate from a special source, such as the sun, or from other surfaces to which the surface of interest is exposed". Such incident radiation is termed irradiation, G. The amount of absorbed thermal energy of an object, G_{abs}, is proportional to the amount of the irradiation on an object. The rate at which radiation is absorbed per unit area is given as:

$$G_{abs} = \alpha G \tag{10}$$

Where the absorptivity of the material, α, is a surface radiative property in the range $0 \leq \alpha \leq 1$. In addition, the value of α varies with the nature of the irradiation. E.g., the irradiation on a surface from the sun may lead to a value of α differing from the values when irradiation comes from a furnace (Incropera et al., 2017, p. 10).

When irradiation on a semitransparent medium occurs, the irradiation will either be reflected, absorbed or transmitted. In Figure 8, incident radiation on a semitransparent surface is illustrated. In addition, Figure 8 illustrates the relationship between irradiation, reflection, absorption and transmission for a semitransparent medium. Reflection radiation is related to the portion of the radiation which is reflected by the surface on which the radiation is incident upon. Absorption refers to the portion of the radiation which is absorbed by the medium and causes an increase in the internal thermal energy of the medium. Transmission radiation is related to

the radiation which passes through a medium (Incropera et al., 2017, p. 715). E.g., when the sun shines through a window, some of the radiation from the sun will be reflected, some will be absorbed by the window and heat up the material and some will be transmitted to the other side of the window.

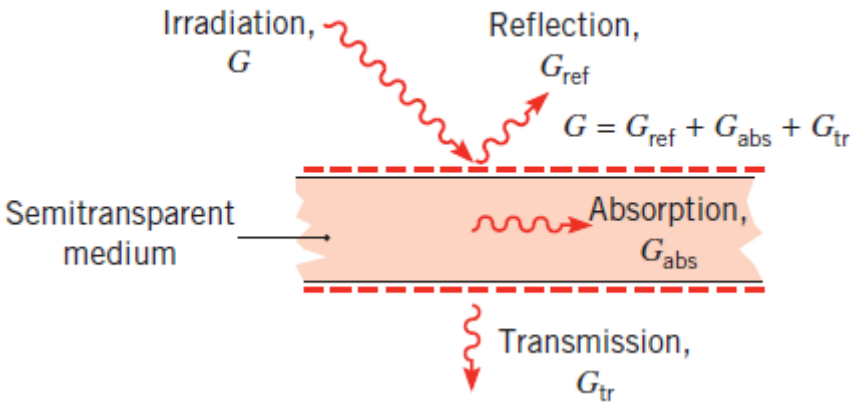

Figure 8: "Radiation at a surface. Reflection, absorption and transmission of irradiation for a semitransparent medium" (Incropera et al., 2017, p. 715)

By defining the reflectivity, ρ, as the fraction of irradiation which is reflected, the absorptivity, α, as the fraction of irradiation which is absorbed as internal thermal energy, and the transmissivity, τ, as the fraction of irradiation which is transmitted, it follows that (Incropera et al., 2017, p. 716):

$$\rho + \alpha + \tau = 1 \tag{11}$$

According to Incropera et al. (2017), "In many engineering problems (a notable exception being problems involving solar radiation or radiation from other very high temperature sources), liquids can be considered opaque (as is the case for metals) or semitransparent (as is the case for sheets of some polymers and some semiconducting materials)". An opaque medium experiences no transmission ($\tau = 0$).

3 Economy

3.1 Costs

To properly evaluate whether a change in the aluminium production process is economically viable, an overview of the costs associated to the change is needed. The addition of a dryer will not lead directly to an increase in revenue, but rather a potential decrease in costs. The nature and size of different costs will be evaluated later, but an assumption is made that the company behaves in a cost-minimizing manner.

The nature of costs vary and are important in most economic aspects, including matters with regards to the profitability of alternative decisions. A differentiation is made between fixed and variable costs. Fixed costs, FC, are costs that do not vary with the output, Q. Such costs should be related to a period in which the costs are fixed. In the long term, most costs are not fixed due to fluctuation in prices and inflation. However, costs that remain constant within a relevant time period are considered fixed. The period needs to be defined, but it should be proportionate to the scale of production and the nature of the costs, e.g, a contract for the lease of property or the depreciation of a machine in a factory. The fixed costs represent the resource consumption to be able to do something, or put differently, they represent the costs associated to building up and maintaining the capacity to be able to do something (Hoff and Helbæk, 2016). Therefore it follows that fixed costs are related to an upper limit in capacity. Furthermore, the fixed cost per unit is inversely proportional to the output quantity. Hence, it is beneficial,*ceteris paribus*, to operate at the upper capacity when considering fixed cost per unit.

In contrast to fixed costs, variable costs, VC, vary with the activity level. For industrial businesses, the output could be the quantity of units produced. In a simplified case where the only variable costs are material cost, the costs would rise proportionally with the increase in production. If the production is zero units, there are no variable costs. In some cases it may be useful to utilize the variable unit costs, VUC, which are the variable costs per unit:

$$VUC = \frac{VC}{Q} \tag{12}$$

At a constant variable unit cost, the increase in cost is proportionate to the increase in output quantity. If the costs increase at a higher rate than proportionally to the output, diseconomies of scale occur. In Figure 9, this case is represented by the green line. If the costs increase at a lower rate than proportionally to the output, economies of scale occur, as illustrated by the red line in Figure 9. In Figure 9, the three main types of cost behaviour at different production volumes are illustrated, but in reality the cost curves of a business can consist of a combination of different types of curves.

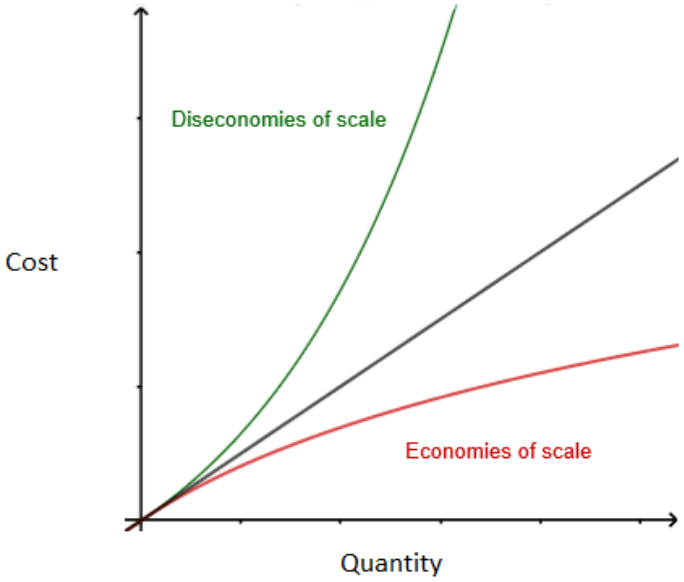

Figure 9: Linear cost increase, economies of scale and diseconomies of scale

The total costs, TC, are composed of the fixed costs, FC, and the variable costs, VC. In Figure 10, an illustration graphically presents the relationship between fixed and variable costs on the total costs, and how the total costs may increase with increasing output quantity. The relation for the total cost is obtained by summing up the costs:

$$TC = FC + VC \tag{13}$$

By differentiating Equation 13 with respect to quantity, Q, the rate of change in costs with respect to output quantity can be investigated. Assuming that the total and variable costs are a function of the output quantity and that the cost-function is continuous and differentiable, the following relation can be obtained:

$$\frac{dTC(Q)}{dQ} = \frac{dVC(Q)}{dQ} = MC(Q) \tag{14}$$

As the fixed costs are constant, the term is eliminated in the differentiation. Thus, the terms in Equation 14 represent the change in costs which arise when the output quantity is changed. This is called the marginal cost, MC. Marginal cost is an often used expression in cost and profitability analyses. Assuming an incremental increase in quantity of one unit, the marginal cost is the cost of producing one more unit. In Figure 10, the rate of change in variable costs is constant, which means that the marginal cost is constant. Thus, for a given increase in quantity produced, the increase in costs is linearly proportional. Though, this is not the norm as cost functions often are nonlinear.

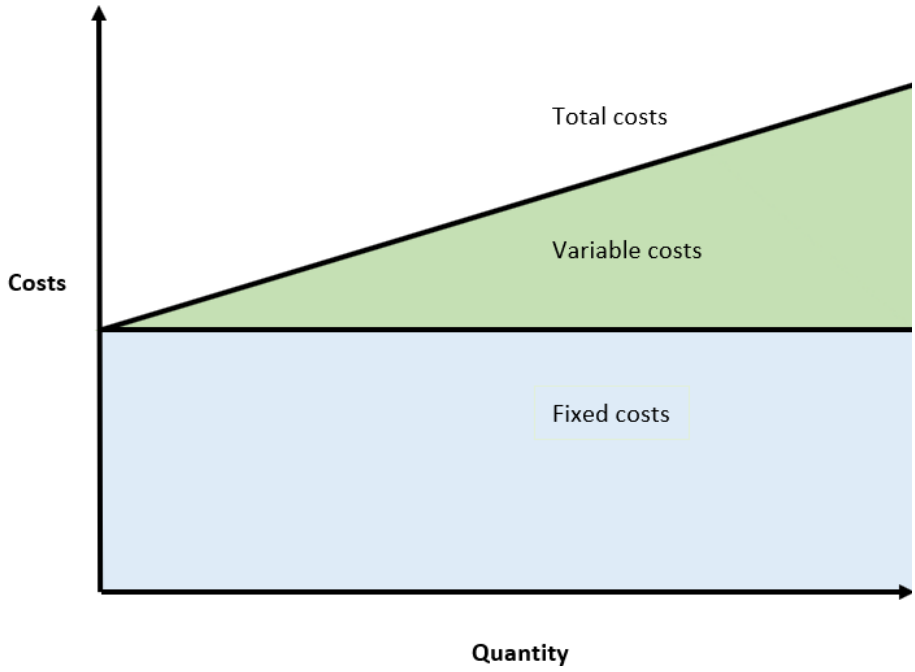

Figure 10: Total, fixed and variable costs as a function of increased quantity of output.

As previously stated in Equation 13, the total costs are the sum of the fixed and variable costs. By considering the total costs in relation to the quantity of produced units, the total unit costs, TUC, can be found as the sum of the fixed costs per unit and the variable unit costs:

$$TUC = \frac{TC}{Q} = \frac{FC}{Q} + VUC \tag{15}$$

This relation is illustrated in Figure 11. In order to determine the quantity of units a business should produce, the optimum cost level should be determined. Total unit cost is the average cost of production per unit. Thus, the lowest average costs per unit is determined as the minimum point on the total unit cost line (Hoff and Helbæk, 2016, p. 199). The average cost per unit is often important to determine, especially in relation to profitability analyses and product calculation due to the fact that the revenue per unit produced is equal to the price of the product subtracted by the total unit costs (Hoff and Helbæk, 2016, p. 187-194).

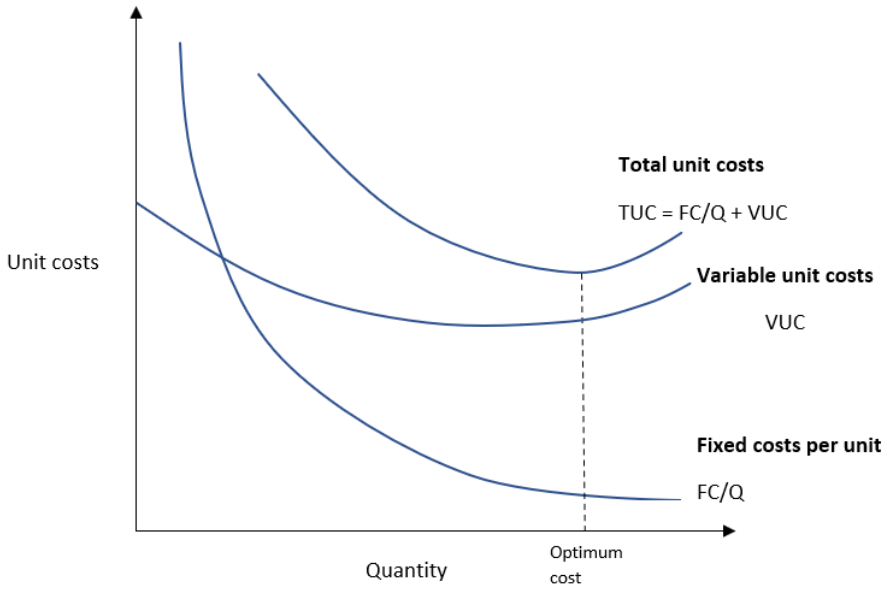

Figure 11: Total unit costs at varying quantity of output. The point of optimum cost on the total unit costs curve is at the minimum point.

3.2 Relevant and differential costs

In a decision-making process it is of importance that the decisions are based on real choices. To firmly grasp what the real choices are in the decision-making process, the knowledge of relevant costs is key. According to (Hoff and Helbæk, 2016, p. 395), the relevant cost is the increase in future total cost of an alternative, in addition to the alternative cost. In all decision-making processes, the relevant costs are the costs which are affected as a consequence of the decision-making. Costs that are unaffected by a decision are deemed irrelevant costs, and should not impact the decision-making. Similarly, costs that are present for all alternative decisions are deemed irrelevant. Furthermore, a sunk cost, or an irreversible cost that has already been incurred, should be deemed as an irrelevant cost. The reason being that costs already incurred are irrelevant when deciding what the future alternative should be. The future cost of each alternative should be the deciding factor

3.3 Circular economy and externalities

In 1968, Garret Hardin's article entitled "The Tragedy of the Commons" was published. The principal argument of the article, according to Graedel and Allenby (2015), is that "a society that permitted perfect freedom of action in activities that adversely influenced common properties was eventually doomed to failure". In his article, Hardin exemplifies his argument by describing overgrazing of a common pasture area which can be utilized by any herdsman. Each herdsman acts independently to maximize their own well-being and consequently concludes that adding

animals to their own herd would lead to an increased income in the short term. At some point the capacity of the pasture area is surpassed, and the overwhelming amount of animals lead to overgrazing. In the end, the pasture is destroyed and disaster strikes all (Graedel and Allenby, 2015, p. 2).

Hardin further explained in his article that the argument of the tragedy of the commons also can be made about pollution: "In a reverse way, the tragedy of the commons reappears in problems of pollution. Here it is not a question of taking something out of the commons, but of putting something in–sewage, or chemical, radioactive, and heat wastes into water; noxious and dangerous fumes into the air, and distracting and unpleasant advertising signs into the line of sight. The calculations of utility are much the same as before. The rational man finds that his share of the cost of the wastes he discharges into the commons is less than the cost of purifying his wastes before releasing them. Since this is true for everyone, we are locked into a system of "fouling our own nest," so long as we behave only as independent, rational, free-enterprisers" (Hardin, 1968). Hardin's focus in this statement is mainly directed towards local pollution like deposition of waste and chemicals in bodies of water and pollution of city air. These are examples of what Graedel and Allenby (2015) deem as "local commons" . Still, his argument is valid for the "global commons", which according to (Graedel and Allenby, 2015, p. 2) is "a system that can be altered by individuals the world over for their own gain, but, if abused, can injure all".

According to Riis (2018), externalities are the effects of individual choices on others in society. In other words, externalities can be deemed as third-party effects. Positive externalities occur when a party acts in a manner that profits other parties in the economy, whilst the acting party receives no compensation, and subsequently does not take into account when making decisions. On the other hand, negative externalities occur when a party acts in a manner that inflicts costs on other parties in the economy, whilst the acting party receives no burden, and subsequently does not take into account when making decisions (Riis, 2018, p. 288). A common example of a negative externality is the pollution that occurs when carbon dioxide is emitted as an industrial by-product without proportionate taxation.

Another definition of externalities is given by Laffont (2018): "Externalities are indirect effects of consumption or production activity, that is, effects on agents other than the originator of such activity which do not work through the price system. In a private competitive economy, equilibria will not be in general Pareto optimal since they will reflect only private (direct) effects and not social (direct plus indirect) effects of economic activity". Here, the argument related to Pareto optimality is introduced. According to Riis (2018), Pareto optimality or Pareto efficiency, is used as well to explain the concept of economical externalities. Pareto optimality is achieved when the individual preference criterion cannot be bettered for any party without negatively affecting at least one other party (Idsø, 2021). The economist who first introduced the concept of economic externalities, Arthur C. Pigou, argued that "negative externalities (costs imposed)

should be offset by a tax" (The Editors of Encyclopaedia Britannica, 2021). Consequently, such taxes were called "pigouvian taxes".

In 2008, Norwegian economist Agnar Sandmo described how pigouvian taxes lead to an internalization of the cost of negative externalities, in the form of marginal social damage, for a producer: "'Pigouvian taxes' is the generic term for taxes designed to correct inefficiencies of the price system that are due to negative external effects. In partial equilibrium terms, the basic idea can be presented as follows: under competitive conditions, utility-maximizing consumers will equate their marginal benefit to the market price Q; we may write this as MB = Q. Similarly, profit-maximizing producers will set their marginal private cost equal to the price, so that MPC = Q. In the absence of externalities, marginal private and social costs coincide: MPC = MSC. Consequently, market equilibrium implies that MB = MSC, which is the condition for efficient resource allocation. If there are negative external effects related to the production or consumption of the good in question, the marginal social cost is higher than the marginal private cost: MSC $>$ MPC. If the market prices facing producers and consumers are identical, this implies that MB $<$ MSC. To restore efficiency, we may levy a tax on the commodity, so that the consumer price is Q while the producer price is Q - t. In the new equilibrium we have that MB = Q and MPC = Q - t; it follows that MB = MPC + t. Since we wish the equilibrium to satisfy the condition that MB = MSC, we must have t = MSC - MPC, which we may define as the marginal social damage. Accordingly, the optimal Pigouvian tax internalizes the externality; producers act as if they took account of the marginal social damage associated with the production of the commodity" (Sandmo, 2018). Furthermore, Metz et al. (2007) states that: "An emissions tax provides some assurance in terms of the marginal cost of pollution control, but it does not ensure a particular level of emissions. Therefore, it may be necessary to adjust the tax level to meet an internationally agreed emissions commitment (depending on the structure of the international agreement). Over time, an emissions tax needs to be adjusted for changes in external circumstances, such as inflation, technological progress and new emissions sources" (Metz et al., 2007, p. 755).

The increased focus on the environmental footprint of carbon dioxide emissions is a result of international climate change mitigation efforts. In 2015 the Paris agreement was adopted by 197 countries at the COP21 in Paris (United Nations, 2021). The aim of the agreement is to reduce the emissions of global greenhouse gases in order to prevent a 2 °C increase in global temperature during this century, and preferably limit the increase to 1.5 °C (United Nations, 2021). The 197 countries who adopted to the agreement are still in the process of implementing the regulations which are necessary to achieve the ambitious 2 °C target.

In 2005 the European Union implemented a cap-and-trade system for carbon called the EU Emissions Trading System (ETS). The aluminium industry in the EU is one of the many industries which is part of this system. According to the European Commission (2015), "The EU ETS is a major tool of the European Union in its efforts to meet emissions reductions targets

now and into the future". Caps which limit the total volume of GHG-emissions, such as CO_2, are decided for the duration of specified periods in time (European Commission, 2015). By lowering the total cap for emissions, period by period, the industry as a whole must adapt to the requirement of lower emissions. Any actor which surpasses their allowed emissions may face a strict fine. As can be understood from the name, an integral part of the ETS is the trade of emission allowances. This trade enables the price which is paid by the actors to reflect the actual price of emitting carbon dioxide, and in addition it promotes the reduction of GHG-emissions where it is most profitable to do so. As is stated by the European Commission (2015), "Trading reveals the carbon price to meet the desired target. The flexibility that trading brings means that all firms face the same carbon price and ensures that emissions are cut where it costs least to do so". Furthermore, firms are allowed to save their allowances if they do not want to trade them. Therefore, a reduction of emissions in one part of the aluminium production process could enable savings in other parts of the process where allowances previously had to be bought. Though, this is a principle which is valid for all firms which are part of the ETS, not only the aluminium industry.

The Paris agreement is designed so that each country determines their contribution towards lowering their environmental footprint in what is named Nationally Determined Contributions (NDC) (United Nations Framework Convention on Climate Change, 2020). Every five years, each country is obliged to update their NDC. This is to ensure that the actions taken by each country remain ambitious. In February 2020, Norway updated their NDCs, stating that the "target is to reduce emissions with at least 50 %, and towards 55 % by 2030 compared to 1990 levels" (The Norwegian government, 2020). Taxation on carbon dioxide emission is an important governmental tool which is used to mitigate emissions. On January 8th 2021, a taxation increase from 590 NOK to 2000 NOK was proposed in the white paper, Meld. St. 13 (2020–2021)(2021), recommended by the Ministry of Climate and Environment. The updated NDC and the white paper underlines the trend of increasing taxation of carbon dioxide emissions. By increasing the taxes on emissions of carbon dioxide, the variable costs of operation is increased. Consequently, processes where less carbon dioxide is emitted become less expensive and possibly profitable. Although Norway is a comparatively small and progressive country with regards to the industrial sector, bigger economies, mainly in the European Union, are implementing measures such as taxation on emissions on CO_2 in order to mitigate GHG emissions (Plumer and Popovich, 2019).

The changes in policies and regulations on industries seen on a global scale which affects the environmental footprint, signifies a change towards a higher level of taxation of carbon dioxide. The cost of emitting carbon dioxide is gradually moving towards a level which internalizes the social cost on the "global commons", which is the environment, in a tax. This introduces a change in the cost calculations and must be assessed when a decision is to be made whether a change in the process, which reduces the amount of carbon dioxide, will be profitable or not. The target of such measures is to promote a change in the production pattern: towards

a greater degree of utilization of resources and recycling, and a lower degree of utilization of unsustainable materials.

4 Literature Review

4.1 Utilizing waste heat

On the topic of using process waste heat for industrial drying of by-products in the aluminium production process, there is no literature available. There are, however, many publications regarding utilization of surplus heat from the aluminium industry processes.

The human impact on the environment is apparent, and in an effort to reduce the emission of greenhouse gasses while enforcing better use of available resources, restrictions are being introduced by many emerging economic powers. Low temperature waste heat is a source of energy which could be exploited with the aim of reducing GHG-emissions. Low temperature waste heat (80-150 °C) in huge amounts is discharged into the atmosphere, and recovery of such heat for useful purposes is challenging (Clos et al., 2017, p. 783). In the Norwegian aluminium industry alone, around 1 TWh/y of heat is rejected as off-gas (Skjervold et al., 2020).

In the aluminium electrolysis, about half of the energy is lost as heat (Ladam et al., 2011, p. 393). Some energy recovery concepts involve redesigning the electrolysis cells by building in heat exchangers into the cell walls, as well as active cooling of the anode yokes (Ladam et al., 2011, p. 393). However, according to (Ladam et al., 2011, p. 397), heat collection from the flue gas is probably the energy recovery concept that has come closest to industrial implementation.

To enable the heat recovery from flue gas, heat exchangers can be used. In the aluminium industry, as well as in other industries, fouling in heat exchangers is a well known problem, according to Clos et al. (2017). Fouling in heat exchangers is depositions that accumulate on heat exchanger surfaces during operation. Fouling retards the heat exchanging capability and causes increased pressure loss and an increased pumping power requirement (Kazi, 2012). Skjervold et al. (2020) states that: "Metallurgical off-gas typically contains particles that can deposit on heat exchanger surfaces, therefore requiring specialized heat recovery solutions for robustness and consistent performance". According to (Clos et al., 2017), there are several available commercial solutions that aim to actively cool down the aluminium pot gas by the use of fouling-resistance enhanced heat exchangers. Notwithstanding the already available technology, Clos et al. (2017) states that the existing solutions are not at a satisfactory level with regards to efficiency. There are however efforts invested into improving the efficiency of heat recovery heat exchangers.

Nikolaisen et al. (2020) investigated cases where key design parameters of heat recovery heat exchangers were monitored with the target of minimizing the surface area. Results of their investigation proved "quite variable" case performance. In their study, Nikolaisen et al. (2020) found that: "When heat exchanger design was restricted by a conservative cross-sectional area ratio, the heat transfer surface area was shown to increase by a factor of three compared to an

"ideal" heat exchanger with a high degree of design freedom". Further, they found that designs that did not restrict the cross-sectional area ratio between the hot and cold sides of the heat exchanger required the least heat transfer area. Consequently, Nikolaisen et al. (2020) state that plate-and-fin type heat exchangers, like the heat exchanger design proposed by Skjervold et al. (2020), are worthwhile investigating further.

In the relevant literature, some thermodynamic cycles are proposed for converting waste heat into power. According to Ladam et al. (2011), Brayton cycles and Rankine cycles are the most relevant means of doing this. The study of surplus energy recovery by means of Rankine cycles is comprehensive, according to Nikolaisen and Andresen (2019). Wang et al. (2012) analysed the performance of organic Rankine cycle for power generation using aluminium reduction cell waste heat in the temperature range of 80°C-140°C, with design concepts involving several working fluids.

4.2 Dryer types

When determining what dryer type and what configuration should to be used, the physical characteristics of the material have to be considered. Whether a continuous or batch-wise drying process is preferred is also a factor in determining which dryer type is optimal. Another distinction, which has to be made, is whether the drying system should be designed for direct or indirect heating. In the following sections, a selection of dryer types are studied. These dryer types differ in distinct ways, presenting some of the main concepts within dryer design. Although the selected dryers which are evaluated cover a significant part of dryer technologies, there is a large amount of dryer technologies available and there are almost countless designs that are omitted from this section.

4.2.1 Rotary dryers

Rotary dryers consist of a cylindrical shell with internal flights which push the material upwards by means of rotation. Most of the drying takes place when the material falls down from the flights, where the convective heat transfer takes place. The dryers are usually angled so that the operation happens at an incline to help the progress of the material. Figure 12 is a sketch of what a rotary dryer could look like. The feed enters at the top and exits at the bottom of the cylindrical shell. The hot air can be entered into the rotary dryer in a cocurrent or countercurrent fashion.

Rotary dryers can be classified as direct, indirect-direct, indirect or special, varying with the heating transfer method used. The direct-heat rotary dryer is the most economical and simple type, and can be used when direct contact between the gas stream and the material is of no

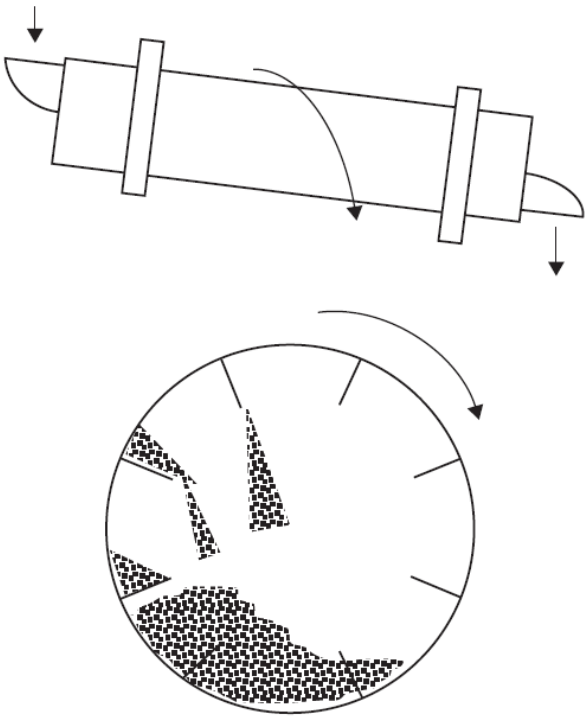

Figure 12: A sketch of a rotary dryer from the side (top), and the cross section (bottom) (Berk, 2008, p. 491).

harmful consequence (Mujumdar, 2007, p. 151-152). The rotary dryer is well suited to minerals and is used frequently in the chemical industry (Berk, 2008, p. 490). Mujumdar (2000) states that the rotary dryer is versatile, flexible and can have a high production rate. According to Wikipedia contributors (2020), rotary dryers "have many applications but are most commonly seen in the mineral industry for drying sands, limestone, stones and soil, ores, fertilizers, wood chips, coal, iron sulphate, filter cakes, sewage sludge, etc". A possible drawback with the rotary dryer is the difficulty of determining the particle residence time, according to Mujumdar (2000),

4.2.2 Drum dryers

Drum dryers are usually applied to dry viscous liquids, concentrated solutions, suspensions, slurries or pastes, according to Mujumdar (2007). Drum dryers have also been successful in drying sludge (Lecomte et al., 2004). On the other hand, a drawback of drum dryers is their lack of versatility with respect to the variety of products that they are able to process.

The drum dryer is a conductive type of dryer. Meaning that the materials are dried when in contact with the drum. In Figure 13, the principle of drum drying is visualized. The feed is sprayed onto the rotating drum. While the material is connected to the drum, it is dried conductively and transported to a doctor's blade, where it is scraped off the drum into sheets (Berk, 2008, p. 482-483). The sheets then fall into a trough or conveyor (Mujumdar, 2007, p. 210).

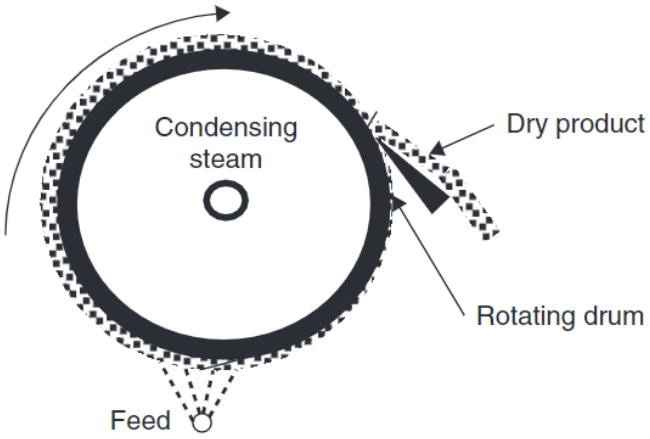

Figure 13: Sketch of a drum dryer with one drum (Berk, 2008).

4.2.3 Fluidized bed dryers

In a fluidized bed dryer (FBD), a high temperature gas stream is used to fluidize the particles that are to be dried. The material which should be dried is placed on a perforated distributor plate at the bottom of the drying chamber. A gas stream is passed through the bottom plate and the layer of the material so that the particles are fluidized. The gas, which is evenly distributed along the perforated bottom plate, envelopes the particles on its way upwards. This ensures a relatively large area of convective heat transfer, because the ratio of surface of each particle and the contact surface between the particles and the gas is high. FBDs can be operated continuously or batchwise, dependent on what is desired (Mujumdar, 2007, p. 174-178).

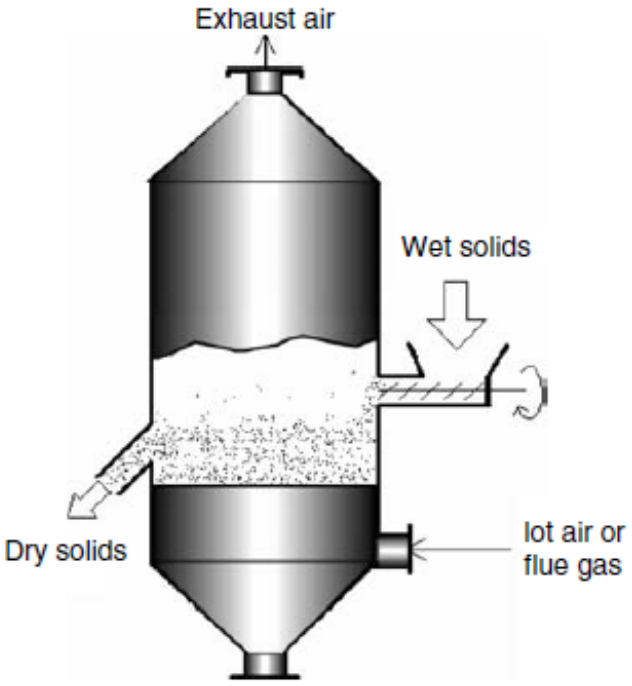

Figure 14: Continuous, well-mixed type of FBD where the feed is continually fed into the drying chamber. Although this type of dryer does not guarantee a completely dry product, it shows the basic set up of a variant of FBD (Mujumdar, 2007, p. 184).

There are many types of FBDs, and each type handles specific materials better than the other. This may be one of the reasons why FBDs are able to handle a wide range of materials. According to Mujumdar (2007), FBDs "are commonly used in processing many products such as chemicals, carbohydrates, foodstuff, biomaterials, beverage products, ceramics, pharmaceuticals in powder or agglomerated form, healthcare products, pesticides and agrochemicals, dyestuffs and pigments, detergents and surface-active agents, fertilizers, polymer and resins, tannins, products for calcination, combustion, incineration, waste management processes, and environmental protection processes". Mujumdar (2007) also states that FBDs "are used extensively for the drying of wet particulate and granular materials that can be fluidized, and even slurries, pastes, and suspensions that can be fluidized in beds of inert solids".

Not all particles are easily fluidized. Geldart recognized this and created the Geldart classification for powders (Geldart, 1973). This classification is based on fluidization quality of dry particles and divides fluidization of powders in four categories where the behaviour of particles in each group is related to the interparticle forces of the powder (Yehuda and Kalman, 2020). In Figure 15, the fluidization regime map is visualized. Group A particles - aeratable particles - are easily fluidized when dry. Group B particles - sandlike particles - are also easily fluidized when dry. Group C particles - cohesive particles - are hard to fluidize when dry. Group D particles - spouted particles - are fluidizable by means of spouted bed fluidization, but are difficult to fluidize.

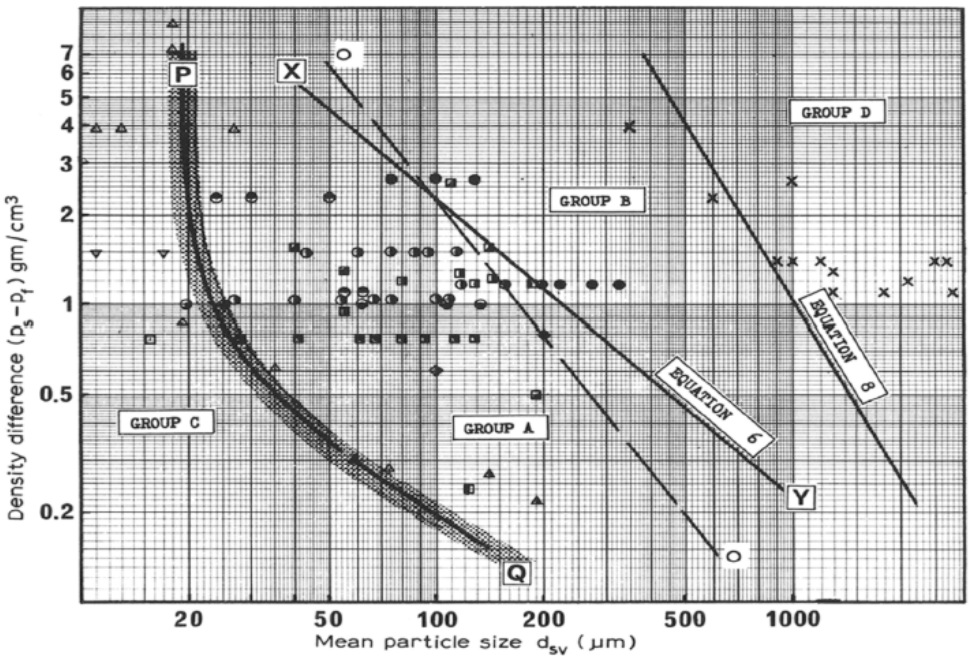

Figure 15: Powder classification diagram for fluization by air (Geldart, 1973).

4.2.4 Spray dryers

In spray drying systems, the material is atomized by a device, either a nozzle or some kind of atomizer (rotary disc atomizers are the most common), and sprayed into hot gas which dries the material. In Figure 16, a comprehensive sketch, from Mujumdar (2007), presents the main features of both a wheel atomizer and a nozzle layout. Spray dryers are used in a wide range of industries and for many different products. Some of these industries and products, according to (Mujumdar, 2007, p. 216), include:

- Chemical industry, e.g., phenol–formaldehyde resin, catalysts, PVC emulsion-type, amino acids, etc.
- Ceramic industry, e.g., aluminium oxide, carbides, iron oxide, kaolin, etc.
- Dyestuffs and pigments, e.g., chrome yellow, food color, titanium dioxide, paint pigments, etc.
- Fertilizers, e.g., nitrates, ammonium salts, phosphates, etc.

Other industries and products include the pharmaceutical and the biochemical industry, environmental pollution control and food and foodstuffs industry, where the drying of milk is a process in which spray dryers often are the preferred choice.

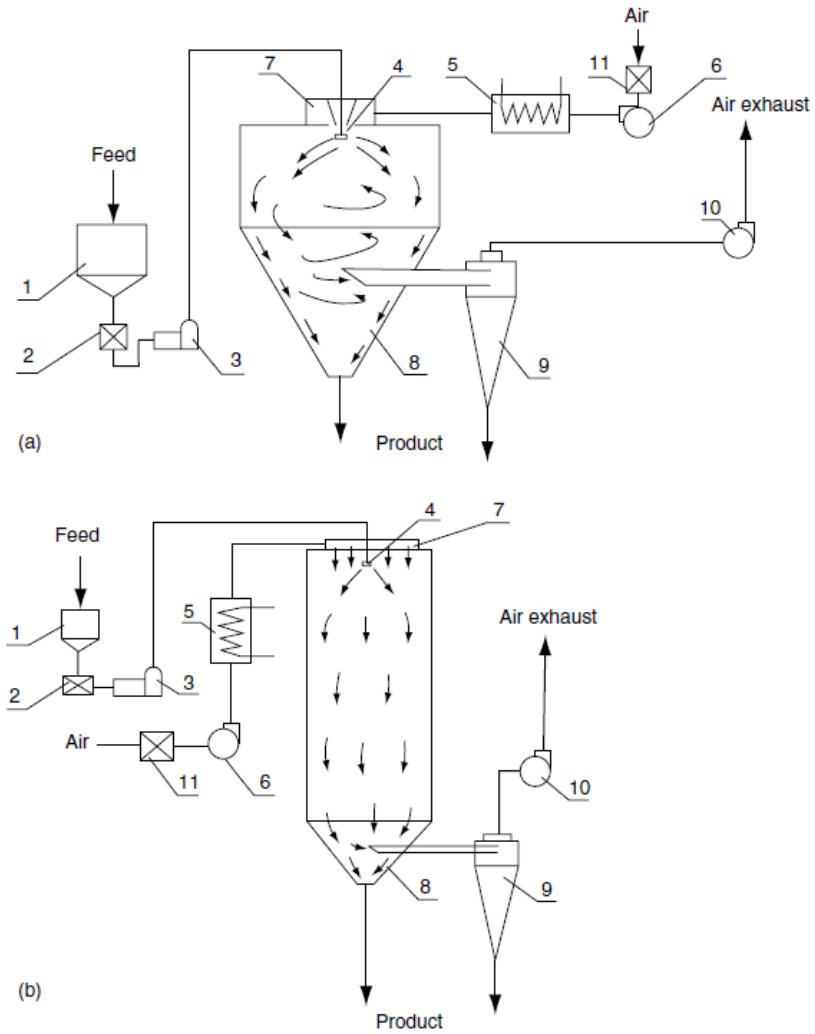

Figure 16: "Spray dryer layout: (a) with wheel atomizer; (b) with nozzle atomizer; (1) feed tank; (2) filter; (3) pump; (4) atomizer; (5) air heater; (6) fan; (7) air disperser; (8) drying chamber; (9) cyclone; (10) exhaust fan"(Mujumdar, 2007, p. 227).

4.2.5 Benefits and drawbacks of some dryer types

In Section 4.2, some dryer technologies have been presented, and here the main benefits and drawbacks of each type are shortly presented:

Rotary dryers:

- Benefits
  - High versatility.
  - Handles both direct and indirect heat.
  - Well suited to the materials in question.
- Drawbacks
  - High rate of particle entrainment.

Drum dryers:

- Benefits
  - Good at handling pastes and slurries.
- Drawbacks
  - Does not have a wide range of products that it can handle.
  - Does only operate at indirect heat.

Fluidized bed dryers:

- Benefits
  - High rate of moisture removal.
  - High thermal efficiency.
- Drawbacks
  - High pressure drop.
  - High electrical consumption.
  - Poor fluidization qualities of some products.

Spray dryers:

- Benefits
  - Good at handling heat sensitive products.
  - Excels at drying liquids.
  - Ability to control particle size of product.
- Drawbacks
  - High installation costs.
  - Lower thermal efficiency.
  - Works mainly for pumpable fluid feeds, but is limited to that.

5 Heat Sources

In the energy balance of the Alcoa Mosjøen plant from Appendix A, the electric energy input into the electrolysis of the plant is given as 2 996 717 MWh per year (8760 hours). This resulted in a total output of around 232 thousand tonnes of aluminium. Although, since the Hall-Héroult process was invented in 1886 there have been steady trends towards a lower specific heat consumption, about half of the energy spent in aluminium electrolysis is lost as heat (Ladam et al., 2011, p. 393).

While utilising waste heat from the electrolysis cell could, in theory, lead to improved efficiency, the complex heat balance of the cell makes it virtually impossible to do so without re-designing the cell. As mentioned earlier, in Section 4.1, designs integrating heat exchangers into the electrolysis cells are being investigated, but those designs are not considered for the purpose of this thesis. According to (Grjotheim and Kvande, 1993, p. 235): "An alumina reduction cell loses a characteristic amount of heat to its surroundings, depending upon its design and thermal insulation. Excessive insulation will prevent the formation of ledge on the side walls and may lead to erosion and early lining failure. On the other hand, if the insulation is insufficient, the ledge may grow so thick that it will be difficult to change anodes. Too little insulation in the bottom of the cell may lead to excessive ledge that covers part of the cathode, and therefore it interferes with the transport of current and the metal and electrolyte movement." This underlines the fact that the heat balance and the size of the side ledge in the Hall-Héroult cell are related and complex variables that could be altered by changing the ambience of the process.

While some of the lost heat is necessary for keeping the bath and the metal molten and at operational temperatures, the geometry of the cell is unfavourable with regards to heat loss. In Figure 17, the heat loss distribution of the cell is shown. According to (Grjotheim and Kvande, 1993, p. 27), only about 20% of the heat produced is actually used for the production of aluminium. So the rest of the heat, i.e. the energy which is not used directly in the process and which is not strictly necessary for keeping the ledge within the operational limits, can be counted as waste heat.

According to (Grjotheim and Kvande, 1993, p. 26): "Optimum thermal insulation of the cathode will save energy. However, in order to maintain a ledge of frozen electrolyte on the side walls of the cathode to protect them from erosion by the bath and metal, the wall insulation must be adjusted to extract a certain amount of heat loss. A proper heat balance is therefore critical to the design of an alumina reduction cell." To consider utilizing surplus heat directly from the electrolysis cells themselves would consequently be hazardous without re-designing the cell. Thus, a direct heat recovery from the electrolysis is not feasible. However, the pot gas of the electrolysis cell is a high temperature gas stream, which could be utilized.

The exhaust gas from the anode baking part of the plant at Mosjøen is also a gas stream which

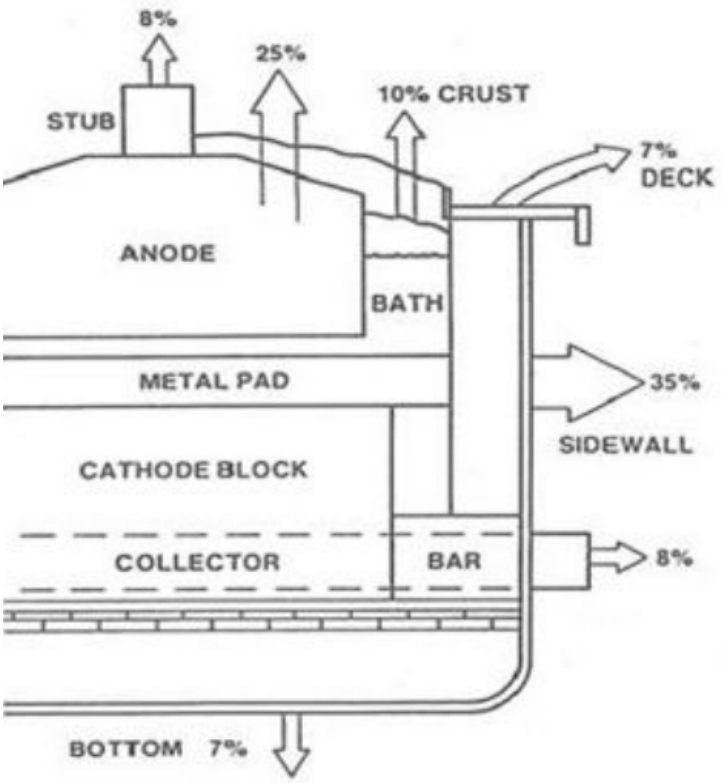

Figure 17: "Typical Hall-Héroult cell heat loss distribution" (Grjotheim and Kvande, 1993, p. 28).

is suited for energy recovery. When the anodes are baked in the ring furnace, they are heated using liquefied natural gas (LNG). At the moment, the petroleum coke used in the anode baking process does not undergo a drying treatment before being used in the baking process. Consequently, the energy expended by burning LNG, turning the moisture in the petroleum coke into vapour, would be replaced by expending process surplus heat.

Shipments of petroleum coke with more than a moisture content of 0.3 % wet basis arrive sporadically. However, the moisture content of the petroleum coke is required to be no more than 0.3 % wet basis, and preferably lower. A higher initial moisture content will adversely affect the quality of the anodes. According to Appendix A, the annual consumption of green anode petroleum coke is around 220 000 tonnes per year. So, even though the moisture content is small, there is a large amount of water to be removed. Around 0.3%, or 660 tonnes of water per year is removed by means of burning LNG. Per annum, 40 tonnes of anode mass is recovered. The anode mass is re-introduced in small amounts into the process without being dried. The moisture content of the anode mass is measured to be around 31.41% wet basis. Hence, approximately 12.6 tonnes of water must be removed by means of burning LNG. In addition, the solid components of the materials are heated by means of burning LNG. Thus, the approximately 219 340 tonnes of petroleum coke and 27.4 tonnes of anode mass must be heated.

Assuming that the latent heat of vaporization of the water is equal to $\Delta H_{vap} = 2256.4$ kJ/kg,

Table 3: Heat source specifications for the exhaust gas from the anode baking.

Anode baking exhaust gas	Unit	Value
Fluid	[-]	"Air Equivalent"
Average temperature	[C°]	190
Average ambient temperature	[C°]	7
Mass flow	$[\frac{Nm^3}{h}]$ $[\frac{Nm^3}{s}]$	185000 51.389
Pressure	[atm]	1

the energy required to heat 1 kg of water from 7 to 100 °C is $Q = 395.25$ kJ, the energy of heating 1 kg of petroleum coke and anode mass from 7 to 100 °C is $Q = 79.05$, the the lower heating value of methane is $LHV = 50$ MJ/kg, and the specific CO_2-emission of methane gas is $\frac{kg_{CO_2}}{kg_{CH_4}} = 2.75$ kg/kg. Thus, 382.488 tonnes of methane, which equates to 1051.842 tonnes of CO_2-emissions is saved. Comparing this to the total input of LNG in the anode baking process, which is 13 500 tonnes per year, the reduction equates to 2.83 %. The same relative decrease of total yearly CO_2-emissions, which in absolute terms equate to 1051.842 tonnes, from the anode baking process could be reduced, in theory, by utilizing the existing surplus heat of the plant.

Table 2: Heat source specifications for the pot gas from the electrolysis.

Electrolysis pot gas	Unit	Value
Fluid	[-]	"Air Equivalent"
Average temperature	[C°]	130
Average ambient temperature	[C°]	7
Mass flow	$[\frac{Nm^3}{h}]$ $[\frac{Nm^3}{s}]$	1600000 444.44
Pressure	[atm]	1

The pot gas output from the electrolysis and the exhaust gas from the anode baking are promising candidates as heat sources in the drying process. In Appendix A, the energy balance and energy streams in the aluminium plant of Alcoa in Mosjøen is tabulated. In Table 2 and Table 3, some key values regarding these flue gas streams are tabulated.

As the mass flows are given as volumetric flow in normal cubic meter, they are converted to real conditions to determine the heat in each stream. Normal cubic metres is a unit of quantity which has a reference temperature of $T = 273.15$ K and pressure of $p = 1$ atm. To convert the temperature and volume in normal conditions to real conditions, Charles's law is used. It can be written as:

$$\frac{\dot{V}_1}{\dot{V}_2} = \frac{T_1}{T_2} \tag{16}$$

Where T[K] is temperature, and $\dot{V}$ $[m^3/h]$ is volumetric flow . The subscripts 1 and 2 are for normal and real conditions respectively.

Hence, to get the volumetric flow at real conditions, the following relation is used:

$$\dot{V_2} = \dot{V_1} \cdot \frac{T_2}{T_1} \tag{17}$$

Where $\dot{V_2}$ $[m^3/h]$ is volumetric flow at real conditions. Dividing by 3600 the volumetric flow per second is obtained.

Using the density of air, ρ, and the heat capacity of air, c_p, at the respective temperatures of each stream and assuming that the temperature difference, ΔT, of each gas stream is between the temperature of the stream and ambient temperature at 7 °C, the theoretical available waste heat amount of each stream is determined as:

$$\dot{Q} = \dot{V_2} \cdot \rho \cdot c_p \cdot \Delta T \tag{18}$$

Where $\dot{Q}$ has dimensions kW because the dimensions of ρ and c_p are $\frac{kg}{m^3}$ and $\frac{kJ}{kg \cdot K}$

Table 4: The calculation of the available heat from the exhaust of the anode baking and the pot gas from the electrolysis. Heat capacity is found using an air density calculator at Engineering Toolbox (2003), while the specific heat of air is found using an online air properties calculator by Berndt Wischnewski (2007).

	Anode baking	Electrolysis
$\dot{V_1}$ $[\frac{Nm^3}{h}]$	185000	1600000
$T_1[K]$	273.15	273.15
$T_2[K]$	463.15	403.15
$\dot{V_2}[\frac{Nm^3}{h}]$	313683.9	2361486.4
$c_p[\frac{kJ}{kg \cdot K}]$	1.02441	1.01561
Δ T [K]	183	123
$\rho[\frac{kg}{m^3}]$	0.761	0.876
$\dot{Q}[kW]$	12430.8	71782.4
$\dot{Q}[MW]$	12.4	71.8

In Table 4, the heat of both gas streams are calculated using the aforementioned expressions. From the last row, it is concluded that the theoretical waste heat output from the anode baking process is $\dot{Q} = 12.4$ MW. From the electrolysis, the theoretical process waste heat output on a yearly average is estimated to be $\dot{Q} = 71.8$ MW.

6 Experiments

Aluminium oxide, anode mass and petroleum coke was sent from the Alcoa plant in Mosjøen. It was vacuum packed during transport, so that the moisture content of the samples in the lab would be equal to the moisture content of the material in the plant. The two goals with the experiments were to:

1. Determine the moisture content and water activity of the materials.
2. Measure the dry weight of the materials.

6.1 Method

The drying experiments were carried out by drying at 150 °C and 105 °C in a VWR DRY-Line Drying Oven DL53 with natural convection, which is pictured in Figure 18. The first experiment could have been conducted in an environmental chamber by measuring water activity at different equilibrium moisture contents. However, the environmental chamber was out of order for an extended period, so other alternatives were used to conduct experiments as a consequence.

Figure 18: VWR DRY-Line Drying Oven DL53 with natural convection.

The first experiment was decided to be a measurement of water activity and weight reduction of moisture content at intervals of 15 minutes. The total duration of the experiments was decided at 75 minutes in the first experiments, but was later changed to 120 minutes in order to be sure that the whole drying process was captured. At a later stage of the experiments, when the temperature in the experiment was 105 °C, the interval was changed to from 15 to 30 minutes. In those instances, the total duration of the experiment was extended so that the whole process

could be captured. After each interval, a sample of each material was removed from the drying oven, then weighed, and about a teaspoon of each material was hermetically sealed in a plastic container and left to equilibrate overnight. This was done so that moisture which potentially was bound in the particles would have time to be transported to the surface. After the samples had reached equilibrium, the water activity at each point in time was measured. In this manner, corresponding measurements of weight and water activity were obtained.

In the second experiment, the dry weight of each material was measured. During the measurement of the dry weight of the solids, the samples were taken out of the drying oven and weighed in intervals of 15 minutes during the first two hours. After the initial two hours, the interval was extended to 30 minutes. After 4.5 hours, the samples were not weighed until the day after. Thus, they had a total residence time of approximately 23 hours in the drying oven. The measurements of weight were carried out using a Mettler Toledo - Precision Balance ME4002 weight, from Figure 19, which has 0.01 g readability (Mettler Toledo, 2012). In some instances, this weight did not have sufficient readability. Consequently, the Mettler AE260 DeltaRange which has a readability of 0.0001 g (Mettler Instruments AG, 1987) was utilized in some instances.

Figure 19: The weights: Mettler Toledo - Precision Balance ME4002 (left); and Mettler AE260 DeltaRange (right), were used in the experiments.

The samples were prepared on aluminium discs that were placed in the drying oven. When a sample was removed from the drying oven, the weight of the sample, m_{sample}, was measured immediately. After that, the samples were hermetically sealed in plastic containers, before being left to equilibrate. Using the AquaLab water activity meter, the water activity, a_w was measured. The AquaLab 4TE, from Figure 20, was used for measuring water activity of the materials. It has an accuracy of $\pm$ 0.003a_w, according to (Meter Group Inc., 2018, p. 5). In addition, (Meter Group Inc., 2018, p. 6) states that measured values of $<$0.03 a_w indicates that samples are too dry to be measured accurately. This was the case for the dry aluminium oxide.

Figure 20: The water activity meter, AquaLab 4TE, was used in the experiments.

6.1.1 Size of samples

Each sample was in the shape of a disc with a diameter of approximately $r = 9.8$ cm and thickness of approximately $d = 7$ mm. When preparing each sample, a large amount of material was filled in each disc and the excess was scraped off from the top using a knife blade. The intention behind this was to ensure uniformity in size with a flat top of each sample. In Figure 21, a tray of samples from the first experiment is shown. From the figure, it is evident that the petroleum coke particles (to the right) are not equal in terms of size. The particle size varied from fine powder to the size of pebbles of several millimetres. As a consequence of this variation in size, these samples were uneven and not as flat on the top as the other samples.

Figure 21: Tray of samples. On the left side, aluminium oxide. In the middle is anode mass. To the right is petroleum coke. This tray is from the first experiment where weight and water activity was measured at 15 minute intervals.

7 Results and Discussion

From the experiments, the dry weight of the aluminium oxide, anode mass and petroleum coke was measured. In addition, drying curves were obtained for the three materials. There were also measurements of moisture ratio and water activity of all three materials at T = 150 °C.

7.1 Drying curves

Drying curves were obtained for the aluminium oxide and anode mass. In Figure 22 the water content in the aluminium oxide, measured in grams, is plotted as a function of time. It is apparent from the figure that the rate of drying was constant the first 60 min, because of the linear behaviour of the curve in this interval. After 60 min, the drying rate decreased. In the interval between 60 min and 90 min, the curve is almost linear. After 90 min, the curve flattens more, before the material eventually was at equilibrium moisture content and the curve is completely flat. Within the first 15 min, the drying curve is not quite as steep as the rest of the first 60 min, probably owing to the heating of the product. The measurements of weight were only taken every 15 min, thus the point of where the real rate change begins is not known. In spite of this, the three changes in slope could be interpreted as phases that correspond with the theory from Section 2.1 describing the constant drying rate and falling rate phases.

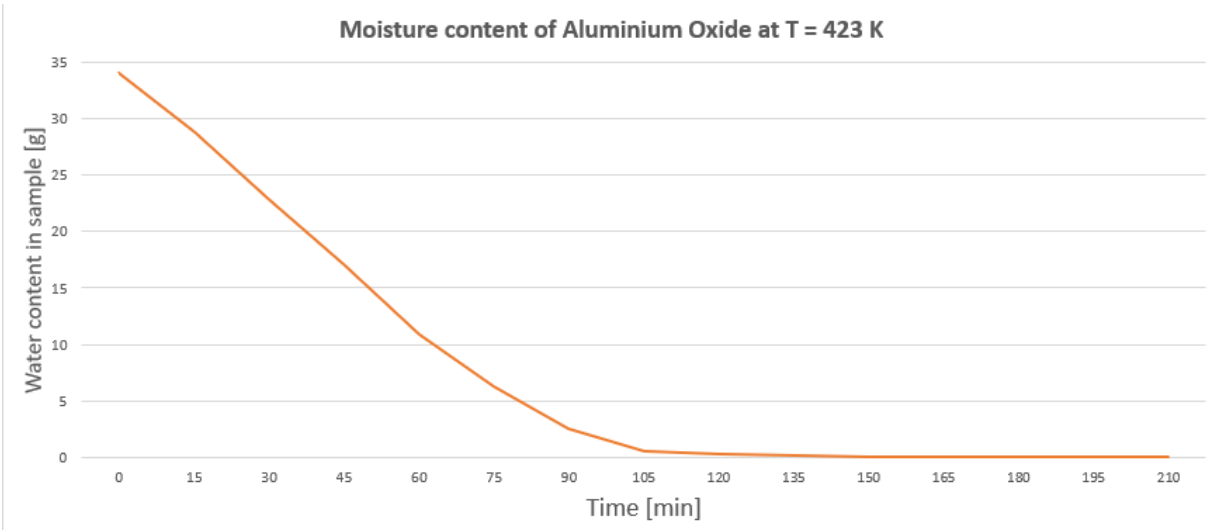

Figure 22: Drying curve of Aluminum Oxide at 150 °C.

In Figure 23, the water content in the anode mass, measured in grams, is plotted as a function of time. From the figure it can be observed that most of the water is removed during the constant drying rate period. From the beginning and until 45 min, the rate of drying was constant. The heating of the product, which occurs in the first interval, was not noticeable when studying the drying curve of the anode mass. Between 45 and 60 min, the slope of the curve is slightly less steep. After 60 min there is a quite sharp flattening.

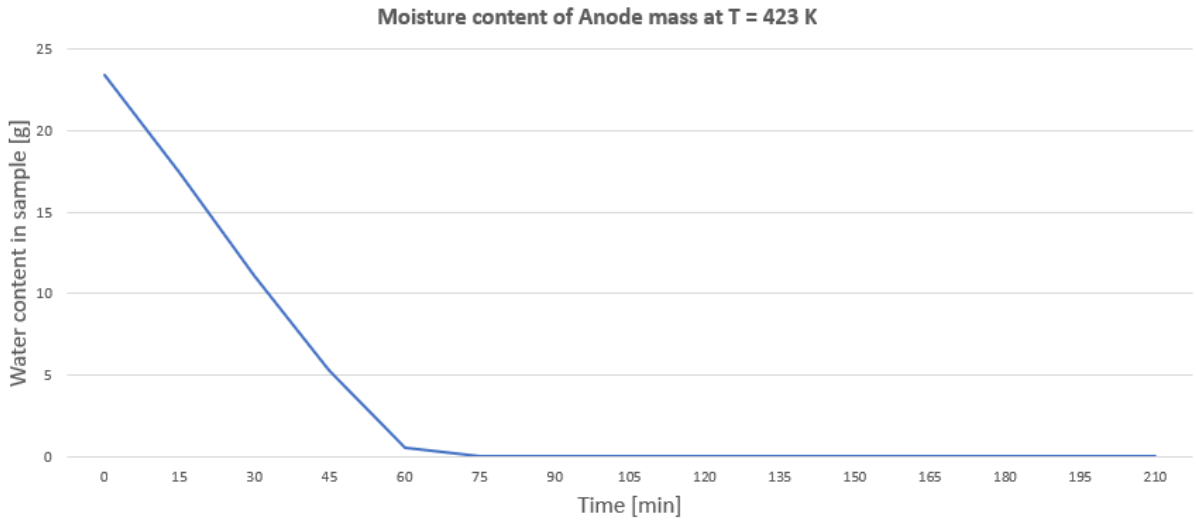

Figure 23: Drying curve of Anode Mass at 150 °C.

Comparing the drying curves of aluminium oxide in Figure 22 and anode mass in Figure 23, it is evident that both drying processes were mainly taking place in the constant drying rate phase. During the first fifteen minutes, the temperature of each product was increased from ambient temperature of approximately 22 °C to 150 °C. In this stage the heat transfer was not at a steady state yet. This effect was most evident for the anode mass, which had a more noticeable change in slope after 15 min. Both curves can be divided into a constant drying rate phase, and two falling rate phases. From both figures, it is evident that the change in slope is only slight, and most of the water has been evaporated before a significant flattening occurs. Hence, the approximation made in the calculation on heat demand in drying that all of the drying happens in the constant rate drying period, is further supported as a fair approximation.

In Figure 24, the drying curve of petroleum coke is illustrated. The water content, in grams, is plotted as a function of time. A noticeable difference in the amount of water which was dried off can be observed by comparing the drying curve of the petroleum coke to the drying curves of the two other materials. As the petroleum coke initially had a water content of approximately 0.1% wet basis, it was comparatively close to being bone dry from the beginning. Due to the fact that the petroleum coke contains almost no water, the heating period of the material was not long. In the sample of anode mass, there was 23.43 g of water before drying, while in the petroleum coke there was only 0.0266 g of water present at the beginning of the experiment. Both materials consist mainly of carbon. The fact that the thermal capacity of carbon is lower than the thermal capacity of water, combined with the high ratio of surface area between the granular particles of petroleum coke and air, meant that the petroleum coke samples were heated quite rapidly. Hence, more of the drying process took place during the first fifteen minutes compared to the drying process of the anode mass.

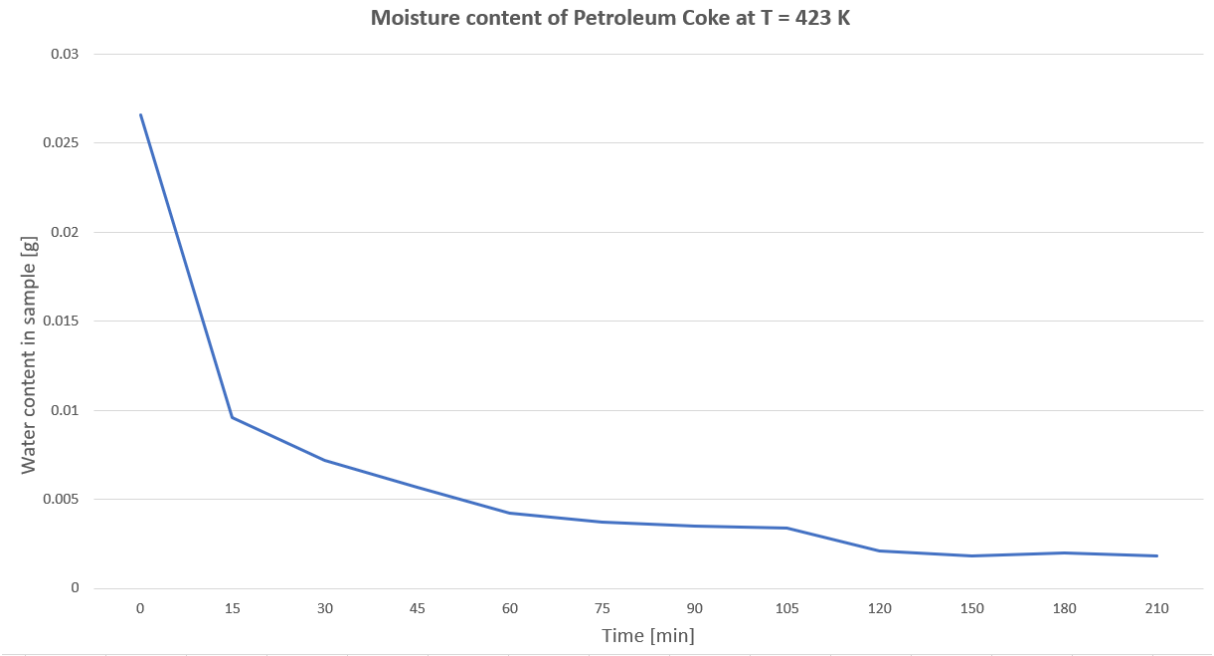

Figure 24: Drying curve of petroleum coke at 150 °C.

Table 5: Dry weight and water activity measured after approximately 23 hours of residence time.

	Initial weight [g]	Dry weight [g]	Water content [% wet basis]	Water activity, a_w, after 23 hours at 150 °C
Aluminium oxide	90.66	56.60	37.57	0.0295
Anode mass	74.59	51.16	31.41	0.1369
Petroleum coke	25.1261	25.0995	0.1059	0.3839

In Table 5, some of the key values obtained in the dry weight measurement are tabulated. The initial weight along with the final weight, which is assumed to be the dry weight, is given. As mentioned, the dry weight is the weight which was obtained after approximately 23 hours of drying at 150 °C. The water activity corresponding to each sample is also tabulated. In the table, water content is calculated as the difference between the initial and the dry weight divided by the initial weight. Thus, the wet basis moisture content is used. The dry basis moisture content and wet basis moisture content of the solids can be calculated using these expressions:

$$M_d = \frac{W_w}{W_d} * 100 \tag{19}$$

$$M_w = \frac{W_w}{W_d + W_w} * 100 \tag{20}$$

Here, M_d [% db] is dry basis moisture content, M_w [% wb] is wet basis moisture content, W_w [kg] is the weight of water in the solid and W_d [kg] is the weight of dry matter. For reference, the dry basis moisture content of the aluminium oxide and anode mass was 60.2 and 45.8 [% db] initially.

The water activity measured after 23 hours of drying for the aluminium oxide was below the threshold of detection of the AquaLab 4te. Thus, it can be assumed that the material was bone dry. The measured water activity for anode mass and petroleum coke was above this threshold. This could be an indication that there was still water present in the product in the form of bound moisture. It could also be a consequence of the sensitivity to moisture of the AquaLab 4te.

7.2 Water activity and moisture ratio

The information of water activity and weight, combined with initial water content and dry weight, was used to derive the moisture ratio, MR, at each measurement point. The moisture ratio is defined as the ratio of moisture content to the initial moisture content of the solid at any point in time, normalized on the total difference in relative weight at the initial moisture and bone dry conditions:

$$MR = \frac{\frac{m_{sample}}{m_{init}}}{1 - \frac{m_{dry,init}}{m_{dry}}} \tag{21}$$

Here, m_{sample} [g] is the weight of the material in a sample after being dried, m_{init} [g] is the initial weight of the material in the same sample when it is at initial moisture, $m_{dry,init}$ [g] is the initial weight of the sample which is used to measure the dry weight of the material, and m_{dry} [g] is the weight of the sample when the dry weight of the material was reached. The ratio in the denominator is recognized as the dry basis moisture content of the material. The reason for using the moisture ratio is that the samples used in this experiment were of different initial weight. Therefore, there was a need to normalize the weight reduction of each sample to apply the values in the same figure.

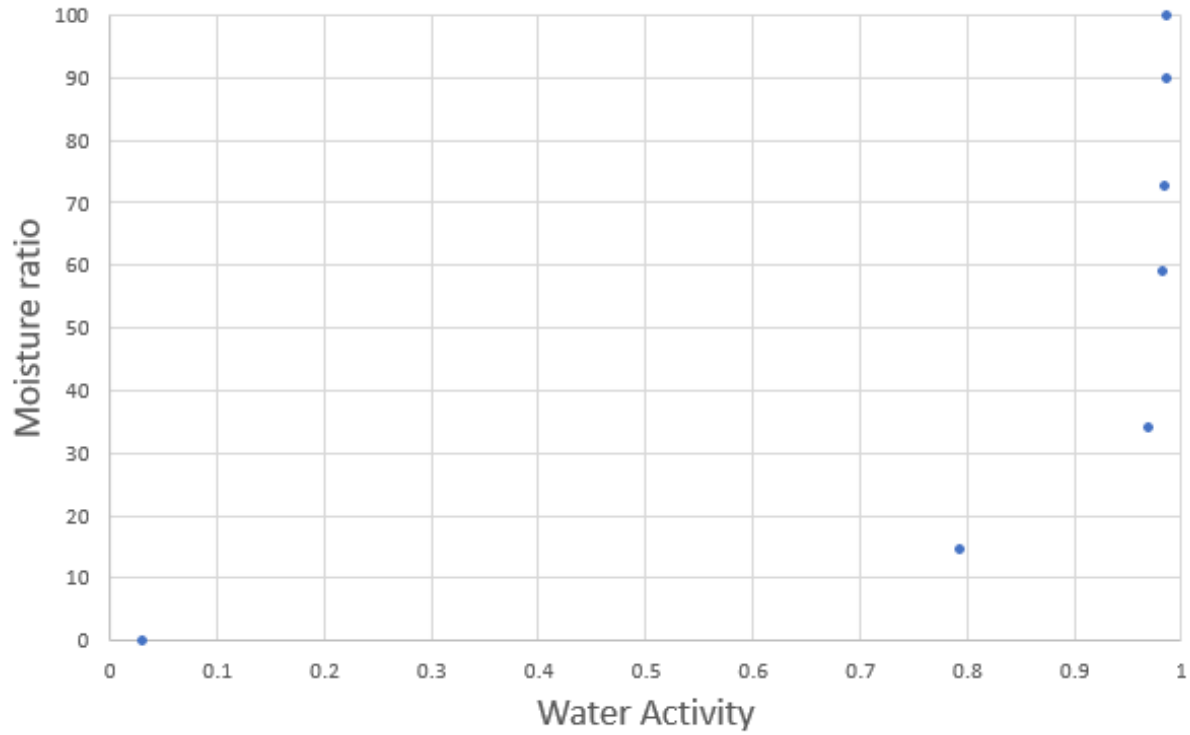

Figure 25: Moisture ratio, MR, and Water Activity, a_w, of Aluminium oxide at Temperature T = 150 °C.

In Figure 25 and 26 the moisture ratio and water activity is plotted for the aluminium oxide. While the values of Figure 25 were measured at 150 °C, the values of Figure 26 were measured at 105 °C. Both of the figures show that the initial reduction in moisture ratio was not accompanied by a similar reduction in water activity. In Figure 25, e.g., the water activity was only reduced from 0.9858 to 0.9681 while 66% of the moisture content is lost. The high rate of reduction in moisture ratio per reduction in water activity supports the assumption that there is a high proportion of free water in the product.

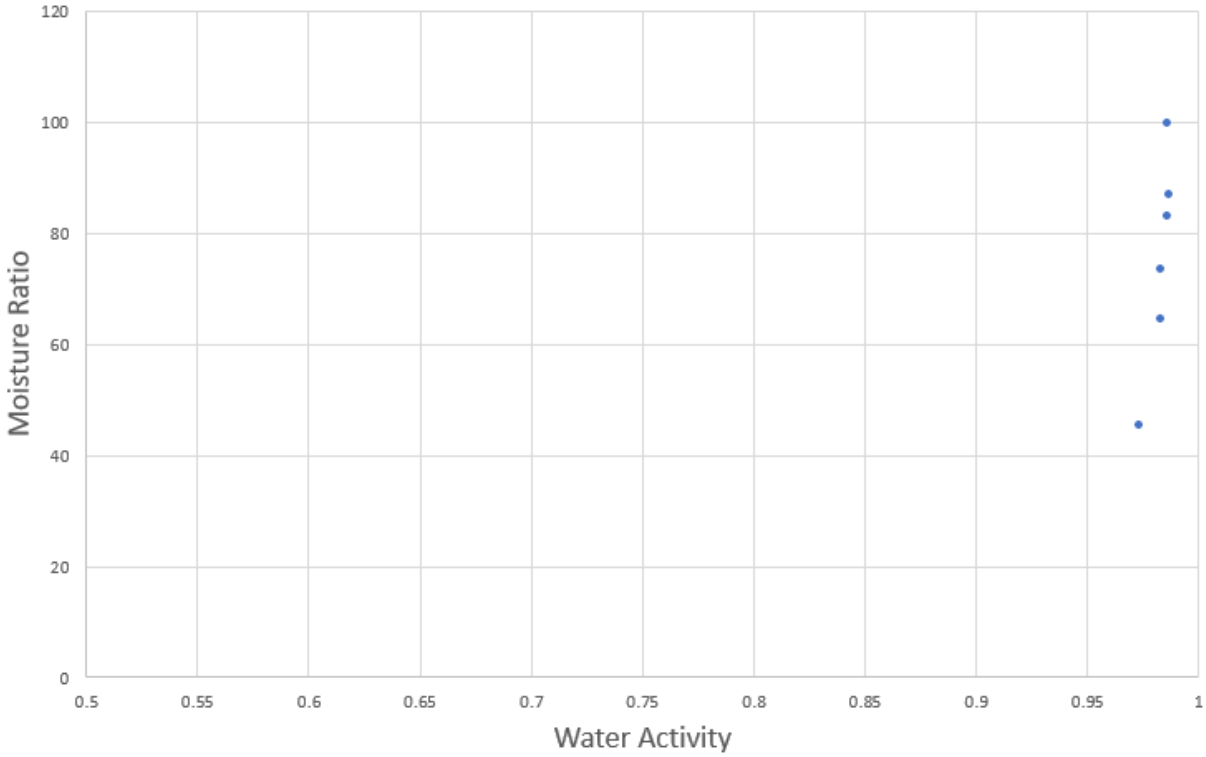

Figure 26: Moisture ratio, MR, and Water Activity, a_w, of Aluminium oxide at Temperature T = 105 °C.

From Figure 26, it can be observed that values of moisture ratio and water activity follow the same pattern as in Figure 25, and the same deduction can be made about unbound water being present in the material. However, as the experiment was conducted over a period of 75 min in total, the drying process had not yet reached a stage where the product was close to dry weight. Thus, the figure proves that the experiment should have been extended by several minutes. It should also be noted that the x-axis is defined from 0.5 to 1 in Figure 26.

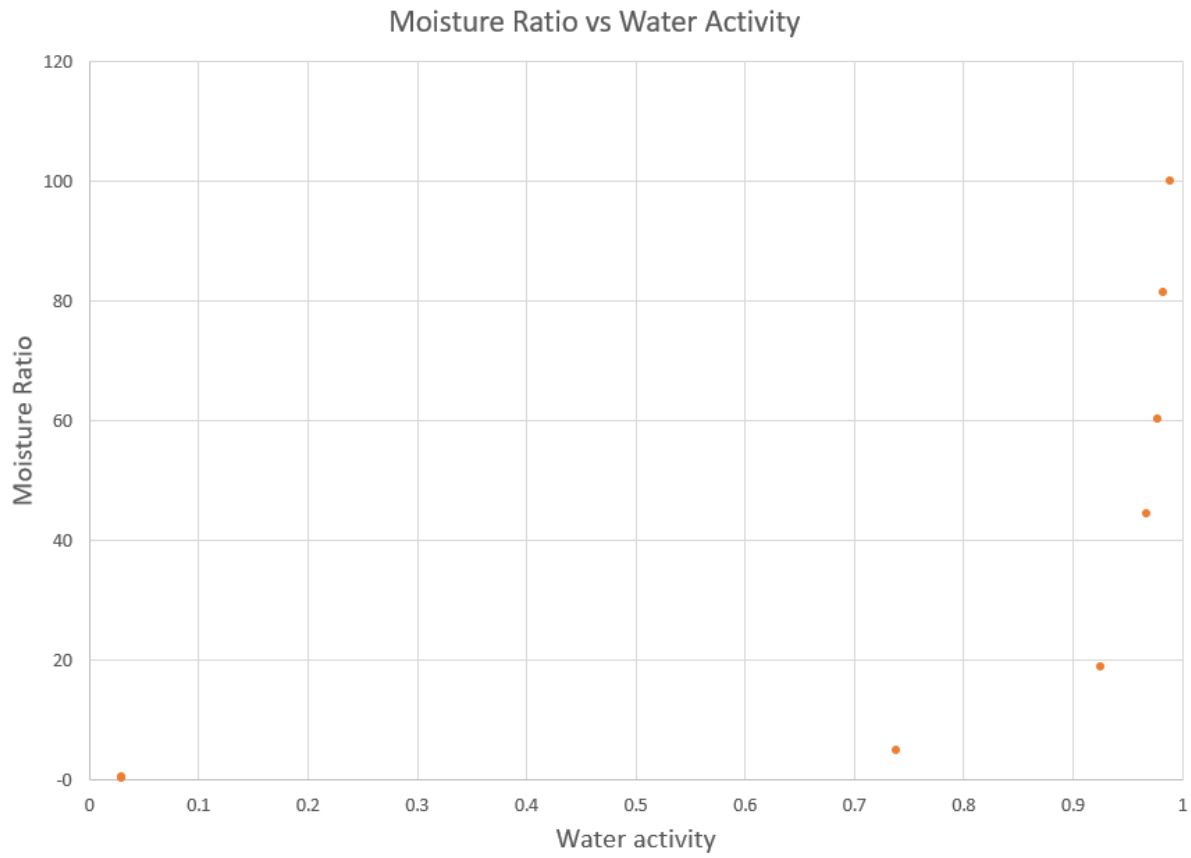

Figure 27: Moisture ratio, MR, and Water Activity, a_w, of Aluminium oxide at Temperature T = 105 °C. The interval length between each point is extended to 30 min in order to fully capture the drying process.

The experiment was repeated with the aim of rectifying the errors which are highlighted in Figure 26. The interval between each measurement was extended from 15 min to 30 min. In addition, the total time of the experiment was increased from 75 to 240 min. In Figure 27, the results of the extended experiment is illustrated. The expected decline in moisture ratio which was not completed in Figure 26 can be observed. In the last three measurement points, the water activity was below the threshold of the water activity meter. Thus, it took between 150 and 180 min for the aluminium oxide to reach a wet basis moisture content of 0 % and water activity equal to 0.

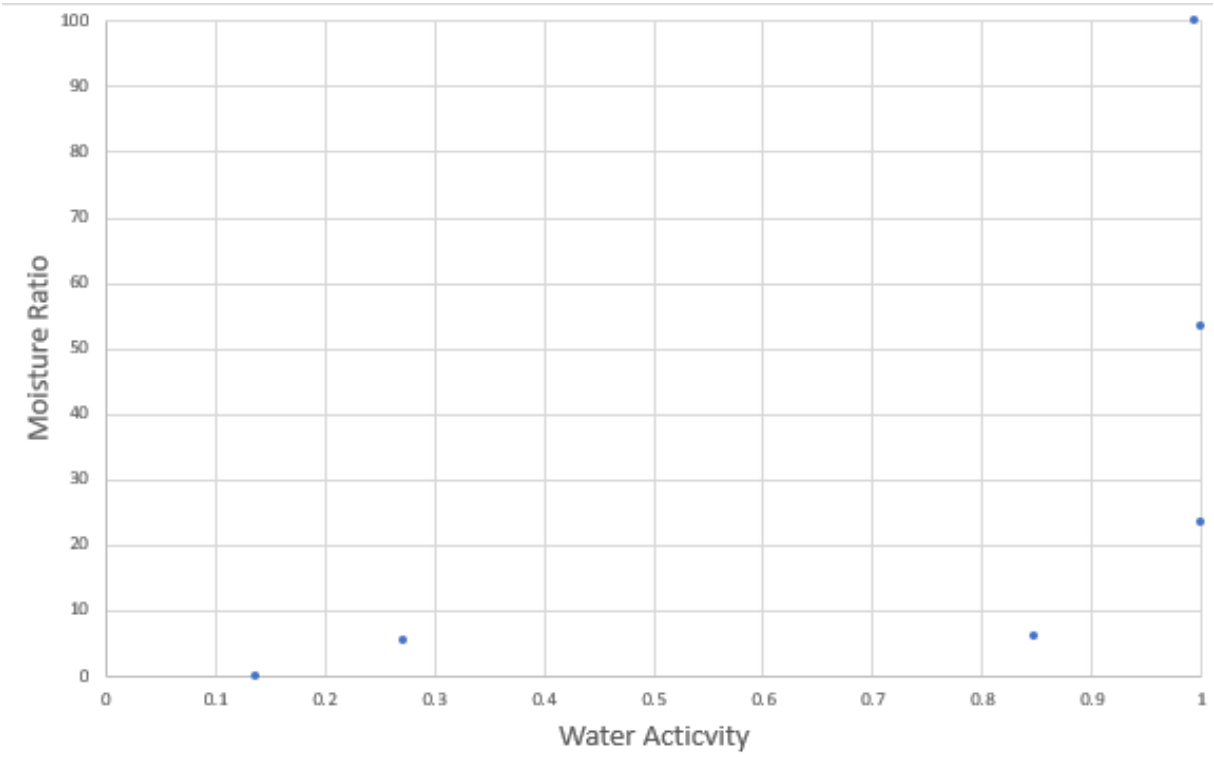

Figure 28: Moisture ratio, MR, and Water Activity, a_w, of Anode Mass at Temperature T = 150 °C.

In Figures 28 and 29 the moisture ratio and water activity is plotted for the anode mass. While the values of Figure 28 were measured at 150 °C, the values of Figure 29 were measured at 105 °C. In both figures, the same patterns can be observed as for the aluminium oxide. A large reduction of moisture ratio occurred without an initial reduction of water activity. This suggests that there was a relatively large amount of unbound moisture in the anode mass samples as well. Even at 105 °C, the anode mass is close to reaching the dry weight after 75 min. In the subsequent section an extended experiment of water activity of the anode mass at temperature T = 105 °C is presented and discussed.

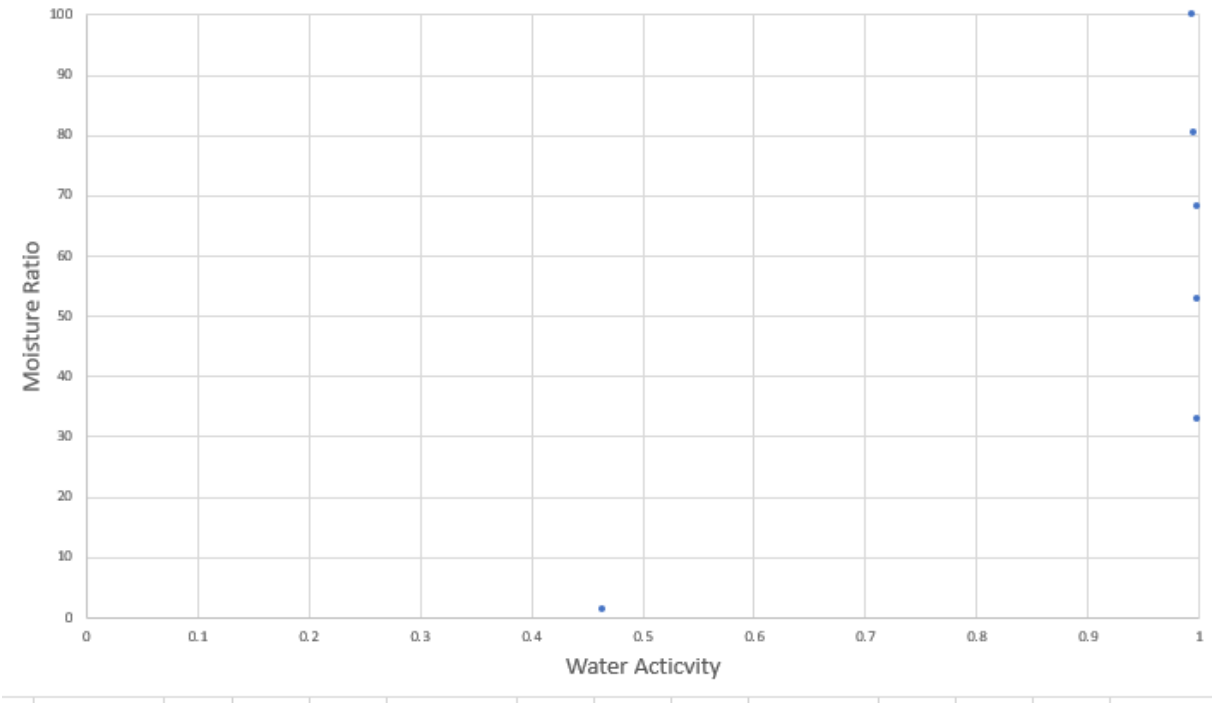

Figure 29: Moisture ratio, MR, and Water Activity, a_w, of Anode Mass at Temperature T = 105 °C.

Similar plots for the petroleum coke yielded curves which were not of sufficient quality to be added. Due to the error of the first drying experiment, at one point during the drying process, the moisture ratio was equal to 300%, while the expected values are between 100% and 0 %. Attempts were made to rectify the results which yielded unsatisfying measurements of moisture ratio and water activity. However, the measurements of water activity were not as expected. Thus, these results are presented in Section 7.3.

7.3 Error sources

There were numerous smaller and larger sources of error which must be taken into account when reviewing the results of the experiments. In this section, a list of various error sources is presented. In addition, the method to counteract or limit the errors which occurred is also given. At the end of the section, uncertainties in the measurement of water activity is discussed.

7.3.1 Various error sources

- Probably the most grave source of error was experienced during the first experiment, when the weight and water activity of the samples were measured. As seen in Figure 21, all the samples of the first experiment were inserted in the drying oven on the same tray. The aluminium oxide and anode mass had a much higher initial moisture content than the

petroleum coke. Thus, some of the moisture that was transferred from the aluminium oxide and anode mass to the air inside the oven, may have been adsorbed by the petroleum coke. This could be the reason as to why the weight of the petroleum coke after 15 min was higher than it was before being inserted into the oven. On the basis of this observation, during the second experiment, where dry weight was measured, it was decided that the petroleum coke would not be dried until most of the moisture had already been evaporated from the other products in the oven. At a later stage, in order to counteract this error, most experiments were conducted with only one type of material in the drying oven at a time.

- During the days between the beginning and the end of the experiments, some material may have dried somewhat when stored due to the difficulty of properly locking zip-lock bags with wet granulated material getting stuck in the lock strip of the bag. To counteract the occurrence of unwanted drying, a purchase of larger zip-lock bags was made with the intention of fitting the larger bags over the smaller bags which were difficult to close.

- The temperature variations when opening the drying oven, in the process of weighing and measuring water activity of the samples, impacted the temperature of the experiments. When the door was opened, the temperature inside the oven dropped rapidly as heat escaped to the ambient. When the oven door was closed, the temperature started to climb, but only quite slowly. In some intervals, the temperature did not even reach the predetermined temperature of the experiment. An effort to correct this inaccuracy was implemented by increasing the temperature inside of the oven so that the average temperature was closer to the intended temperature.

- Although an effort was made to ascertain that samples were of equal and uniform thickness, there were some uneven samples. Shrinkage of some samples was more noticeable than of other samples, which could indicate that some samples of the same material had a higher initial moisture content than others.

- The water activity meter is a sensitive instrument which is affected by very slight differences in humidity. To test the sensitivity of the meter, a sample with low water activity was re-inserted into the water activity meter after being subjected to an exhalation of breath. The measured water activity of that sample increased significantly, to a water activity corresponding to humid air. Hence, it is possible that other samples were affected by this sensitivity. Some trial measurements of water activity yielded varying water activity of some dry materials.

- In the process of making the samples, the first samples that were created were exposed to air for a significant amount of time before being put inside the drying oven. On a tray there is available space for up to fifteen samples, and each sample has a preparation time of a few minutes. Whenever a sample was prepared, it was weighed immediately afterwards, before it was placed on the tray that was going in the oven. It was observed

that some samples had lost a few grams of water in the time between being prepared and weighed, and until they were in the oven. Measures intended to counteract this was taken by decreasing the number of samples on each tray and thereby decreasing the preparation time of a tray.

- In order to measure the weight of the petroleum coke samples, a scale with higher resolution was utilized. The scale, a Mettler AE260 DeltaRange, has a chamber which protects the sample from drafts. By weighing samples which were removed from the drying oven at 150 °C immediately on the scale, air inside the chamber was heated up by the sample. When the sample was removed from the chamber and the chamber was closed, the weight of the air inside the chamber had been reduced, This affected the weight measurements typically by approximately 0.0020 g. The total weight reduction in the experiment which aimed at determining the dry weight of petroleum coke was 0.0266 g. Hence, an error of 0.0020 g would mean a 7.5 % margin of error. To counteract this inaccuracy, the difference in the weight of the air of the chamber before and after the weighing was subtracted from the weight which was measured.

- During the experiments which were conducted in the spring, the anode mass formed a solid crust during a drying experiment at 105 °C. The same crust formation did not occur during similar drying conditions during experiments in December. The material which was used in the two experiments came in different shipments from Alcoa Mosjøen. The first shipment was received in the fall of 2020, while the second shipment was received in the spring of 2021. There was a noticeable difference in the material composition of the anode mass in the two shipments in terms of particle size. While the first shipment contained anode mass which was mainly fine-grained with a only a few larger lumps of petroleum coke, the second shipment contained anode mass with composition consisting of a larger fraction of larger lumps of petroleum coke. Although this has only been observed visually during the experiments, the lower moisture content of the samples of the anode mass used in the drying experiments which were conducted in the spring may confirm this observation. As the lumps of petroleum coke contain a smaller fraction of moisture than the fine-grained paste, the mixture containing a higher fraction of lumps contains less moisture. As a consequence of the larger amount of lumps in the anode mass, the preparation of the samples intended for drying had to be altered. The preferred method of scraping off surplus material with a knife in order to get an even surface resulted in the large lumps of coal dragging anode mass off the disc. Consequently, a spoon was used to distribute anode mass as evenly as possible in the aluminium disc. The anode mass was compressed while using the spoon to evenly distribute the anode mass, and this compression of the anode mass could potentially be the reason why the crust was formed only on the samples which were part of the drying experiment with the latest shipment.

  The crust of each sample was observed to be increasingly harder and thicker as each sample was removed with every 30 min passing. Small samples were to be removed

from aluminium trays and sealed in containers in order to measure the water activity. The water activity samples were filled with material from the solidified crust, which had to be broken up before being inserted into the water activity measurement container, in addition to material from beneath the crust.

In Figure 30, the relation between moisture ratio and water activity of anode mass from experiments in the fall of 2020, which will be referred to as the blue series, which is depicted in the succeeding two figures, and the anode mass from from experiments in the spring of 2021, which will be referred to as the orange series. The points in the blue series are the same as in Figure 29. The main difference in the method between the two experiments which yielded the two series is the aforementioned difficulties with distributing the anode mass, and the time interval. The time interval between each sample was taken out of the drying oven was 30 min in the orange series, compared to every 15 min in the blue series. As mentioned, this was done in order to properly assess the complete drying process at 105°C, because the blue series did not have enough measurements close to the dry weight. Another difference between the series is the final, leftmost, measurement in the orange series. This data point is gathered at the dry weight of the sample, measured after 1344 min, or 22.4 hours. This dry weight measurement provides a basis for calculating the moisture ratio. For the blue series, the moisture ratio was calculated using the dry weight experiment which was conducted as a separate experiment.

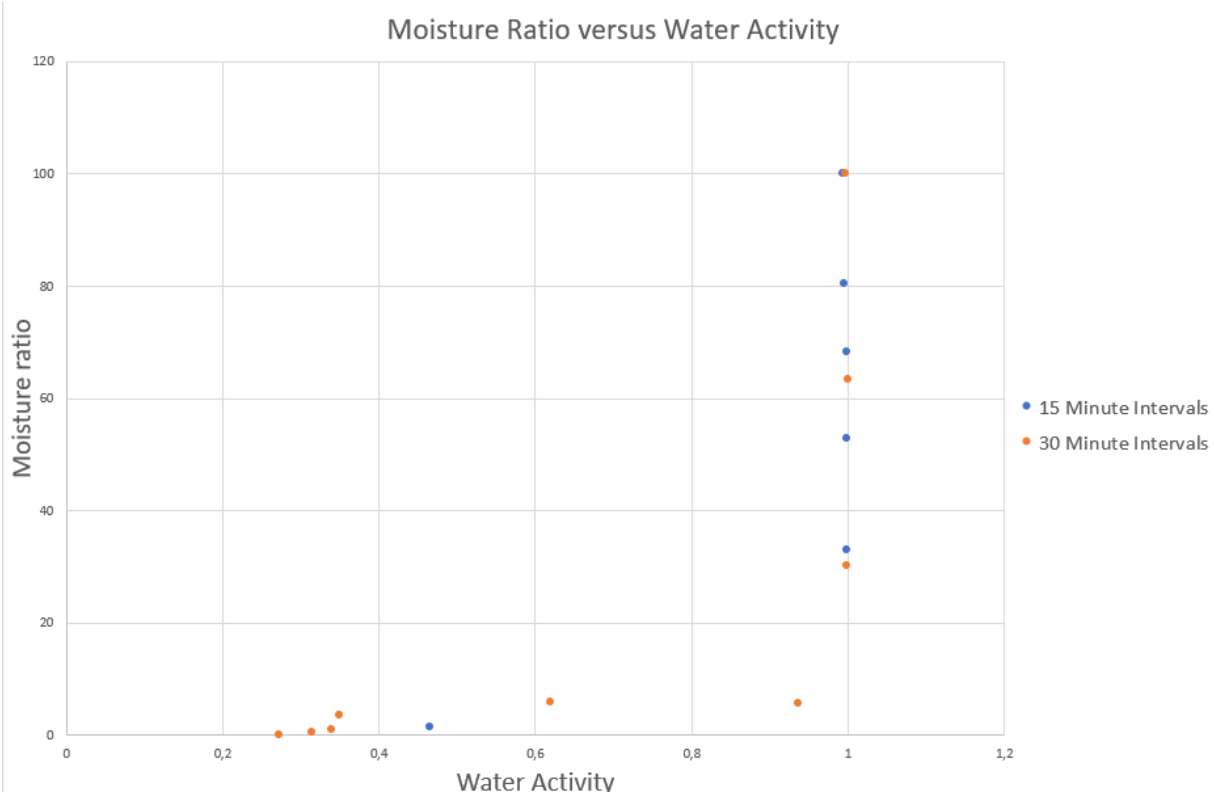

Figure 30: Moisture ratio and water activity in anode mass dried at 105 °C. The blue series is the same as in Figure 29, from the experiments conducted in 2020, while the orange series is from the experiments conducted in 2021. In the blue series, a sample was removed every 15 min, while in the orange series a sample was removed every 30 min. The leftmost data point is a dry weight sample of the same series as the other orange data points.

Figure 31 is similar to Figure 30 but the timestamp of each data point in the orange series is provided in order to underline inconsistent results. From 0 to 90 min there is a rapid reduction of moisture in the material, while the water activity reduction is comparatively small. This is expected, as the free moisture in the material is evaporated. At 120 min, the sample had a higher moisture ratio than the sample at 90 min, although only by a margin in the moisture ratio of 0.12. Thus, this difference could be due to differences in material composition, i.e., some samples had a larger fraction of petroleum coke lumps. Hence, the moisture ratio value at 120 min is within the expected range considering the error sources in the experiment.

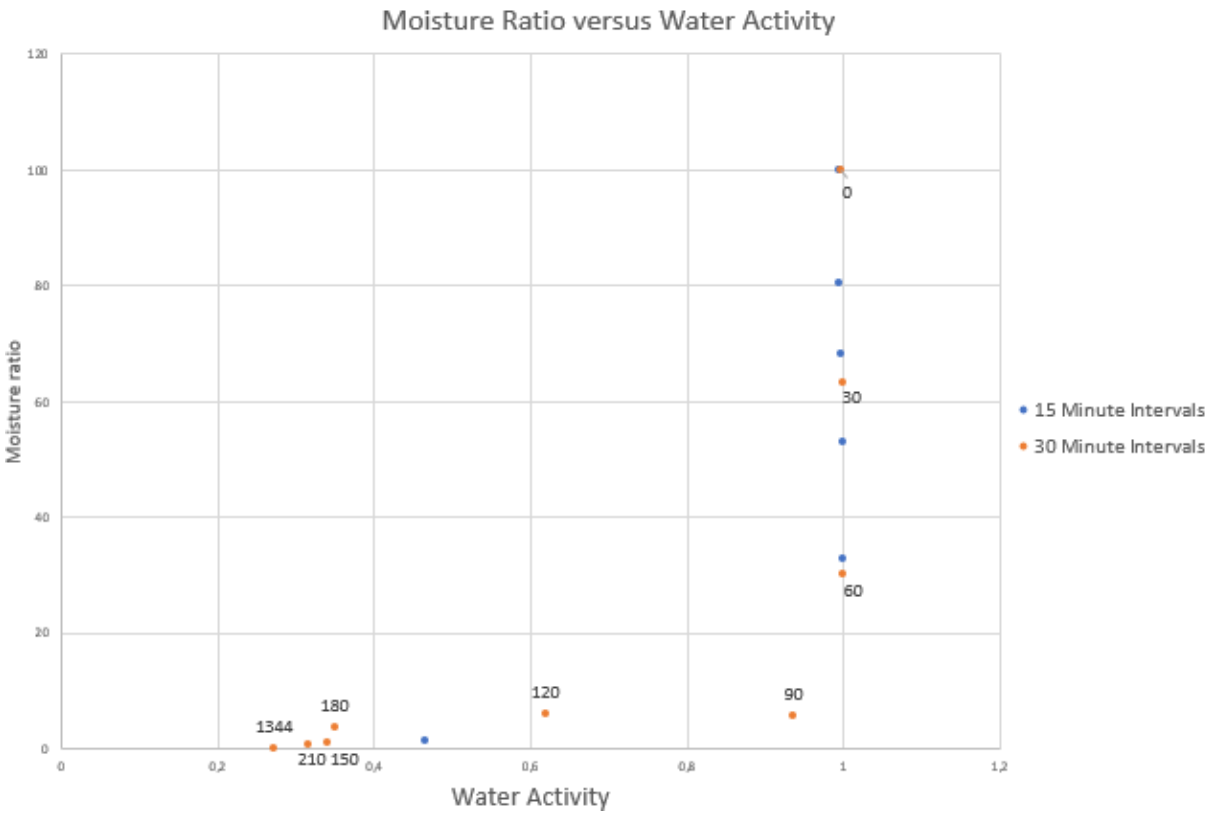

Figure 31: Here, Figure 30 is altered with emphasis on the timestamps of each data point in the orange "30 minute interval" series. As can be observed, the water activity and moisture ratio at 150 and 180 min are not as expected.

After 120 min, the samples had lost more moisture. And after 150 min, the mass of that sample had reduced from 59.40 g to 44.92 g, which yielded a moisture ratio, which has a range of 0 to 100, of 0.99. However, after 180 min, the weight of the sample was measured at 61.03 g and 46.55 g at 0 and 180 min respectively. This means that the decrease yields a moisture content of 3.63. Hence, the reduction of weight of the sample which was removed from the drying oven after 180 min had a relatively lower decrease in weight compared to the sample which was removed after 150 min. While the same argument can be made here, as in the previously discussed case of the sample which was removed after 120 min, the water activity was measured to be higher after 180 min compared to the sample removed after 150 min. The increase in water activity is not an expected result. The water activities were measured at 0.3399 and 0.3495 at 150 and 180 minutes respectively. This increase of 0.0096 is larger than the accuracy of the AquaLab 4TE of $\pm$ 0.003. Further inconsistencies in measurements of water activity suggests that there is either an error in the method which is used for determining water activity or the measurement technique when utilizing the water activity meter, or the water activity meter is not able to properly measure water activity at low values. These inconsistencies are elaborated upon in Section 7.3.2.

7.3.2 Uncertainties and inconsistencies in water activity measurements

Further experiments were conducted in order to ascertain the moisture ratio and water activity of petroleum coke, as well as the dry weight and drying curve. A scale with higher accuracy than the previously used Mettler Toledo Precision Balance ME4002 was required in order to measure the weight of water which was evaporated during the experiment. The Mettler AE260 DeltaRange which has a readability of 0.0001 g (Mettler Instruments AG, 1987) was utilized. From the experiment, which was conducted with the more accurate scale, determining the moisture ratio and water activity of the petroleum coke, Figure 32 was produced. Each data point is generated at 15 minute intervals at a temperature of 150 °C. From Figure 32, it is not evident in which order the data points are structured. To provide clarity, a curve was produced in Figure 33 to visualize the development of the moisture ratio and water activity.

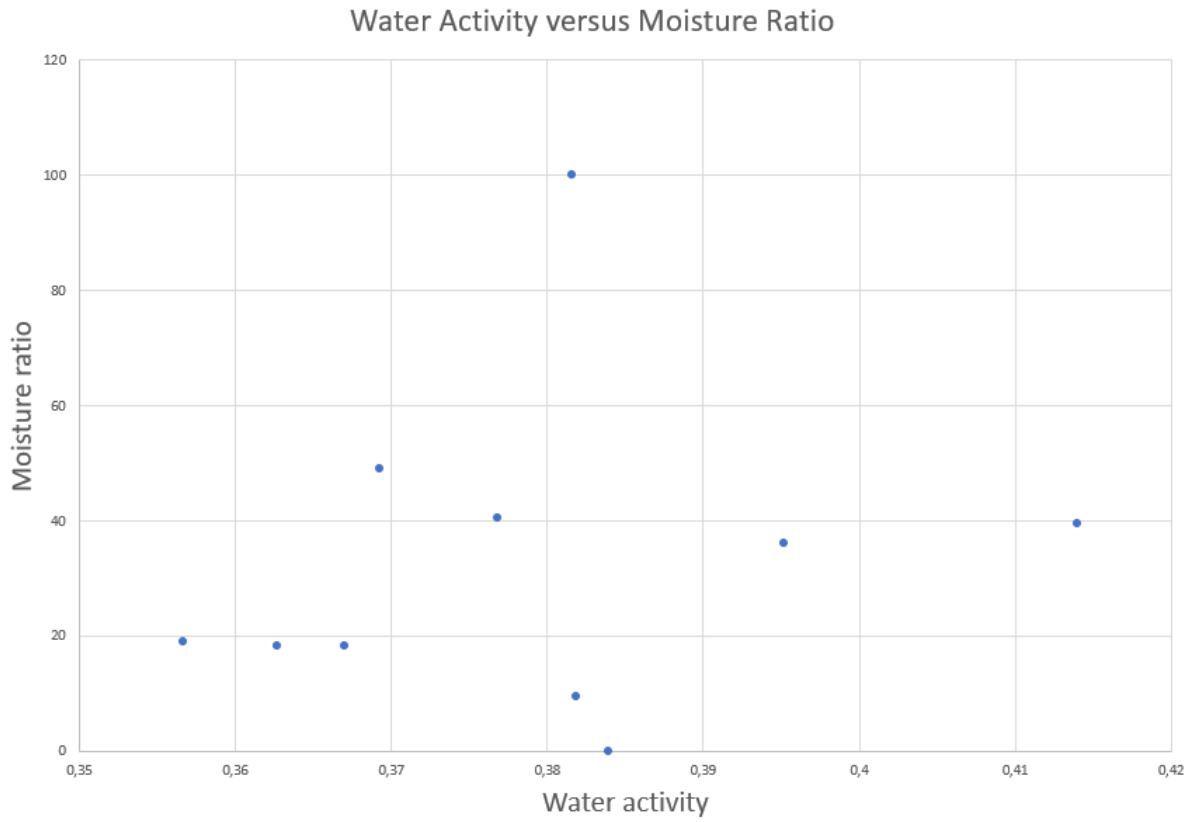

Figure 32: Moisture ratio, MR, and water activity, a_w, of petroleum coke, measured at temperature T = 150 °C. The data points are seemingly disorganized.

The curve in Figure 33 underlines the inconsistent results from the water activity measurements. While the reduction in moisture ratio is as expected, the water activity at the beginning and at the end of the experiment is almost identical. In fact, the difference between the measured water activity at moisture ratios 100 and 0 is 0.0023. This difference is less than the accuracy of the water activity meter of 0.003. In addition, the water activity is observed to be increasing and decreasing throughout the experiment, while the expected result would be the water activity should only be decreasing.

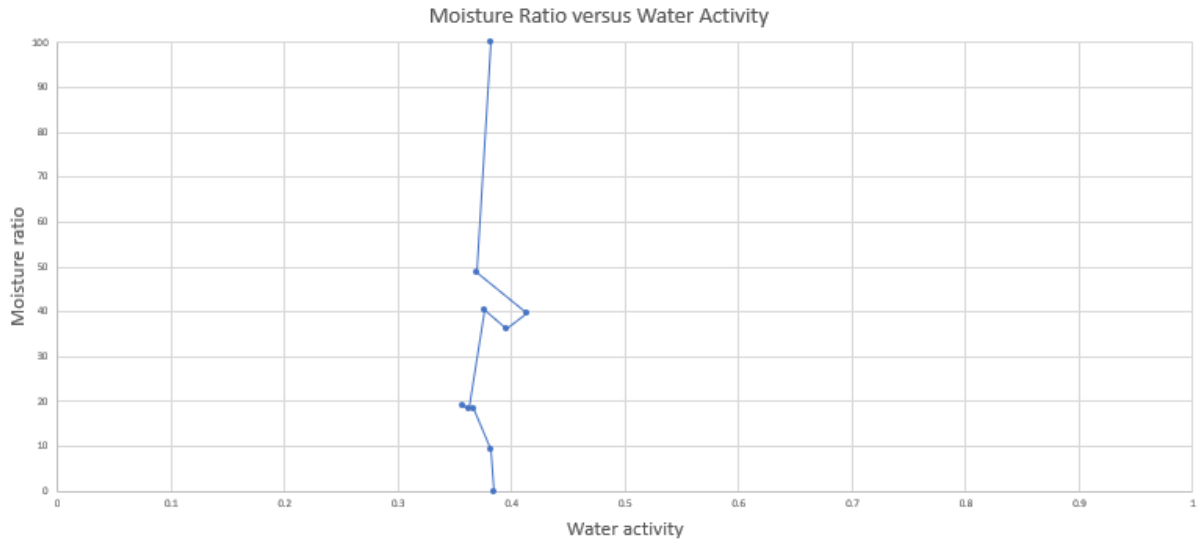

Figure 33: Moisture ratio, MR, and water activity, a_w, measured at temperature T = 150 °C. The seemingly disorganized data points of Figure 32 are presented in the form of a curve with the range in water activity between 0 and 1 on the x-axis.

There were conducted multiple experiments aiming at ascertaining the moisture ratio and water activity of petroleum coke. Some of the failed experiments yielded results which were unsatisfactory in terms of accuracy of moisture ratio due to an insufficiently accurate scale, so the experiments had to be carried out again. In spite of this, the measurements of water activity were obtained with an identical method as in the successful experiment. Figure 34 illustrates the moisture ratio and water activity from an experiment where the moisture ratio is not correct. The same "clustering of data points" can be observed here, albeit at lower values of water activity than in the other experiment.

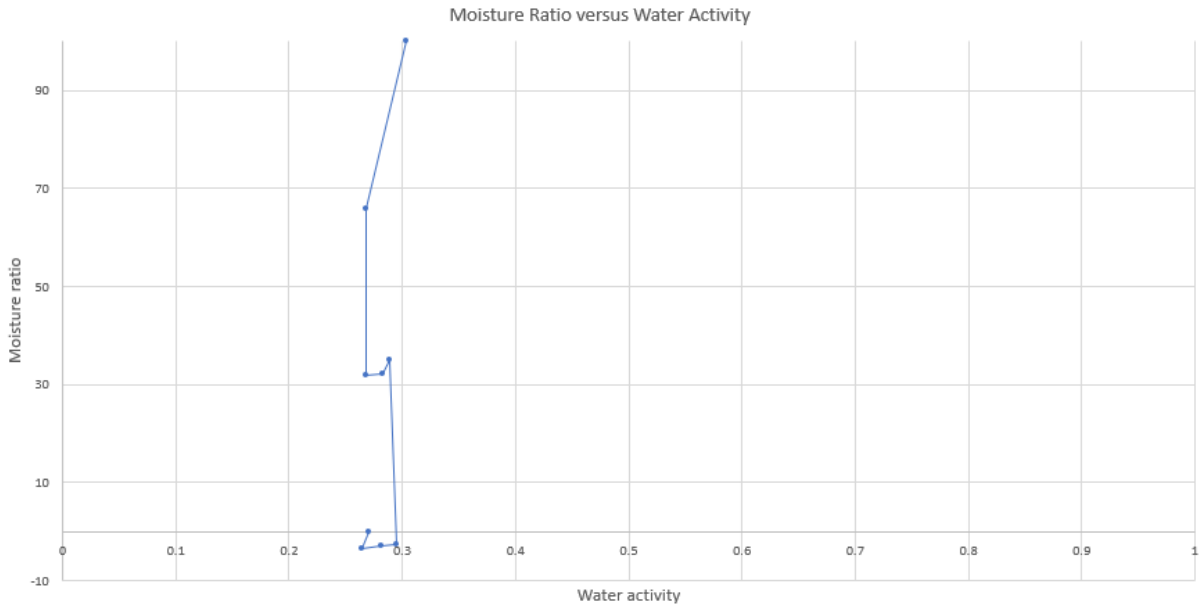

Figure 34: A measurement of moisture ratio, MR, and water activity, a_w, of petroleum coke, measured at temperature T = 150 °C. The moisture ratio is incorrect because the scale which was used was not sufficiently accurate. However, the same "clustering" can be observed with regards to water activity.

Another experiment was conducted in order to rectify the inconsistent results of the previous experiments. Instead of performing the experiment like it was conducted previously, the petroleum coke was wetted for 24 hours before being dried. Thus, in the 24 hour period before the experiment, the petroleum coke adsorbed water until it was in equilibrium with the water. The water was then strained out of the petroleum coke, and drying experiments were conducted in the same manner as in previous experiments. In Figure 35, the moisture ratio and water activity is plotted. As the moisture ratio is normalized on the total loss of moisture, the moisture ratio in Figure 35 ranges from from a wet basis moisture content of approximately 27.7 % to zero. However the moisture ratio of the petroleum coke which was not wetted ranges from from a wet basis moisture content of approximately 1 % to 0 %.

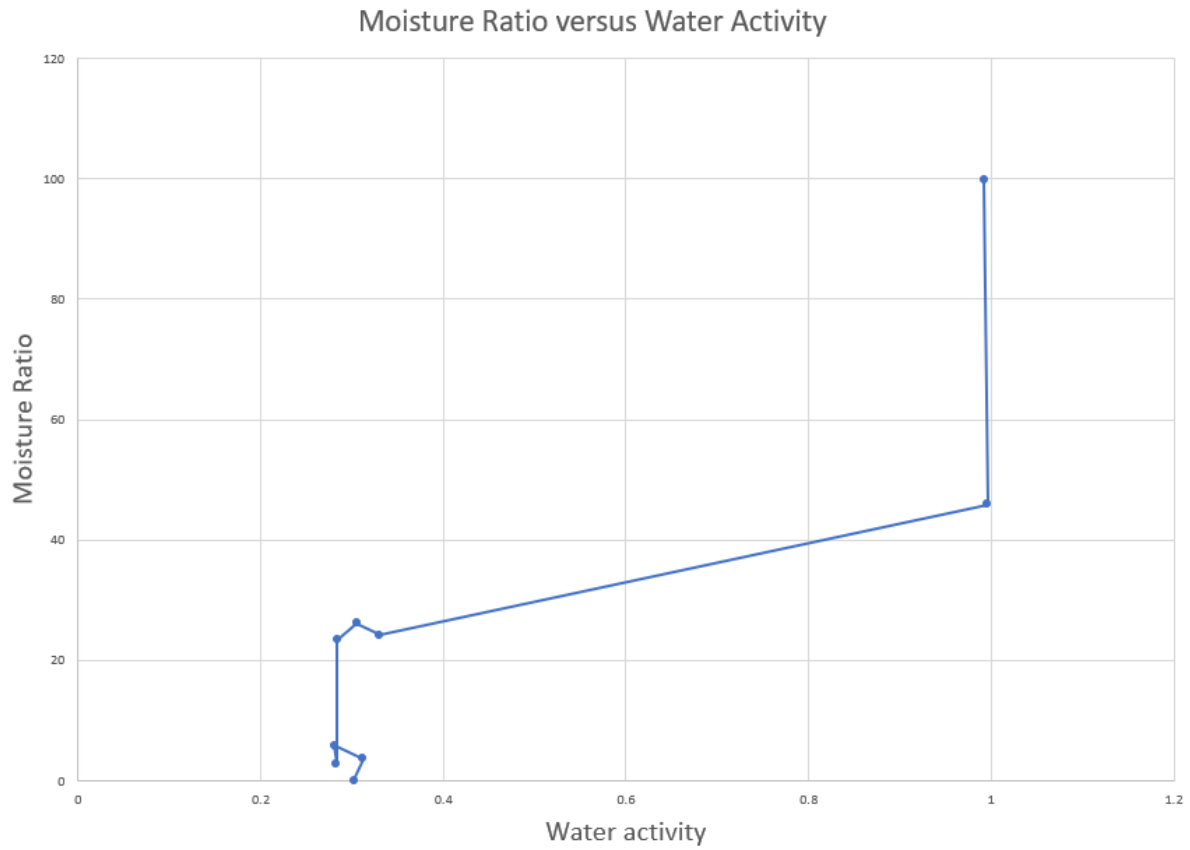

Figure 35: Moisture ratio and water activity of petroleum coke which was wetted for 24 hours before being dried, measured at temperature T = 150 °C.

The uncertainty of these results prompted uncertainty as to whether an error has been made in the handling of the water activity meter or whether the water activity meter accurately measured the water activity of the petroleum coke. Especially at lower values of water activity, the results were not as expected. There was not found any literature regarding the water activity of petroleum coke which could aid in explaining the results. Hence, it is suggested that further work is required to establish why the water activity is at such high levels. In spite of this, for the purpose of drying petroleum coke intended for use in carbon anodes, the results are satisfactory in the sense that the production of anode mass is not compromised by the uncertainties and inconsistencies which were experienced in the experiments.

7.4 Specific energy requirement of drying

As discussed in Section 2.4, the energy required to dry the product will be that of the latent heat of vaporization of the water in the product, in addition to the energy expended while heating the product.

Using Equation 4 for the calculation of the specific heat of each material, and assuming that the drying process occurs after the heating of the product has occurred, the specific energy required

for drying of each material will be given as:

$$Q_{drying} = \Delta H_{vap} \cdot mf_{water} + (mf_{water} \cdot c_{p,water} + mf_{material} \cdot c_{p,material}) \cdot \Delta T \qquad (22)$$

Here, ΔT is the temperature difference between the average material temperature and the drying temperature. The latent heat of vaporization, ΔH, is assumed to be the one corresponding to the drying temperature.

Table 6: Calculation of heat requirement of drying, assuming a drying temperature of 150 °C.

	Mass fraction of water	Mass fraction of solid	Latent heat of vaporization [kJ]	Energy of heating from 7 to 150 degrees	Energy requirement	Unit
Aluminium Oxide	0.3757	0.6243	2113.7	303.8	1097.9	kJ
Anode mass	0.3141	0.6859	2113.7	274.6	938.53	kJ
Petroleum coke	0.0011	0.9989	2113.7	122.5	124.8	kJ

Table 7: Values of variables in the calculation of heat requirement of drying the materials.

Variable	Value	Unit	Reference
$c_{p,water}$	4.25	kJ/kgK	Engineering Toolbox (2004*a*)
ΔH_{vap}	2113.7	kJ/kgK	Engineering Toolbox (2004*b*)
$c_{p,aluminiumoxide}$	0.8450	kJ/kgK	National Institute of Standards and Technology (1979)
$c_{p,anodemass}$	0.8532	kJ/kgK	National Institute of Standards and Technology (1978)
$c_{p,petroleumcoke}$	0.8532	kJ/kgK	National Institute of Standards and Technology (1978)

In Table 7, the values of thermal properties used in the calculation of the specific energy required for drying. The average value of specific heat of water between 7 °C and 150 °C was used. The latent heat of vaporization of water at 150 °C, ΔH_{vap}, was utilized in the calculations. When calculating the specific heat of aluminium oxide, the average value between the specific heat at 7 °C and 150 °C was used. Interpolation in the tables referenced in Table 7 was done in order to obtain values at the aforementioned temperatures.

When determining the specific heat of aluminium oxide, an assumption was made that 100% of the material was α-aluminium oxide. In reality, the aluminium oxide consists of approximately 50% α-aluminium oxide and 50% β-aluminium oxide. Values of the β-type were difficult to obtain and verify. Other types of aluminium oxide: α, δ, γ, and κ were compared with each other. The size of the heat capacities was close to equal for some of the types of aluminium oxide. The largest variation between the different heat capacities at the reference temperature of 25 °C, was of approximately 4.8 %. Consequently, it was evaluated that an assumption of 100% α-aluminium oxide for the calculation of specific heat would not cause a large margin of error. Similarly, approximations were made when determining the heat capacity for the anode mass and the petroleum coke. The anode mass consists of petroleum coke and pitch, both of which mainly consist of carbon. Thus, the specific heat of pure carbon was used for both materials in the calculations.

Table 8: Final calculations on heating demand

Material	Energy requirement	Unit		Mass flow	Unit		Mass flow	Unit		Heat requirement	Unit
Aluminium Oxide	1097.9	kJ/kg		500000	kg/year		0.0158549	kg/s		17.4	kW
Anode mass	938.5	kJ/kg		40000	kg/year		0.00126839	kg/s		1.2	kW
petroleum coke	124.8	kJ/kg		220000000	kg/year		6.97615424	kg/s		870.3	kW

In Table 8, the calculations on specific energy requirement and total power requirement are tabulated. Comparing the values of Table 8 with the theoretical heat supply, which is calculated in Section 5 and tabulated in Table 4, it is apparent that the heat supply from the pot gas and exhaust gas at the plant is larger than the calculated heat requirement of drying. Summing up the heat requirements for each material in Table 8, the total heat required is approximately 889 kW. Although the total heat available in the two waste heat streams are 12.4 and 71.8 MW respectively. By substituting the measured water content of the petroleum coke, with the expected moisture content of 1% wet basis, the amount of heat required is increased to approximately 2.7 MW. This is still significantly less than the heat supplied by the exhaust gas. Consequently, the conclusion is that there should be enough surplus heat in the Alcoa Mosjøen plant to cover the heat demand of drying the by-products and raw materials evaluated in this thesis.

8 Rotary Dryer Considerations

The benefits and drawbacks of several dryer technologies were presented in Section 4.2. The qualitative arguments presented in Section 4.2.1 regarding the suitability and versatility of utilizing a direct rotary dryer, means that the rotary dryer is preferred.

8.1 Dryer placement

In determining where the dryer should be placed, both engineering and economic factors are important to evaluate. The large area which is occupied by the aluminium plant at Alcoa means that there are long distances between the different buildings where the processes occur. This could prove challenging. Considerations regarding the minimisation of costs and loss of energy are crucial. The key factors which are considered in the choice of placement of the dryer are the following:

- Availability of space.
- Distance to heat source.
- Distance to mass sources.

There is space which is available close to the anode baking furnace which is a heat source of 12.4 MW. The space is also close to the silo where petroleum coke is stored. The area which is available is large enough to fit a rotary dryer.

8.1.1 Availability of space

The availability of space is one of the most important aspects which must be considered when determining the most suitable placement of a dryer. The sizeable scale of the aluminium plant is occupied by large buildings where processes occur at high temperatures and heavy machinery move between the buildings while doing various tasks. Strict security protocols are in place so as to minimize the risk of injury to the numerous workers employed at the plant. Any change in the aluminium production process, in this case, related to installing a dryer, should aim at not affecting any of the existing security protocols and standards already in place. Therefore, a suitable space for a dryer would be a space where a dryer would infringe minimally on the current operations and safety protocols. The available space, which is close to the anode baking, satisfies the requirement.

8.1.2 Distance to heat source

In order to minimise thermal losses and cost, the distance between the exit of the flue gas from the anode baking and the dryer should be kept at a minimum. The hot gas which is used in the anode baking process is transported through pipes to the dryer. Thermal heat loss from the pipe to the environment is undesirable, as the temperature at the inlet of the dryer should be kept as high as possible. In addition to the negative impact of large heat losses which is a consequence of long pipes, the cost of a pipe is rising linearly with the length of the pipe. Thus, the value of keeping the distance short between the heat source and the dryer can be defined in terms of heat losses and economic losses. The aforementioned available space is located approximately 50 metres from the outlet of the anode baking flue gas. This is an acceptable distance to the heat source, especially when considering the vast area of the aluminium production plant.

8.1.3 Distance to mass sources

In the endeavour to find the optimal placement of the dryer, the distance between the sources of mass should be considered. The cost of moving large amounts of material to and from the dryer increases with the distance the material has to travel. From Table 8 it is evident that the mass flow rate of petroleum coke is, by far, the largest. The location which is considered as most promising is located right next to a silo where petroleum coke is stored. The possibility of making the feed of petroleum coke continuous means that the majority of the costs of supplying petroleum coke to the dryer can be attributed to the initial investment. The anode mass is another mass stream which must be accounted for. Since the anode mass already is moved from the cooling pool of the anodes and to the anode baking, moving it to the dryer will not affect the cost of the process greatly. This is also because the dryer is close to the anode baking facility. Finally, the aluminium oxide must be considered. The aluminium oxide is located in the artificial lake which is quite close. A system for storing aluminium oxide on land after it has been excavated could be considered if there is available space. If the aluminium oxide is stored in a container with a fine mesh sieve in the bottom, excess water could run off into the deposition pool while the aluminium oxide is stored before being entered into the dryer. The operation of bringing the wet aluminium oxide from the deposition pool and bringing the dry aluminium oxide to the electrolysis will require some labor. Therefore, investing in infrastructure to store the aluminium oxide on land before drying it could reduce operating costs and could help dewater the material by filtration somewhat before drying.

8.2 Continuous or batch feed

The dryer is located in an area close to a silo which contains petroleum coke. Ideally, pipes could be fitted so that the mass flow of petroleum coke is continuous. The other materials need to be

brought in batches. Thus, it is suggested that the preferred design of the dryer is a combination of continuous and batch, where only the petroleum coke is provided by a continuous flow. This must be discussed with the manufacturer of a dryer, and if it is not possible, then the alternative must be that the dryer is a batch dryer, as the materials need to be kept separate from each other.

8.3 Air stream

The direction of the stream of hot air inside the rotary dryer affects the drying process. On the effect of how countercurrent air flow dictates the drying rate, Berk states: "The starting rate of drying is lower but it is possible to dehydrate the product to the lower final moisture content" (Berk, 2008, p. 488). As the importance of reaching a bone dry product is crucial for the aluminium oxide, the flow of air must be countercurrent.

8.4 Trials with a manufacturer

According to Mujumdar (2007), the residence time of particles in rotary dryers is difficult to determine. In order to properly design a rotary dryer which fits the process, tests must be conducted on a rotary dryer. Due to the high importance of producing bone dry output from the dryer, tests with real conditions in a dryer is necessary to provide assurance that the output of the dryer will have no moisture.

During the experiments in the rotary dryer, it is important to determine the drying rate of the three materials in different phases of drying. Due to the geometry of the dryer and the internal flights, in addition to characteristics of each material, an understanding of how much water can be removed from each material type at different stages of the drying process must be established. In Section 4.2.1, it was explained that most of the convective heat transfer occurs when the material falls from the flights inside the dryer. Conversely, it is also during this phase that most of the convective drying occurs. The difference in how each material is affected by the geometry of the internal flights, i.e., how the material is affected by the lifting action of different flight geometries, should lead to an evaluation where a trade-off between the most efficient flight design for each material should decide which internal flight geometry is optimal. Thus, only after having made agreements with a supplier of a rotary dryer which is willing to provide a rotary dryer that is designed to fit the mass flow rate and moisture removal rates of the materials which have been evaluated, can the right design be made.

8.4.1 Residence time

In a rotary dryer, material is conveyed by means of several mechanisms, from the inlet to the outlet of the dryer. Mujumdar (2007) states that the three distinct mechanisms which affect the movement of particles inside the dryer are: cascade motion as a result of the lifting action of the internal flights and the slope of the dryer; kiln action, which occurs as the particles slide over the shell of the dryer or over one another; and bouncing, which occurs when particles fall. The holdup in the rotary dryer, H, and the feed rate, F, can be utilized to determine the average residence time, $\bar{\tau}$:

$$\bar{\tau} = \frac{H}{F} \tag{23}$$

By utilizing this relation, a simple estimate of the average residence time as a function of volumetric holdup in a dryer of length, L = 10 m, and diameter, radius, r = 2 m, is illustrated in Figure 36. The feedrate of petroleum coke, F, is used. In addition, an assumed density of coke of ρ = 0.8 $\frac{kg}{m^3}$ is assumed. The holdup of the material in the dryer is dependent on the slope of the dryer.

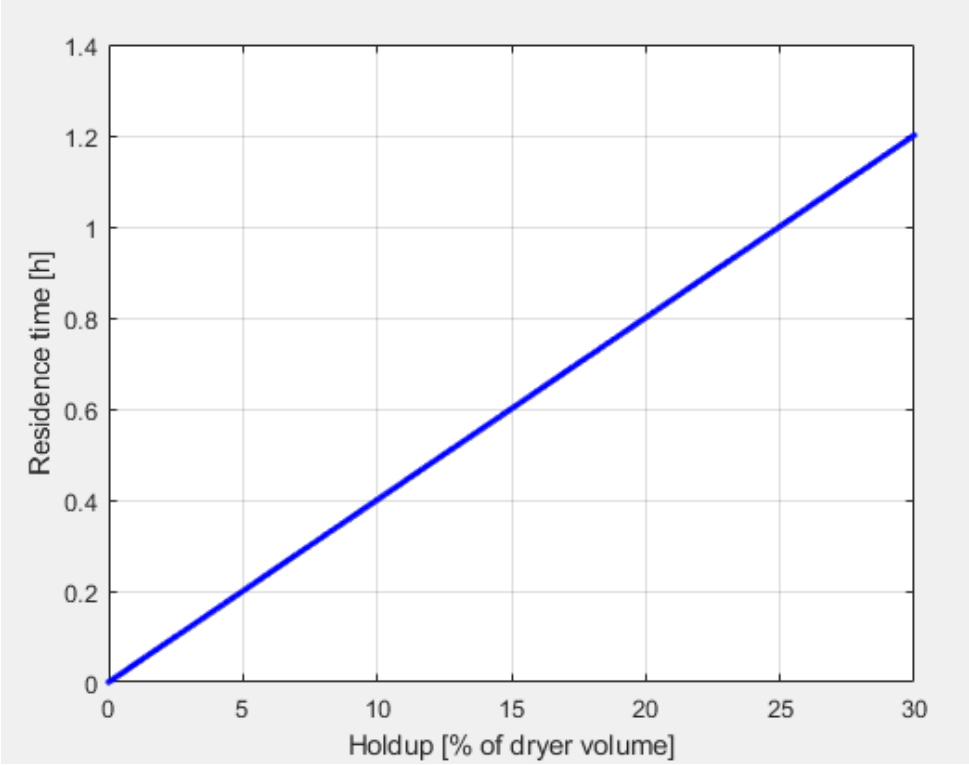

Figure 36: The residence time [h] of petroleum coke versus the volumetric holdup in the rotary dryer.

Furthermore, according to Mujumdar (2007), most of the studies on residence time consider the average holdup in the dryer, and Mujumdar (2007) presents an empirical equation in order to

determine the average residence time, $\bar{\tau}$, of a material:

$$\bar{\tau} = \frac{0.0433(Ln)^{0.5}}{DNtan\alpha} \tag{24}$$

Where $\bar{\tau}$ [s] is the residence time, L [m] is the length, D [m] is the diameter, N [r/min] is the rotational speed, α is the is the slope of the dryer, and n [degrees] is the dynamic angle of repose (Mujumdar, 2007, p. 156). In this instance, the angle of repose, which is dependant on moisture content among other factors, would be a variable which should found through trials in order to estimate the theoretical residence time of each material. The slope of the dryer, α, must also be determined. However, several empirical equations are proposed, and a study of which equations are suitable for the three materials which have been evaluated, as well as the dryer and internal flight geometry must be determined. Models on holdup and residence time which take flight geometry into account exist, and one is provided by Van Puyvelde (2009), where the *GFRlift*-model is presented. This model proposes some shapes of internal flights, and is, like the empirical relation in Equation 24, dependent on the angle of repose of the materials.

8.4.2 Drying rate

In the experiments, the drying curves have been presented graphically. Whereas the curves prove that the drying of the materials at the given temperatures is suitable, the experiments do not provide the exact drying rate for the conditions which will be present in the rotary dryer. The surface-area-to-volume of the particles which are dried by convective heat transfer, in addition to the velocity of the air stream inside the rotary dryer which provides forced convection when the materials fall down from the flights, yields the assumption that a higher rate of drying can be achieved in a rotary dryer than in the experiments inside a natural convection dryer.

9 Calculation of Costs

As explained in Section 3.3, the costs associated with each alternative decision must be compared in order to assess which is the most profitable decision. In this section, an attempt will be made to provide an overview of the relevant operating costs and investment costs in the analysis of the profitability of adding a dryer to the process, compared to the current situation where no dryer is utilized. The payback period of the investment is a key factor in the decision-making process, and there are several economic uncertainties related to the available decisions.

9.1 Investment costs in the current situation

In the current situation, there are no investment costs which are necessary to evaluate in order to continue the operation.

9.2 Operating costs in the current situation

In the current situation there are several operating costs that are eliminated by introducing a dryer to the process. The most significant operating costs that are affected by adding a dryer are related to the following:

- Deposition of aluminium oxide.
- Material cost of aluminium oxide which is deposited.
- Burning of LNG.
- Cost of mixing wet and dry petroleum coke.

9.2.1 Deposition of aluminium oxide

On average, each year 500 000 kg of wet aluminium oxide is removed from the aluminium oxide deposition pool at Alcoa Mosjøen. The cost of depositing this mass in a facility is an estimated 1 000 000 NOK per year. Thus, utilizing a dryer so that aluminium oxide does not need to be sent to a material deposition facility will lead to savings of 1 MNOK.

9.2.2 Material cost of aluminium oxide which is deposited

Considering the aluminium oxide, which in the current situation is deposited instead of being re-introduced into the process, the savings on direct material costs related to drying the material

and re-introducing it would be equal to the price of the amount of the dried aluminium oxide. This is valid under the assumption that the aluminium oxide which is saved would be equally valuable for the company as the aluminium oxide which is bought. By drying and re-introducing the aluminium oxide which would otherwise be discarded, the quantity of aluminium oxide, which is bought at a price of 3 NOK/kg, would decrease. The aluminium oxide which is bought is assumed to be bone dry. As mentioned in Section 9.2.1, the amount of wet aluminium oxide which is removed from the deposition pool at the aluminium plant is approximately 500 00 kg/year. It is assumed that the wet aluminium oxide has the moisture content which is tabulated in Table 5, and that the moisture content after drying is 0 % wet basis. Consequently, the weight of the dry aluminium oxide is 312 150 kg. As the price of aluminium oxide is given as 3 NOK/kg, the savings in material cost of drying aluminium oxide is calculated at 936 450 NOK/year.

9.2.3 Burning of LNG

Liquefied Natural Gas (LNG) is used in the anode baking process in order to provide heat. Per annum, 220 000 tonnes of petroleum coke is used as input in the anode baking process. The moisture in the petroleum coke is currently removed by means of drying it with heat which is generated from burning of LNG. Furthermore, heat from burning of LNG is used to increase the temperature of the petroleum coke in the anode baking process. Similar arguments can be made about anode mass which is gathered from the basin where the anodes are cooled during the baking process. The wet anode mass, which amounts to 40 tonnes per year, is mixed into the anode baking process while wet. Consequently, the anode mass is also currently dried and heated with the heat which is generated from burning LNG.

The price at which Alcoa purchase LNG is given as 4 NOK/Sm^3, where Sm^3 is Standard cubic metres. The Lower Heating Value (LHV) of methane is assumed to be 50 MJ/kg. To calculate the price of LNG in NOK/kg, the ideal gas equation is used:

$$pV = nRT \tag{25}$$

Where p [Pa] is pressure, V [m^3] is volume, n [mol] is the amount of substance of gas, R [J/K $\cdot$ mol] is the gas constant which is equal to 8.3145 and T [K] is the temperature.

By using the following relation about molar mass:

$$n = \frac{m}{M} \tag{26}$$

Where m [g] is the weight, and M [g/mol] is the molar mass, we get the following equation which is used to convert Standard cubic meter to kilogram:

$$pV = \frac{m}{M}RT \tag{27}$$

It is assumed that the standard conditions of gas is given at temperature T = 288,15 K and pressure p = 101325 Pa. Furthermore, it is known that the volume v = 1 m^3 and that the molar mass of methane is $M_{methane}$ = 16.043 g/mol. By using these values, the mass of methane at standard conditions is calculated as m/V = 0.6785 kg/m^3. Using this result, the price of LNG, p_{LNG}, can be stated in NOK/kg as:

$$p_{LNG} = 4[NOK/Sm^3] = 4/0.6785 = 5.8954 \tag{28}$$

The amount of LNG which is required is calculated in Section 5, and it is estimated to approximately 382.488 tonnes of LNG. By applying the price which is calculated in Equation 28, the annual operating costs which are reduced by utilizing a dryer becomes 2254903.5 NOK/year, or 2.25 MNOK/year. This means that Alcoa will save approximately 2.83 % of the costs related to purchasing LNG.

9.2.4 Cost of mixing wet and dry petroleum coke

During the course of normal operations, the aluminium plant receives large loads of petroleum coke by ship. The shipments are subject to strict scrutiny with respect to material quality. One such quality requirement which the material must meet is that the content of water should be below 0.3 %. Occasionally, the moisture content of the petroleum coke does not satisfy the standards for carbon anode production. In these cases, the shipment of petroleum coke may need to be shipped to Rotterdam, where Alcoa have a facility where the petroleum coke from the shipment can be mixed with drier petroleum coke in order to lower the moisture content of the mixture, which is to be sent back to the Alcoa plant in Mosjøen. A different solution to this problem, which currently also is used, is that the petroleum coke could be mixed with the petroleum coke which is already in stock at Mosjøen.

This solution, where petroleum coke is shipped to Rotterdam and treated, is costly. Although the exact cost is not specified by Alcoa, the better option economically would be to use surplus heat for drying. In addition, the emissions of greenhouse gases due to unnecessary shipping of petroleum coke can be deemed a negative externality of this solution. By designing a dryer set-up which is able to dry the petroleum coke shipments that are not at a satisfactory moisture content, the need to ship and mix the material is eliminated. Since the costs associated with mixing dry and slightly less dry coke which is already present at the plant is not quantified, there can be made a qualitative argument that the addition of a dryer provides added value and flexibility in the process of drying petroleum coke. Hence, the benefit of adding a dryer will not have a direct impact on the analysis of the profitability.

9.3 Investment costs associated with adding a new dryer

There are investments required in order to incorporate a drying system into the aluminium production process. The costs of these investments in fixed assets can be depreciated over the expected useful life of the assets. If, e.g., a linear depreciation model is utilized, the annual costs of associated with the investments would be a fixed cost. The main investment costs associated with the change is discussed in this section. The focus will be on the cost of these areas, which represent the most significant changes:

- Dryer unit
- Piping for heat and product feed
- Deposition pool rebuilding

9.3.1 The dryer unit

Inquiries have been made to several companies about the price of an industrial rotary dryer. Due to different circumstances, no company located in Europe were willing or able to provide a price estimate of an industrial rotary dryer after being given a detailed description of the conditions of the process. The details used in the enquiry were made on the basis of information about the process which was already available publicly online, the name of the company name was not specified. Several manufacturers of industrial rotary dryers from India were able to provide a price point of dryers, though the prices which were provided were not for dryers that were designed specifically for the conditions that were specified.

Table 9: Price of certain industrial rotary dryers. The price is originally given in Indian Rupee and converted to Norwegian Kroner.

Country	Company	Price [rupee]	Price [NOK]	Tabulated Capacity [tonnes per hour]	Reference
India	Laxmi Engineers	3500000	385000	3 to 20	Laxmi Engineers (n.d.)
India	Excellent En-Fab Incorporation	2200000	242000	0.5 to 30	Excellent En-Fab Incorporation (n.d.)
India	Baharath Industrial works	540000	59400	Not available	Bharat Industrial Works (n.d.)

In Table 9, a selection of dryers are chosen to represent the variety of what dryers are available from Indian manufacturers, and at what price they are available. At a required capacity of just above 25 tonnes per hour, not all dryers in Table 9 would be able to manage such a large mass flow rate. In addition, it is evident that the differences in price is significant. The most expensive dryer is almost 6.5 times as expensive as the cheapest one. An evaluation of the quality and durability of the dryers is needed to ascertain whether the quality of the cheaper options are of the required standard and reliability.

In order to calculate the payback period of installing a dryer, a price has to be chosen. As there is no certainty as to what a dryer which is properly adapted to the conditions which are specific to this task, and considering that there may be costs that are unforeseen, an estimation is made that the cost of a drying unit can be expected to be approximately 50 % more expensive than the most expensive dryer which is tabulated. Thus, the value of an industrial dryer is chosen to be 577500 NOK. However, after ascertaining the other costs, the price of the price of the dryer can be changed in a sensitivity analysis where the payback period is examined.

9.3.2 Piping

Pipes are needed in order to bring surplus heat from the anode baking process to the dryer. The pipes, which have a total length of around 100 metres, run from the anode baking to the dryer and back to the fume treatment of the anode baking facility. Installation costs of the piping is expected to be 220 000 NOK, while the price per length of the pipes is known to be 6 500 NOK/m. The material of the pipes is corten steel, or weathering steel. Taking this information into account, the total cost of purchasing and installing pipes will be 870 000 NOK.

9.3.3 Deposition pool rebuilding

Figure 2 shows the artificial lake in Mosjøen where aluminium oxide is deposited temporarily before being sent to a deposition treatment facility. The possibility of rebuilding the deposition pool in order to facilitate easy retrieval of aluminium oxide, in addition to environmental restrictions, is considered, and the cost of the rebuild of the pool is estimated at 10 MNOK.

There is a possibility that Alcoa will be required to rebuild the deposition pool in order to comply with regulations due to concerns of conservation of nature. In the current situation, aluminium oxide and other effluents are deposited temporarily in the deposition pool, before being deposited permanently at a treatment facility. The particles of aluminium oxide are brought to the deposition pool by a stream of water from the wet scrubber. As the water decreases in speed when the water enters the lake, the particles are deposited along the lake bed. The principle is similar to when rivers run into a body of water, forming a river delta. Excavators are utilized in order to empty the pool, and the motion caused by excavating leads to particles being whirled up into the stream. Hence, particles of aluminium oxide could be escaping from the deposition pool and into the ocean in the process of emptying the pool.

Although the problem of aluminium oxide particles being carried by the stream into the ocean is present with or without a dryer, the frequency of excavating aluminium oxide may increase when the need for aluminium oxide for the dryer arises. Currently, the aluminium oxide is only excavated every few years. If the aluminium oxide is to be dried, the assumption is that the need to excavate aluminium oxide would arise more frequently. Thus, the payback period of

the investment, including a rebuild, will be investigated in Section 9.6.

9.4 Operating costs associated with adding a new dryer

9.4.1 Batch operations

The main operating cost associated with adding a dryer is the cost of moving product to and from the dryer. This cost is variable, in the sense that a smaller amount of material being moved will lead to fewer labour hours spent by workers on moving material, which in turn means that less is spent on wages. The same logic applies to an increase in material needing to be moved. The wear and tear of equipment which is used in order to perform the batch operations is also proportional to the workload. The dryer placement is assumed to be close to the silo where petroleum coke is stored, and the silo is situated close to where the anode production process occurs. This placement is chosen partly in order to minimize the length that the petroleum coke has to be transported, due to the large amounts of petroleum coke compared to the mass flow of the other materials. Thus, the piping is ensuring that the flow of material from the silo is transported continuously.

However, aluminium oxide and anode mass must be brought to the dryer in batch operations. There are existing costs related to gathering and re-introducing the anode mass into the current anode baking process. Consequently it is estimated that the costs associated with this task is in the same magnitude as bringing it to the dryer and back to the anode baking process. Therefore, the cost of batch operations required to dry anode mass does not need to be taken into account when evaluating the differences in costs of the two alternatives.

The costs of the batch operations which are required to bring aluminium oxide to the dryer are variable. As mentioned above, the costs related to batch operations vary with the level of activity. It is expected that the marginal costs of this activity is constant. However, the marginal cost may increase if the labor hours required to perform the tasks leads to workers exceeding their hours such that overtime pay is needed. An estimated 300 000 NOK per year is estimated as the cost of paying for this comparatively labor intensive activity. As there is uncertainty regarding the magnitude of this cost, the effect of increasing the operating costs associated with batch operations is investigated in Section 9.6.

9.5 Payback period of dryer installation

The payback period of the dryer is the time it takes before the initial investment is recovered. In other words, the payback period is the time it takes for the accumulated total costs of keeping the current process to be equal to the costs associated with purchasing, installing and utilizing

a dryer.

In Figure 37, the total costs associated with the two decisions is demonstrated graphically. From the figure, the abscissa of the point defined by the intersection of the green and the blue lines can be interpreted as the payback period. The initial investment which is required for purchasing and installing a dryer is larger than the investment cost of the alternative decision. On the other hand, the operating costs associated with the utilization of an industrial dryer are lower than the operating costs in the current situation.

The lines which are used in the calculation of payback period are a result of using the information of costs which was discussed above. The general equation for a line is given as:

$$y = mx + b \tag{29}$$

Where y [NOK] is the total accumulated cost, x [years] is time, m [NOK/year] is the slope of the line and b [NOK] is the value of y when x is equal to zero. To determine the slope of the lines which represent the total cost, the annual operating costs determine the slope of the line while the investment costs are interpreted as the value of b.

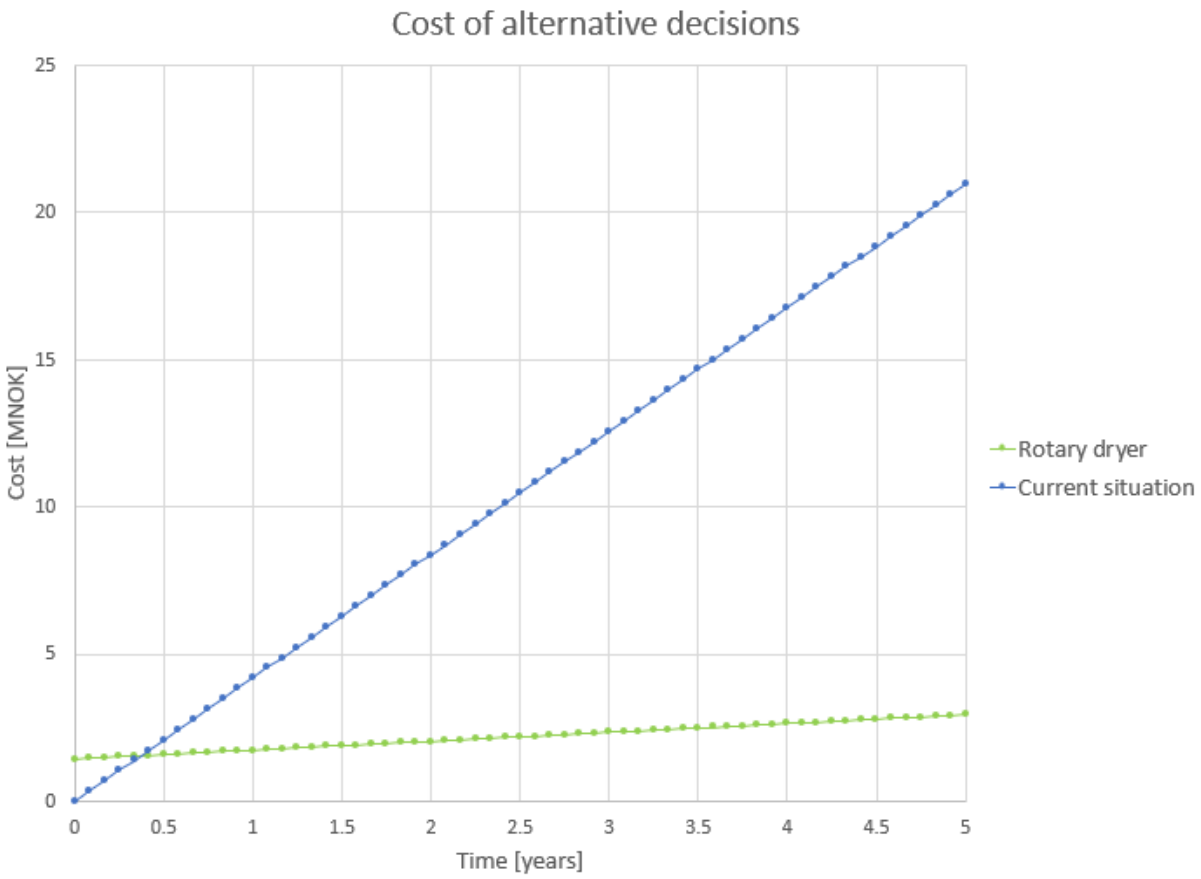

Figure 37: Total costs of the two decisions. Each point on the line is the expected cumulative cost at the beginning of each month with a total horizon of five years time. The dimension of the y-axis is in millions of NOK, or MNOK.

It can be observed from Figure 37 that the slope of the line representing the total costs of the current situation is steeper than the line representing the total costs associated with installing a dryer. This is a consequence of the difference in operating costs associated with the two alternatives. The operating costs associated with installing a dryer is lower than the alternative, which is to not alter the current process. From Figure 37, it is evident that the payback period of installing a dryer is between four and five months. Some of the factors which have been discussed previously are quite definitive while other factors are uncertain and will be investigated in a sensitivity analysis in Section 9.6. Another aspect which must be considered, is the variable unit costs related to the investments. As the costs associated with the investments are fixed over the useful life of the fixed assets, it is important that the dryer is operated at the right capacity. A decrease in output will result in a system which is more expensive per unit of dried matter. The time value of money is factor which is not considered in the payback period calculations. However, calculating the net present value of the investment with an 8 % yearly discount rate still yields a payback time of between four and five months. Thus, it can be concluded that it is profitable to utilize process waste heat for the purpose of drying the raw materials and by-products which have been investigated in this thesis .

9.6 Sensitivity analysis on payback period

A sensitivity analysis on the payback period is beneficial in a decision-making process because a more extensive insight is gained and a broader knowledge of which future improvements in the process may be more cost effective. By varying the variables associated with incorporating a dryer into the process, the change in individual variables will display how the change affects the payback period. In the sections above, a discussion of costs has been presented. Some of the costs are less certain than others. For instance, the cost of rebuilding the aluminium oxide deposition pool is not yet considered when calculating the payback period, but the cost of this project is estimated to be approximately 10 MNOK. Another relevant example is how a change in moisture content of petroleum coke would affect the payback period. The moisture content of the petroleum coke varies with each new shipment. Consequently, in the sensitivity analysis of uncertain variables, variables in an a suitable range is used to illustrate the change in payback period.

9.6.1 Deposition pool rebuild

The estimated cost of the deposition pool rebuild is 10 MNOK. As mentioned in Section 9.3.3, the rebuild of the pool may happen irrespective of the dryer being incorporated into the process, albeit at a later time. However, for the sake of investigating its effect on the payback period, the whole cost is placed on the scenario where a dryer is installed. In Figure 38, the graphical representation of the cost curves shows that the payback period is expected to be close to three

years. This scenario is the worst-case scenario, and it is unreasonable to place the whole cost of rebuilding the pool on the investment cost of a dryer.

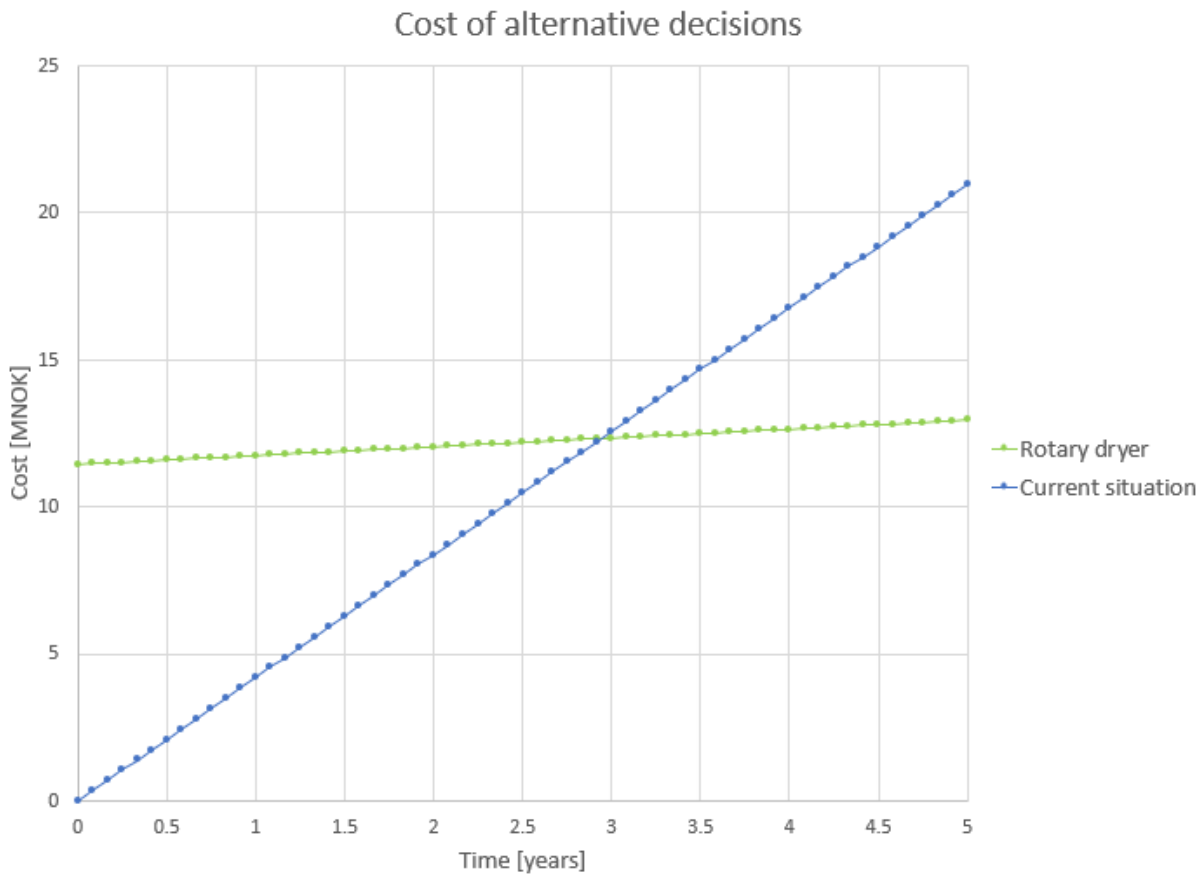

Figure 38: Total costs of the two decisions. Each point on the line is the expected cumulative cost at the beginning of each month with a total horizon of five years time. The dimension of the y-axis is in millions of NOK, or MNOK. In this scenario, the whole cost from the deposition pool rebuild is placed on the scenario where a dryer is installed.

9.6.2 Increase in price of LNG

The price of LNG is dependent on the price of CO_2. For the aluminium industry in the EU, the price of CO_2 is decided by the ETS. In the future, CO_2-emissions are probably going to be taxed at a higher rate than they are today. Thus, in this scenario the price of LNG is increased by 50% as a consequence of strict environmental policies. This price increase is not assumed to be conservative, and such a price increase is not necessarily expected imminently. However, it is of interest to investigate how such a drastic price increase would affect the payback period. In Figure 39, the price increase is implemented while the cost of the deposition pool rebuild is also still included. From Figure 39, it can be observed that the payback period of this scenario is approximately two years and three to four months. Comparing this payback period to the payback period presented in Figure 38, it can be determined that the difference in payback period is approximately 8 months.

The payback period with the same increase in price of LNG leads to a reduced payback period of approximately one month if the deposition pool rebuild is not accounted for. Though it should be stressed that the price of CO_2 on

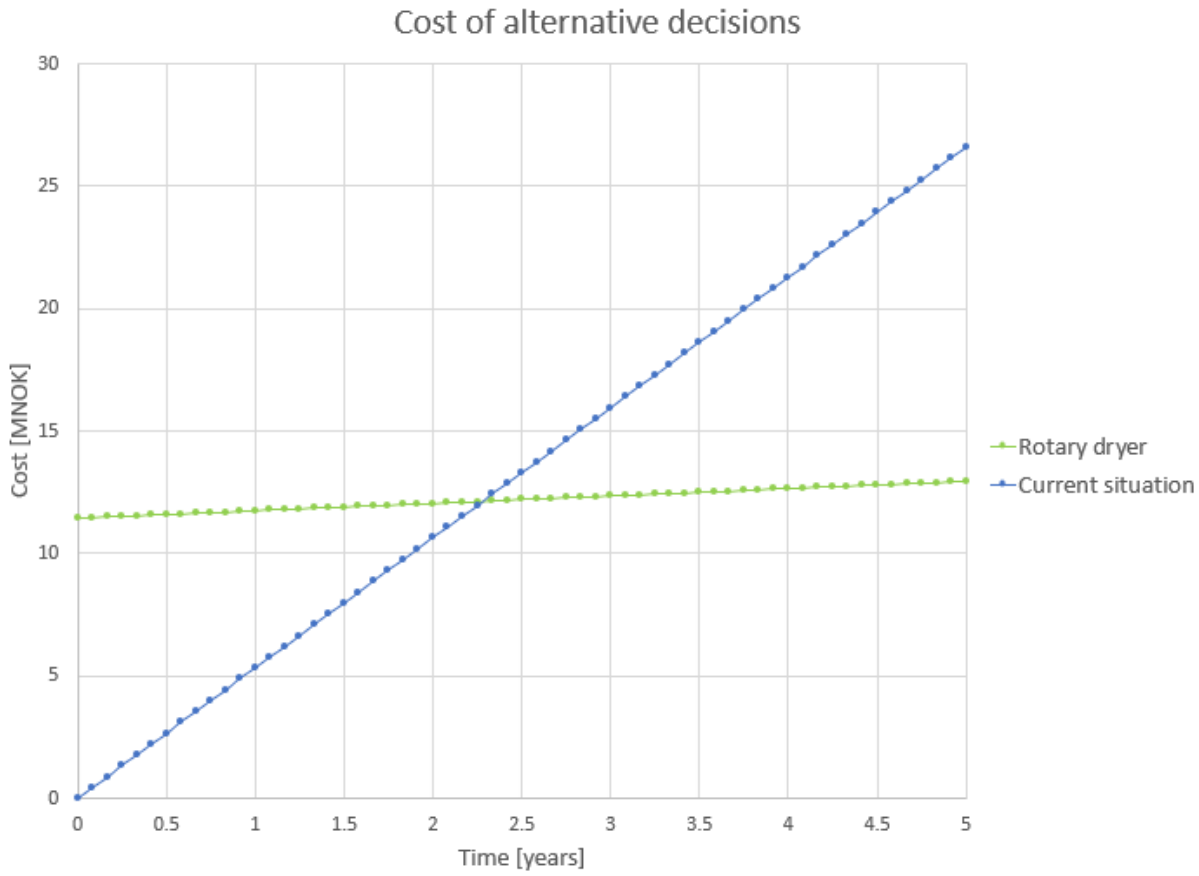

Figure 39: Total costs of the two decisions. Each point on the line is the expected cumulative cost at the beginning of each month with a total horizon of five years time. The dimension of the y-axis is in millions of NOK, or MNOK. In this scenario, the whole burden of cost from the deposition pool rebuild is placed on the scenario cost of installing a dryer. In addition, the price of Methane is increased by 50%

9.6.3 Lower moisture content of petroleum coke

The amount of LNG which is saved when the petroleum coke is dried and heated before being introduced to the anode baking process is dependant on the moisture content of the material. While there is a strict criterion regarding the wet basis moisture content in the anode baking process of no more than 0,3 %, the moisture content in some shipments are above and below this threshold. In Section 5, the amount of LNG which is required to remove the amount of water which shall be removed in a dryer is calculated. In this calculation, the wet basis moisture content is estimated to be 0.3%. However, it is also of interest to investigate how a reduced moisture content would affect the payback period. Therefore a scenario where the wet basis moisture content of petroleum coke of 0.1% is investigated. From Figure 40 it can be observed that the payback period is approximately six months. Comparing this to the payback period

presented in Figure 37, where the payback period was calculated as four to five months, it becomes evident that the relatively small change in moisture content changes the payback period somewhat. As there is a mass flow of 220 000 tonnes of petroleum coke each year, even a small difference in moisture content results in a large reduction of water which is heated and evaporated. The reduction is large in absolute terms due to the large amount of petroleum coke.

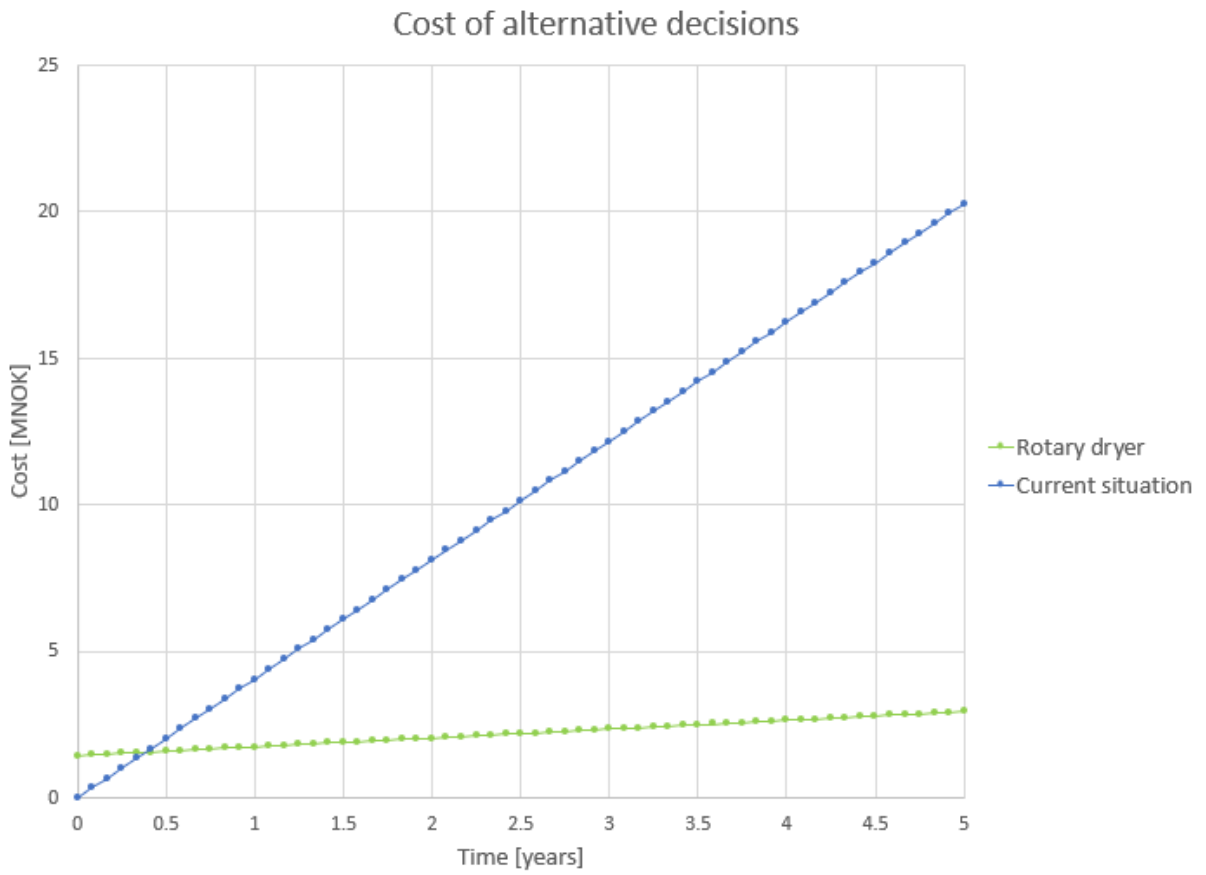

Figure 40: Total costs of the two decisions. Each point on the line is the expected cumulative cost at the beginning of each month with a total horizon of five years time. The dimension of the y-axis is in millions of NOK, or MNOK. In this scenario, the wet basis moisture content of petroleum coke is changed from 0.3% to 0.1%

9.6.4 Increase in batch operation costs

The costs of operations related to bringing material to and from the dryer, called batch operations, was previously discussed in Section 9.4.1. Due to the amount of labor hours required to perform this type of task, it is assumed that the task is quite labor-intensive. However, by designing a process which is continuous for the petroleum coke while the other materials must be loaded in batches, the intent is to shift the process over to a more capital-intensive process. As the batch operations cost is the only relevant operating cost of the scenario where a dryer is incorporated, it would be beneficial to have some knowledge about what an increase in operating costs would mean for the payback period. Therefore, in this scenario, the batch operation costs are increased from 300 000 NOK/year to 1.5 MNOK/year. As is evident from Figure 41,

the payback period is affected, compared to the best-case scenario. An increase in payback time of approximately two months can be observed, with a total of 6 to 7 months of payback period.

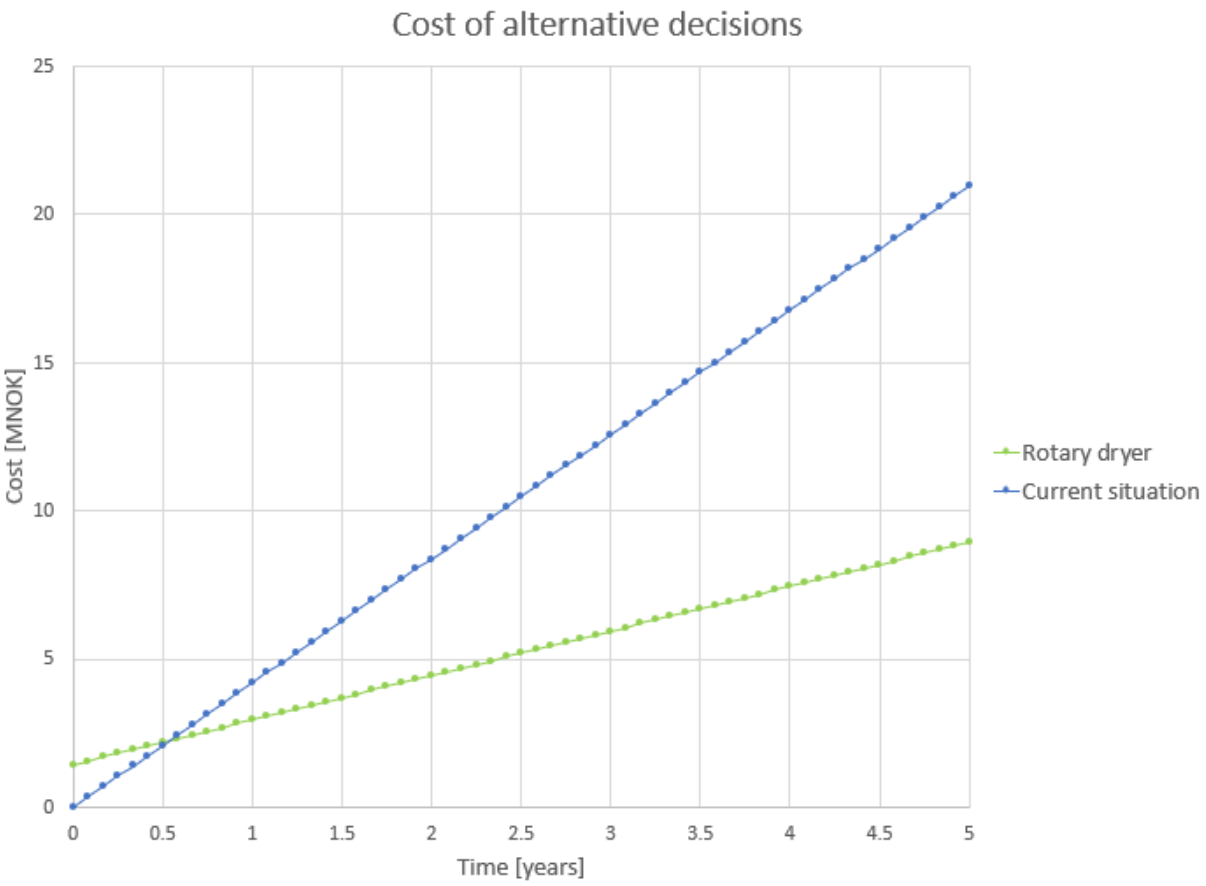

Figure 41: Total costs of the two decisions. Each point on the line is the expected cumulative cost at the beginning of each month with a total horizon of five years time. The dimension of the y-axis is in millions of NOK, or MNOK. In this scenario, the operating costs associated with batch operations are increased by a factor of 5.

9.7 Increased cost of dryer unit

The price of purchasing a dryer unit is currently unknown. Thus, it is of importance to estimate the payback period if the price of a rotary dryer is higher than anticipated. An increased price of the rotary dryer may occur due to many circumstances, e.g., if there are conducted tests at a manufacturer to determine the optimal geometry of flights, or if the system which is required for continuous feed of petroleum coke is higher than first anticipated. Therefore, in this scenario, the price of a rotary dryer is increased by a factor of 3. Hence, the investment cost is increased from 577 500 NOK to 1 732 500 NOK. As can be observed in Figure 42, the payback period in this scenario is approximately 8 months. This is an increase of 3 to 4 months, compared to the best-case scenario.

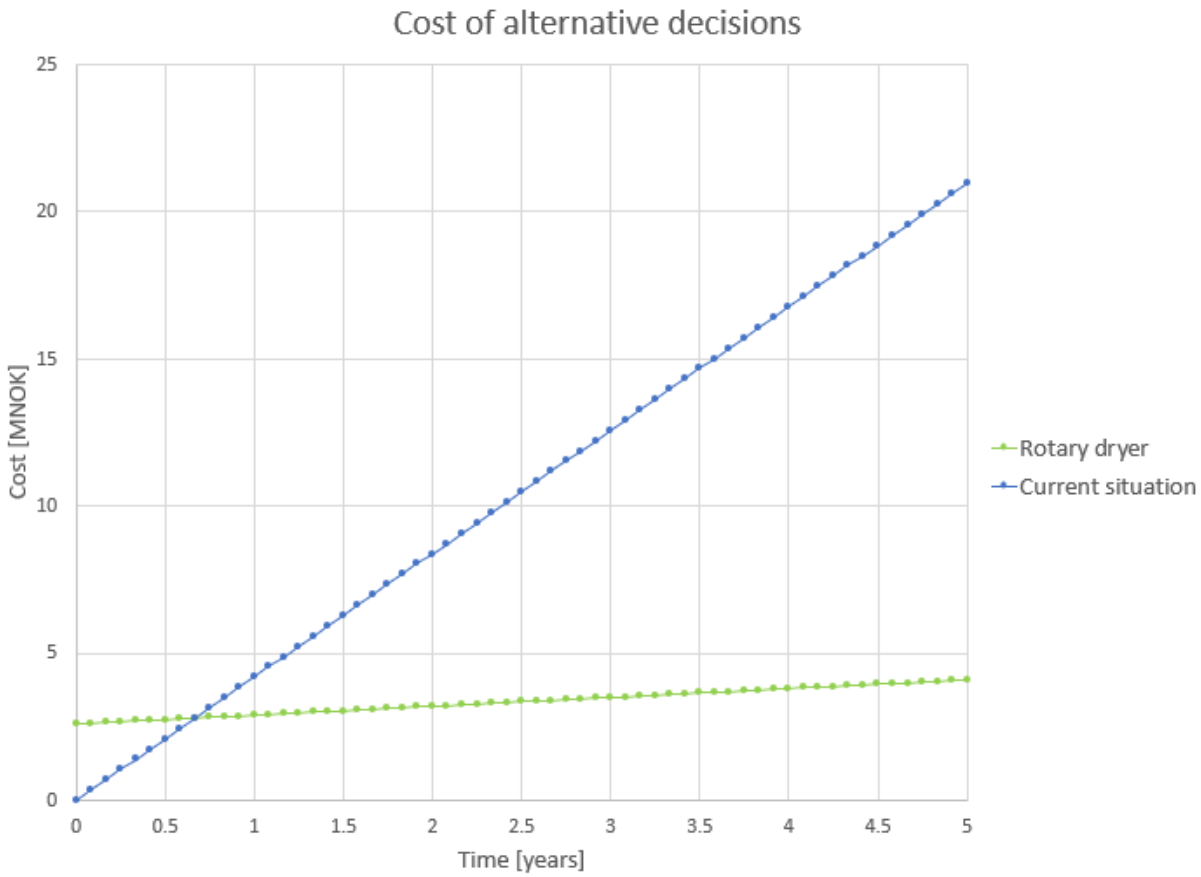

Figure 42: Total costs of the two decisions. Each point on the line is the expected cumulative cost at the beginning of each month with a total horizon of five years time. The dimension of the y-axis is in millions of NOK, or MNOK. In this scenario, the investment costs of buying a dryer is increased by a factor of 3.

9.7.1 Conclusion from the sensitivity analysis

Based on the sensitivity analysis which is provided, it can be concluded that the profitability of the decision to alter the existing process in order to incorporate a dryer makes sense in terms of saving costs. The sensitivity analysis reveals that the payback period would be between approximately four months at best and three years at worst, depending on the ranges of parameter values which have been previously discussed. The acceptable payback period is a decision which must be made by the company.

10 Further Work

The following work is proposed in order to fully implement an industrial rotary dryer at Alcoa Mosjøen:

- The acceptable payback period of the project must be decided by the company. Information regarding the profitability of the project is provided in this thesis, but there may be circumstances which have not been taken into account yet. However, based on the information about the payback period which is provided, a return on investment would occur relatively quickly.
- A deal must be made with a manufacturer of a rotary dryer for the design of a dryer which is custom-built for the purpose of drying the three different materials. With the manufacturers, trials should be conducted in order to optimise the rotary dryer to the conditions of the process. By utilizing the given information in Section 8.4.2, the dimensions of a rotary dryer, drying rate, residence time of the material and angle of inclination of the dryer should be possible to determine.
- If the moisture content reduction of the petroleum coke and anode mass is not at an acceptable level after being dried in a rotary dryer, then further studies on the water activity of petroleum coke and anode mass may be needed to determine what conditions would be required to ensure a lower water activity than was achieved in this master's thesis.

References

Berk, Z. (2008), *Food Process Engineering and Technology*, Elsevier Science & Technology, chapter 22, pp. 459–510.

Berndt Wischnewski (2007), 'Calculation of thermodynamic state variables of air'. [Online Accessed 16-December 2020].
URL: *https://www.peacesoftware.de/einigewerte/luft.html*

Bharat Industrial Works (n.d.), 'Industrial dryers'. [Online Accessed 8-June 2021].
URL: *https://www.bharathindustrialworks.co.in/dryers.html*

Chevarin, F., Azari, K., Ziegler, D., Gauvin, R., Fafard, M. and Alamdari, H. (2016), 'Substrate effect of coke particles on the structure and reactivity of coke/pitch mixtures in carbon anodes', *Fuel (Guildford)* **183**, 123–131.

Clos, D. P., Andresen, T., Nekså, P., Johnsen, S. G. and Aune, R. E. (2017), Enabling efficient heat recovery from aluminium pot gas, *in* 'Light Metals 2017', The Minerals, Metals & Materials Series, Springer International Publishing, Cham, pp. 783–791.

Engineering Toolbox (2003), 'Air - density, specific weight and thermal expansion coefficient at varying temperature and constant pressures'. [Online Accessed 16-December 2020].
URL: *https://www.engineeringtoolbox.com/air-density-specific-weight-d_600.html*

Engineering Toolbox (2004*a*), 'Water - specific heat'. [Online Accessed 16-December 2020].
URL: *https://www.engineeringtoolbox.com/specific-heat-capacity-water-d_660.html*

Engineering Toolbox (2004*b*), 'Water - specific heat'. [Online Accessed 16-December 2020].
URL: *https://www.engineeringtoolbox.com/water-properties-d_1573.html*

European Commission (2015), 'EU ETS Handbook'. [Online; accessed 20-June 2021].
URL: *https://ec.europa.eu/clima/sites/clima/files/docs/ets_handbook_en.pdf*

Excellent En-Fab Incorporation (n.d.), 'Rotary dryer'. [Online Accessed 8-June 2021].
URL: *https://www.indiamart.com/excellentenfabinc/industrial-dryers.html#rotary-dryer-131599220*

Gautam, M., Pandey, B. and Agrawal, M. (2018), Chapter 8 - carbon footprint of aluminum production: Emissions and mitigation, *in* S. S. Muthu, ed., 'Environmental Carbon Footprints', Butterworth-Heinemann, pp. 197 – 228.
URL: *http://www.sciencedirect.com/science/article/pii/B9780128128497000088*

Geldart, D. (1973), 'Types of gas fluidization', *Powder Technology* **7**(5), 285 – 292.
URL: *http://www.sciencedirect.com/science/article/pii/0032591073800373*

Graedel, T. and Allenby, B. R. (2015), *Industrial ecology and sustainable engineering*, Pearson.

Grjotheim, K. and Kvande, H. (1993), *Introduction to aluminium electrolysis : understanding the Hall-Héroult process*, 2nd ed. edn, Aluminium-Verlag, Düsseldorf.

Hardin, G. (1968), 'The tragedy of the commons', *Science* **162**(3859), 1243–1248.
URL: *https://science.sciencemag.org/content/162/3859/1243*

Hoff, K. G. and Helbæk, M. (2016), *Bedriftens økonomi*, 8. utg. edn, Universitetsforlaget, Oslo.

Idsø, J. (2021), 'Pareto-optimalitet'. [Online; accessed 12-April 2021].
URL: *https://snl.no/Pareto-optimalitet*

Incropera, F. P., DeWitt, D. P., Bergman, T. L. and Lavine, A. S. (2017), *Incropera's Principles of heat and mass transfer*, 8. utg. global ed. edn, Wiley, Singapore.

Kazi, S. (2012), *Fouling and Fouling Mitigation on Heat Exchanger Surfaces*.
URL: *https://www.researchgate.net/publication/221927710_Fouling_and_Fouling_Mitigation_on_Heat_Exchanger_Surfaces*

Ladam, Y., Solheim, A., Segatz, M. and Lorentsen, O.-A. (2011), *Heat Recovery from Aluminium Reduction Cells*, John Wiley & Sons, Ltd, pp. 393–398.
URL: *https://onlinelibrary.wiley.com/doi/abs/10.1002/9781118061992.ch70*

Laffont, J. J. (2018), Externalities, *in* 'The New Palgrave Dictionary of Economics', Palgrave Macmillan UK, London.

Laxmi Engineers (n.d.), 'Rotary dryer'. [Online Accessed 8-June 2021].
URL: *https://www.laxmi-group.com/rotary-dryer.html#rotary-dryer*

Lecomte, D., Fudym, O., Carrère-Gée, C., Arlabosse, P. and Vasseur, J. (2004), 'Method for the design of a contact dryer-application to sludge treatment in thin film boiling', *Drying Technology* **22**(9), 2151–2172.
URL: *https://doi.org/10.1081/DRT-200034229*

Meld. St. 13 (2020–2021)(2021) (2021), ': Klimaplan for 2021–2030'.
URL: *https://www.regjeringen.no/no/dokumenter/meld.-st.-13-20202021/id2827405/*

Meter Group Inc. (2018), *METER AquaLab 4 Manual Web*, METER.

Mettler Instruments AG (1987), 'Operating Instructions Mettler Analytical Balance AE260 DeltaRange'. [Online; accessed 24-May 2021].
URL: *https://www.marshallscientific.com/v//vspfiles/files/manuals/MTAE260.pdf*

Mettler Toledo (2012), 'Precision Balance ME4002'. [Online; accessed 7-December 2020].
URL: *https://www.mt.com/gb/en/home/products/Laboratory_Weighing_Solutions/Precision_Balances/Standard/ME_Precision_Balances/ME_4002.html*

Metz, B., Davidson, O. R., Bosch, P. R., Dave, R. and Meyer(eds.), L. A. (2007), 'Climate change 2007: Mitigation of climate change, contribution of working group iii to the fourth assessment report of the intergovernmental panel on climate change'.
URL: *https://www.ipcc.ch/site/assets/uploads/2018/03/ar4_wg3_full_report-1.pdf*

Moran, M. and Shapiro, H. (2015), *Principles of engineering thermodynamics*, 8th ed., si version. edn, Wiley, Singapore.

Mujumdar, A. (2000), 'Classification and selection of industrial dryers', *Exergex Corp.* .

Mujumdar, A. S. (2007), *Handbook of industrial drying*, 3rd ed. edn, Taylor & Francis, Boca Raton, Fla.

National Institute of Standards and Technology (1978), 'NIST-JANAF Thermochemical Tables - Carbon'. [Online Accessed 16-December 2020].
URL: *https://janaf.nist.gov/tables/C-002.html*

National Institute of Standards and Technology (1979), 'NIST-JANAF Thermochemical Tables - Aluminium Oxide, Alpha'. [Online Accessed 16-December 2020].
URL: *https://janaf.nist.gov/tables/Al-096.html*

Nikolaisen, M. and Andresen, T. (2019), Optimization of system operation and heat exchanger sizing in rankine cycles - a case study on aluminium smelter heat-to-power conversion, *in* 'Proceedings of the 5th International Seminar on ORC Power Systems'.

Nikolaisen, M., Skjervold, V. T. and Andresen, T. (2020), 'Evaluation of heat recovery heat exchanger design parameters for heat-to-power conversion from metallurgical off-gas', *Science et technique du froid* .

Pedersen, B. (2017), 'Hall–héroult-prosessen'. [Online; accessed 12-December 2020].
URL: *https://snl.no/Hall%E2%80%93H%C3%A9roult-prosessen*

Pedersen, B. (2018), 'Aluminium'. [Online; accessed 27-October 2020].
URL: *https://snl.no/aluminium*

Plumer, B. and Popovich, N. (2019), 'These Countries Have Prices on Carbon. Are They Working?'. [Online; accessed 3-May 2021].
URL: *https://www.nytimes.com/interactive/2019/04/02/climate/pricing-carbon-emissions.html*

Prasad, S. (2000), 'Studies on the Hall-Heroult aluminum electrowinning process', *Journal of the Brazilian Chemical Society* **11**, 245 – 251.

Riis, C. (2018), *Moderne mikroøkonomi*, 4. utg. edn, Gyldendal akademisk, Oslo.

Sandmo, A. (2018), *Pigouvian Taxes*, Palgrave Macmillan UK, London, pp. 10312–10315.
URL: *https://doi.org/10.1057/978-1-349-95189-5_2678*

Skjervold, V. T., Skaugen, G., Andresen, T. and Nekså, P. (2020), 'Enabling power production from challenging industrial off-gas – model-based investigation of a novel heat recovery concept', *Science et technique du froid* .

Tangstad, M. (2013), *Metal production in Norway*, Akademika Publ, Oslo.

The Editors of Encyclopaedia Britannica (2021), 'Arthur Cecil Pigou'. [Online; accessed 23-April 2021].
URL: *https://www.britannica.com/biography/Arthur-Cecil-Pigou*

The Norwegian government (2020), 'Norway steps up 2030 climate goal to at least 50 % towards 55 %'. [Online; accessed 20-April 2021].
URL: *https://www.regjeringen.no/en/aktuelt/norge-forsterker-klimamalet-for-2030-til-minst-50-prosent-og-opp-mot-55-prosent/id2689679/*

United Nations (2021), 'The Paris Agreement'. [Online; accessed 14-April 2021].
URL: *https://www.un.org/en/climatechange/paris-agreement*

United Nations Framework Convention on Climate Change (2020), 'Nationally determined contributions (ndcs)'. [Online; accessed 20-April 2021].
URL: *https://unfccc.int/process-and-meetings/the-paris-agreement/the-paris-agreement*

Van Puyvelde, D. R. (2009), 'Modelling the hold up of lifters in rotary dryers', *Chemical Engineering Research and Design* **87**(2), 226–232.
URL: *https://www.sciencedirect.com/science/article/pii/S0263876208002566*

Wang, Z., Zhou, N. and Jing, G. (2012), 'Performance analysis of orc power generation system with low-temperature waste heat of aluminum reduction cell', *Physics procedia* **24**, 546–553.

Wikipedia contributors (2020), 'Rotary dryer — Wikipedia, the free encyclopedia'. [Online; accessed 20-December 2020].
URL: *https://en.wikipedia.org/w/index.php?title=Rotary_dryer&oldid=934851677*

Yehuda, T. and Kalman, H. (2020), 'Geldart classification for wet particles', *Powder technology* **362**, 288–300.

List of Figures

List of Tables

Appendices

A Energibalanse Alcoa

B Risk Assessment

C Draft Scientific Paper

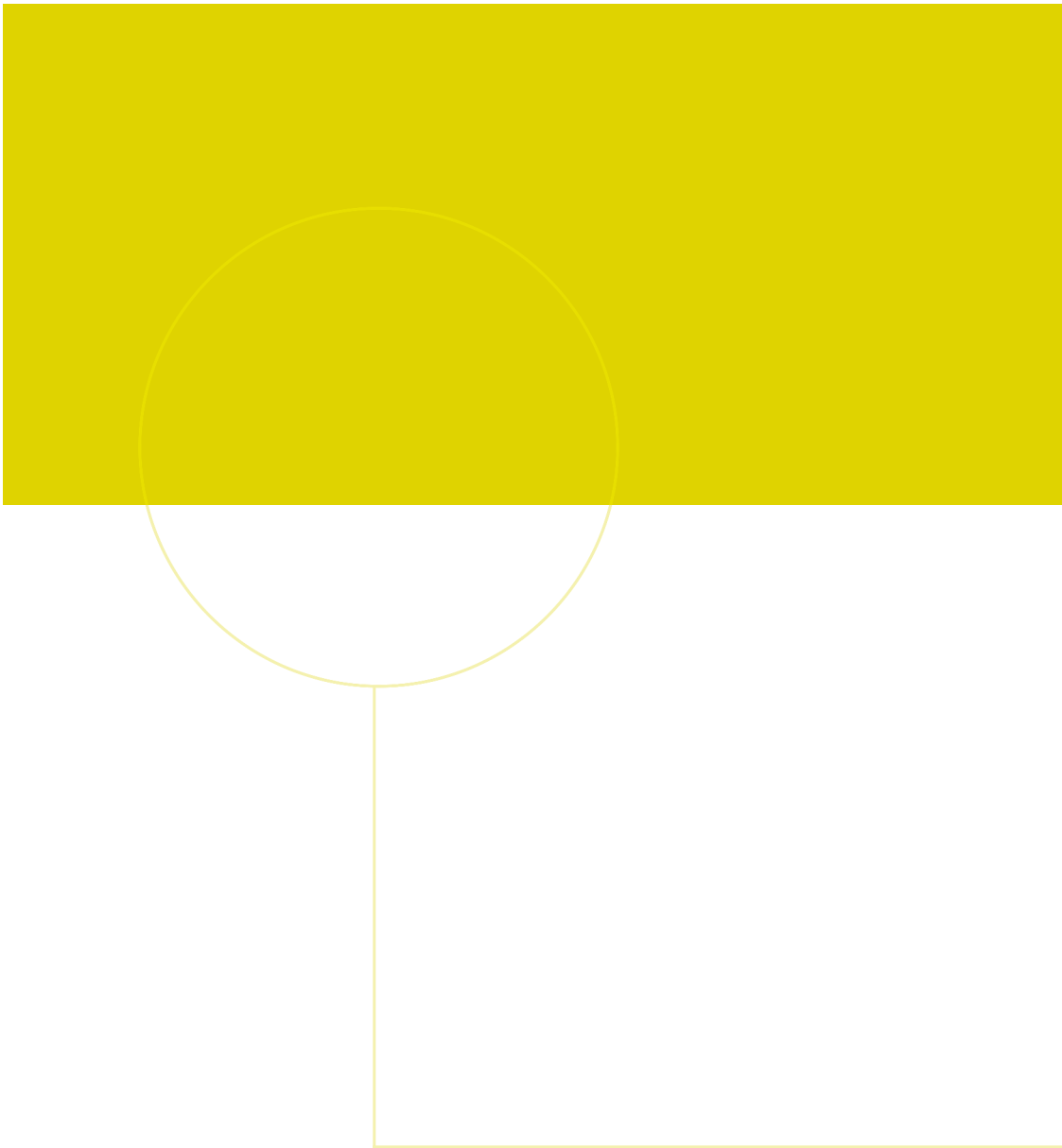

NTNU

Kunnskap for en bedre verden